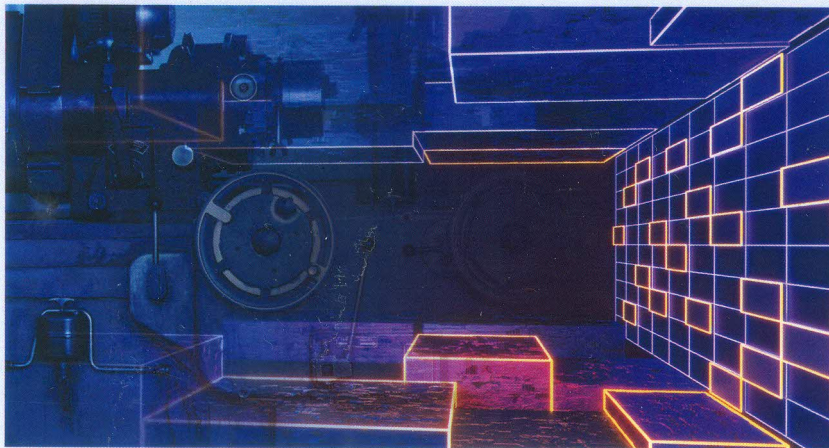


# Journal of Physics Conference Series



# 1605

Volume 1605

Online ISSN: 1742-6596 Print ISSN: 1742-6588

[jpcs.iop.org](http://jpcs.iop.org)

**IOP** Publishing

# **Journal of Physics: Conference Series**

**Volume 1605 (Part II)**

Edited by

**M. Popovic & Y.Q. He**

- 012087 An experimental study on the discharge coefficient of a sharp-edged hydraulic orifice**  
*Wenlin Wang, Xiaochang Cao, Xin Kong and Yongming Wu*
- 012088 Study on the characteristics of metal magnetic memory signal of X70 pipeline steel**  
*Xiyong Zhang, Yun Chen and Yonghong Chen*
- 012089 Research on Equipment Life Cycle Cost Prediction Based on GA-LSSVM**  
*Yong-hong Chen, Yong-sheng Su and Xiang-hua Du*
- 012090 Simulation Analysis of Installation Process of Long stern Shaft of Large Ship**  
*J H Zhou and H Shi*
- 012091 A Nozzle Structure of Wire Drawing Prevention for 3D Printing Fused Deposition Manufacturing**  
*Fu Jieqiong, Bu Leping, Zeng wenping and Zhang yong*
- 012092 Summary of ten innovations in the machinery field--the analysis on material processing contrary the mechanical principles etc.**  
*C M Li, X L Yin, Y Zhang, F Sun, H Cao, Q Liu and X Liu*
- 012093 Multi-parameter joint optimization of self-piercing riveting on aluminum alloy plate**  
*Y H Zhang, B J Shi and J B Zhong*
- 012094 Hydraulic Control Research of Working Device of Grab Arm Cleaning Machine for Heavy Load and Large Depth**  
*Chen Yuanlong, Wang Ziquan and Chen Rongna*
- 012095 Equivalent Mechanical Model for Conducting Polypyrrole Actuator**  
*Jinyou Chen and Sukun Tian*
- 012096 Dynamic Performance and Fatigue Analysis of ASP Pump Rotor**  
*Niu Qichen, Zhang Gongxue, Meng Yanhui, Yang Sen, Tuo Yinfeng and Ma Zhi*
- 012097 A design method of acoustic metamaterials with buckling vibrators**  
*Shenghui Qin, Xiaoming Wang and Yulin Mei*
- 012098 A Design Method for Labyrinth Sound Absorption Structure with Micro-perforated Plates**  
*Dequn Yu, Xiaoming Wang and Yulin Mei*
- 012099 Experimental Research and Mechanical Analysis of Levelling Parametric Characterization of 3D Printer**  
*Zeng Lianghua*

## A Nozzle Structure of Wire Drawing Prevention for 3D Printing Fused Deposition Manufacturing

Fu Jieqiong<sup>1a</sup>, Bu Leping<sup>1b, 2a</sup>, Zeng wenping<sup>1c</sup>, Zhang yong<sup>2b</sup>

<sup>1</sup>Guangzhou City constructing College, Guangzhou 510925

<sup>2</sup>College of Mechanical and Electrical Engineering, Inner Mongolia Agricultural University, Hohhot 010018

First author Fu, Jieqiong: Female, born in 1982, associate professor, Master of Engineering, research direction: mould designing and manufacturing as well as numerical control, E-mail:332460235@qq.com

Corresponding author Bu, Leping: Male, born in 1958, professor, Doctor of Engineering, graduate student tutor, research direction: material processing technology and equipment, E-mail:buleping1958@126.com

**Abstract:** The working principle of 3D printing fused deposition Manufacturing is introduced. The reasons for the problems of nozzle material flow and product wire drawing in the process of product printing are pointed out. The structure of traditional nozzle is analyzed, and a new structure of nozzle is proposed. The main feature of the new nozzle structure is that it can generate negative pressure in the closed space when the wire is withdrawn, thus it can effectively prevent the nozzle flow and product drawing. At the same time, by optimizing the heat dissipation system of the new nozzle structure, the stability of the nozzle printing process can be improved. The practical application shows that this new nozzle structure is effective and worth popularizing.

### 1. Introduction

3D printing is a kind of additional material rapid proto-typing technology, which is based on a kind of digital model file, it has utilized materials of special wax material, photosensitive resin, powder-like metal or plastic, etc to manufacture three-dimensional objects by printing layers of binding materials. Whereas, fused deposition Manufacturing (Shortened form FDM) has heated and melted the filiform hot melting material (Which is generally to be PLA or ABS wire)then it has squeezed and sprayed filiform hot melting onto the working platform to pile up in layer for moulding via a nozzle whose diameter is generally to be 0.4mm, as is shown by figure 1. As during the 3D printing process of the fused deposition manufactureing, the printing nozzle needs constant moving, when the nozzle moves from one printing point to the next printing point, it will appear drawing phenomenon because the fused shape material in the nozzle had not been stopped in time or spilled over, as is shown by figure 2, which therefore has greatly affected the printing quality[1]. Although method for improving draw-bench has properly setting the printer parameters, such as pumpback distance, pumpback speed, fuse temperature, distance of dangling movement, etc., but these are to solve the problem[2] in processing parameter layer; however the design has reached the purpose of completely improving drawing problem of fuse deposition manufactureing product by starting from nozzle structure of the printer.



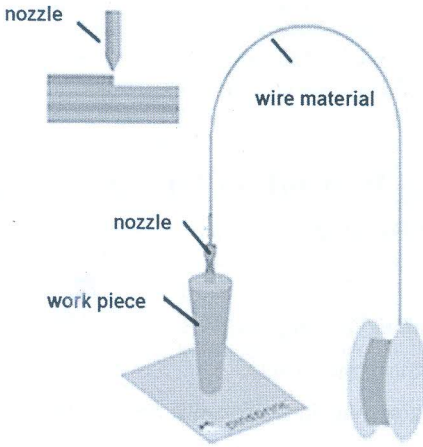


Figure 1 Schematic diagram of fused deposition manufacturing

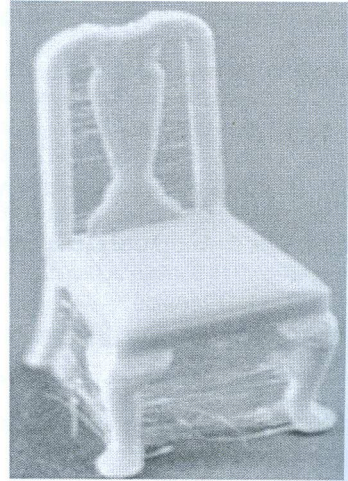


Figure 2 Schematic diagram of product drawing phenomenon

## 2. Structural Design of Traditional Nozzle

### 2.1. Structure of Traditional Nozzle

Nozzle of traditional structure is shown as figure 3 and figure 4, whose main components have included hollow throat, heat dissipation, heating chamber, heating block, nozzle, fixed block and thermal insulation pillar, etc.

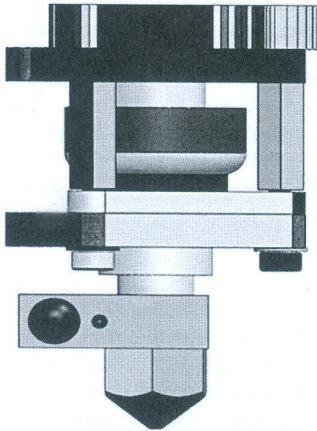


Figure 3 Three-dimensional structural figure of traditional nozzle

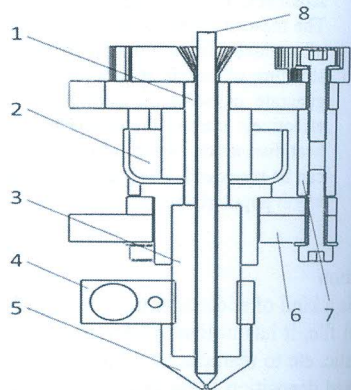


Figure 4 Two-dimensional structural figure of traditional nozzle  
1 Hollow throat 2 Heat dissipation 3 Heating chamber 4 Heating block  
5 Nozzle 6 Fixed block 7 Thermal insulation pillar 8 Printing wire material

### 2.2. Defect of Traditional Nozzle in Anti-drawing

There are two aspects for defects of the structure of traditional nozzle has existed in anti-drawing[3]: one is that the 3D printing wire material is heated after it enters into the heating chamber, when the printing wire is pumped back, it will flow in the molten state in the heating chamber; so the printing material in the molten state still will be spilled out along the nozzle, which therefore will appear condition of wire re-leaking, with-wire and wire-flowing and will affect product quality; secondly, the printing nozzle structure has mainly dissipated by the thermal baffle and the auxiliary blower, whose dissipation point is rather concentrated and the airflow is too dispersed, which is difficult to reach very

wire aisle. And the cooling fin becoming bigger from down to upper has been designed on the external part of the radiating tube; the wind scooper with downward ventilation mouth is installed outside the cooling fin, the cooling fan of 30mmx30mm is fixed on the wind scooper.

### 3.2. *Advantages after the Improvement*

Via the practical tracking to the nozzle after improvement, the practice has shown that the nozzle after the improvement has had structural features and advantages of below aspects:

(1)The silicon gel sealing sleeve is inset between the radiating tube and the hollow throat. The silicon gel is a kind of new type macro-molecule elastic material, which has had very good high-temperature resistance (180-200°C); at the same time, it has possessed very good physical stability. Under the tight locking of the radiating tube, it has conducted surrounding sealing to the wire material make the internal part of the hollow throat form the sealing space within the area surrounded by the silicon gel sealing sleeve, printing wire material and the nozzle. Thus in the process of the printing, when the printing nozzle needs the wire-stopping movement to coordinate with the drawing-back of the wire material of the wire-squeezing electric machinery, i.e., the printing wire material will be lifted upward for a section of distance; because of the existence of the sealing chamber, extent negative pressure will be formed at the wire material place of the nozzle head molten state, which will recycle the wire rod of the molten state upward, which therefore has prevented the happening of the drawing phenomenon. Via the experiment, the printing wire material of D1.75 generally needs to set the drawing back distance into 2-3mm as proper; however to printing wire material of D3, then setting it into 1.5-2mm is ok.

(2)By matching the feature that the temperature has been gradually reduced from down to up of the heating tube and the process that the printing wire needs a temperature accumulation to be enhanced to the molten state, which therefore has designed the cooling fin of the radiating tube into a structure being gradually bigger from down to up. The wind scooper has been installed on the outer ring of the radiating tube, which has intensively conducted the radiating airflow away from the cooling fin and it has increased the radiating effect; however the ventilation mouth that guiding the wind to the lower end of the nozzle has been added at the downside of the wind scooper, which has partially conducted the airflow at the bottom to the printing wire of the nozzle; it has not only strengthened the dissipation of the printing wire, but also has reduced some lower airflow and has strengthened the effect that the temperature is gradually reduced upward. Via the test, the upper temperature of the radiating canister has been kept at 60~70°C, which therefore has guaranteed that the wire material will not occur thermoplastic variation at the place of silicon gel sealing sleeve; it let the wire material will not be too hot to occur deformation then lose sealing effect at this place, drawing-back and it has also guaranteed the negative pressure enhancing effect of the sealing chamber at the nozzle mouth; and the temperature of the down part is among 130~150°C, which has promoted the formation of the molten effect for the printing wire. Additionally, it has conducted parts of the wind to the two sides of the nozzle mouth, which has accelerated the heat evolution at the nozzle mouth and at the sprayed out melting wire; it has also played the role of guaranteeing the product printing quality and the stability of the printing.

### 3.3 *The Experimental Data after the Improvement*

It has conducted experimental verification to the nozzle after the improvement, which has adopted the assembly machine whose type is Reparp i3 and it has used PLA printing wire material of 3mm diameter, whose wire feeder is near-end material feeding; related data for moulding printing into the 3D model of the same vase is shown as the table in the article (Except the data on the table, other parameters have kept same), whose testing result is shown as the experimental data table of the research. From the table, it can be seen that when it is 205 °C, 50mm/s and the drawing-back distance is 1.5mm, the degree of finish for all joints of its finished printing pieces are very good and there is no obvious defect, which has effectively improved the generation of drawing phenomenon in 3D printing fused deposition manufacturing.

good dissipation effect; therefore it will affect the stability of the heating chamber of the printing wire material, and that finally will affect the quality of the 3D printing product[4].

### 3. The Improvement of the Nozzle Structure

#### 3.1. Structure of Traditional Nozzle

The nozzle structure after the improvement is shown as figure 5 and figure 6. Schematic figure of ventilation and dissipation is shown as figure 7.

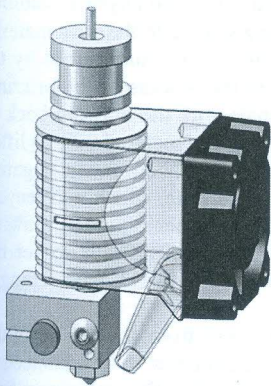


Figure 5 Three-dimensional figure of the nozzle structure after the improvement

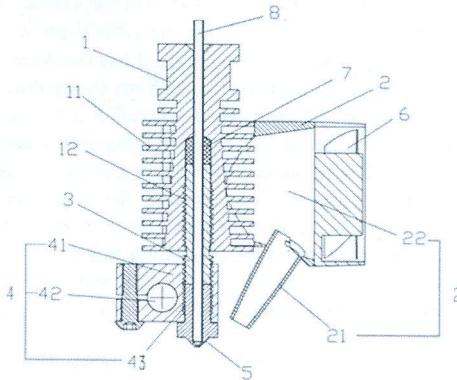


Figure 6 Section view two-dimensional figure of the nozzle structure after the improvement  
1 The radiating tube 2 The radiator system (21 Downward ventilation mouth, 22 The wind scooper)  
3 Hollow throat of the printing wire 4 The heating block (41 The heating fixed block, 42 The heating tube, 43 Thermistor) 5 Nozzle 6 Fan 7 Silicon gel sealing sleeve 8 Printing wire material

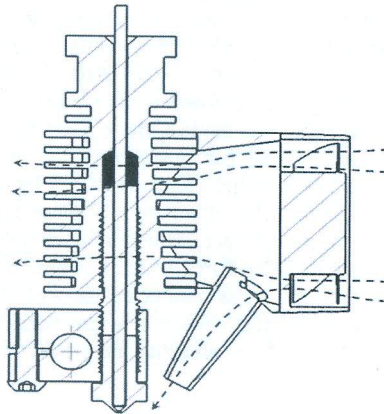


Figure 7 The radiator system after the improvement

The new type anti-drawing 3D printing squeezed-out type nozzle structure[5] has included the radiating tube, hollow throat, the heating apparatus, the cooling fan, the wind scooper, the nozzle and the silicon gel sealing sleeve; the heating fixed block in the heating apparatus has been equipped with the heating tube and the thermocouple, being used as heating control and fixed piece, the lower end of the hollow throat and the nozzle has been connected into the heating fixed block via the screw joint; the upper end of the hollow throat also has been connected onto the radiating tube via the screw joint; the silicon gel sealing sleeve is inset inside the radiating tube and the upper end of the hollow throat tube; the middle hole of the radiating tube, the middle hole of the silicon gel sealing sleeve, the middle hole of the hollow throat and the middle hole of the nozzle have connected into a stripe of printing

Table 1 Experimental Data Table for this Research

No.	Diameter of the nozzle mouth	Temperature of the nozzle mouth	Printing speed	Drawing-back distance	Printing effect	Appearance quality
1	0.4mm	195 °C	50mm/s	1.5mm	The printing route is rather obvious	It sometimes has wire lacking and wire drawing
2	0.4mm	195 °C	50mm/s	2mm	The printing route is rather obvious	It sometimes has wire lacking but has not wire drawing
3	0.4mm	195 °C	70mm/s	1.5mm	The adhesive force of the printing layer has some defects	It sometimes has wire lacking and wire drawing
4	0.4mm	195 °C	70mm/s	2mm	The adhesive force of the printing layer has some defects	The wire lacking is rather obvious
5	0.4mm	205 °C	50mm/s	1.5mm	The surface is very exquisite and has no obvious defects	No obvious wire drawing and wire lacking
6	0.4mm	205 °C	50mm/s	2mm	The surface is very exquisite and has no obvious defects	No wire drawing and wire lacking
7	0.4mm	205 °C	70mm/s	1.5mm	The surface is very exquisite and it is a little warping	No obvious wire drawing and wire lacking
8	0.4mm	205 °C	70mm/s	2mm	The surface is very exquisite and it is a little warping	No obvious wire drawing and wire lacking

#### 4. Conclusion

The design has conducted the design improvement of the printing nozzle structure mainly aiming at the common defect-wire drawing of 3D printing fused deposition manufacturing, whose main measure is to add silicon gel sleeve between the radiating tube and the hollow throat in order to form the sealing space inside the hollow throat therefore to make it form extent negative pressure at the nozzle mouth place when the wire material draws back and to make the wire material of the molten state at the head of the nozzle mouth halt and recycle, which therefore has prevented the occurrence of the wire drawing phenomenon. At the same time, it has optimized the structural design of the cooling system and it has prevented the wire material's deformation at the place of silicon gel sealing sleeve, which therefore has guaranteed the reliability of the sealing space formed interior the hollow throat. Additionally, the design has also improved the ventilation system by letting wind from one part blow to the two sides of the nozzle mouth to make the nozzle mouth and the wire material heat just squeezed from the nozzle mouth drop off very quickly in order to improve the effect of 3D printing.

#### Research project

Inner Mongolia Natural Science Funds (2009MS0802), Inner Mongolia Office of Personnel Services Talent Funds, National Natural Science Foundation of China (61563042)

#### References

- [1] Ma, Yuqiong; Wang, Tiecheng; Zheng, Hongwei; Wang, Wei. Structural Design as well as Movement Research of FDM Multiple Nozzle 3D Printing[J]. Machine Tool and Hydraulic Pressure, 2019. (8) : 29-32
- [2] Li, Cheng Double Nozzle Equipment Development as well as Technology Parameter Research Based on FDM Technology[D]. Nanjing: Nanjing Normal University, 2014: 15-20
- [3] Huang, Zifan; Ma, Yuelong; Li, Junmei, etc. Research of Fuse Deposition Moulding Colorful



- 3D Printer[J]. Machine Tool and Hydraulic Pressure, 2017.45 (4) : 21-25
- [4] Yang, Xiangdong; Zhang, Pengfei; Chen, Wenjun, etc. Research of Desktop Type 3D Printer Technology[J]. Mechanical and Electrical Engineering Technology , 2016.45 (4) : 65-67
- [5] Chen, Jiwen; Yang, Hongjuan. Knowledge Engineering and Mechanical Innovation Design[M]. Beijing: Chemical Industry Press, 2016.
- [6] Research of Moulding Quality and Parameter Setting Relation for 3D Printing Model[J]. Liu, Lilin. Plastic Industry. 2018(05)

Online ISSN: 1742-6596 Print ISSN: 1742-6588  
Journal of Physics: Conference Series Vol.1605  
Electronically available at <http://iopscience.iop.org>

Vijayan Sugumaran  
Zheng Xu  
Huiyu Zhou *Editors*

# Application of Intelligent Systems in Multi-modal Information Analytics

Proceedings of the 2020 International  
Conference on Multi-model  
Information Analytics (MMIA2020),  
Volume 2

Vijayan Sugumaran · Zheng Xu ·  
Huiyu Zhou  
Editors

# Application of Intelligent Systems in Multi-modal Information Analytics

Proceedings of the 2020 International  
Conference on Multi-model Information  
Analytics (MMIA2020), Volume 2

 Springer

*Editors*

Vijayan Sugumaran  
Department of Decision and Information  
Sciences, and Center for Data Science  
and Big Data Analytics  
Oakland University, School of Business  
Administration  
Rochester, MI, USA

Zheng Xu  
Shanghai University of Medicine  
and Health Sciences  
Shanghai, China

Huiyu Zhou  
Department of Informatics  
University of Leicester  
Leicester, UK

ISSN 2194-5357                      ISSN 2194-5365 (electronic)  
Advances in Intelligent Systems and Computing  
ISBN 978-3-030-51555-3              ISBN 978-3-030-51556-0 (eBook)  
<https://doi.org/10.1007/978-3-030-51556-0>

© Springer Nature Switzerland AG 2021

This work is subject to copyright. All rights are reserved by the Publisher, whether the whole or part of the material is concerned, specifically the rights of translation, reprinting, reuse of illustrations, recitation, broadcasting, reproduction on microfilms or in any other physical way, and transmission or information storage and retrieval, electronic adaptation, computer software, or by similar or dissimilar methodology now known or hereafter developed.

The use of general descriptive names, registered names, trademarks, service marks, etc. in this publication does not imply, even in the absence of a specific statement, that such names are exempt from the relevant protective laws and regulations and therefore free for general use.

The publisher, the authors and the editors are safe to assume that the advice and information in this book are believed to be true and accurate at the date of publication. Neither the publisher nor the authors or the editors give a warranty, express or implied, with respect to the material contained herein or for any errors or omissions that may have been made. The publisher remains neutral with regard to jurisdictional claims in published maps and institutional affiliations.

This Springer imprint is published by the registered company Springer Nature Switzerland AG  
The registered company address is: Gewerbestrasse 11, 6330 Cham, Switzerland

# Contents

<b>Part I: Multi-modal Informatics in Industrial, Robot, and Smart City</b>	
<b>Noise Data Removal Method of Frequency Response Curve Based on MNKriging Interpolation Algorithm . . . . .</b>	<b>3</b>
Ling Wei, Zijuan Guo, Shaolei Zhai, Cong Qi, En Wang, Tao Deng, Wenhua Chen, and Bing Lu	
<b>An Analysis Method of Multi Round Interactive Semantics for Power Enterprises Based on Solr Engine . . . . .</b>	<b>11</b>
Zheheng Liang, Jijun Zeng, Daohuan Jiang, and Gongfeng Zhu	
<b>Simplification Method of Two-Level Stroke Line Based on Painting Sequence . . . . .</b>	<b>17</b>
Yu Lin	
<b>Typical Risk Situations in Driving Situations . . . . .</b>	<b>24</b>
Yulei Liu	
<b>Construction of Smart Campus Under the Background of Big Data . . .</b>	<b>32</b>
Peilu Feng	
<b>Mass Fashion Life Service Space in Intelligent Cities . . . . .</b>	<b>37</b>
Hesen Li	
<b>Development Background of China’s Energy Internet Industry and Experiences . . . . .</b>	<b>43</b>
Shanshan Wu, Xingpei Ji, Qingkun Tan, and Rui Tang	
<b>Probe on Curriculum Design of Electronic Circuit Based on Multisim14.0 . . . . .</b>	<b>49</b>
Guangjun Yuan, Jiyuan Sun, Zhenjun Lei, and Yang Lu	
<b>Coupling Dynamics of Complex Electromechanical System . . . . .</b>	<b>56</b>
Zhouhong He and Xiaowen Liao	

<b>Development Strategy of Educational Robot Industry Based on Big Data Analysis</b> .....	62
Jingqiu Yang and Yiquan Shi	
<b>Selection of Urban Rail Transit Connection Mode Under Nested Logit Model</b> .....	69
Tao Liu	
<b>Design Method of Aerobics Teaching Assistant Platform Based on 5G Technology</b> .....	75
Qiong Huang and Fubin Wang	
<b>Transformation and Upgrading of Manufacturing Industry Under the Background of the Digital Economy</b> .....	82
Haiyan Jiang and Xuhui Chen	
<b>Effect of Heat Treatment on Microstructure and Properties of Wear-Resistant Cast Steel with High Strength and Toughness</b> .....	88
Haijun Cui, Bo Zhang, and Meng Wang	
<b>Computer Aided Design and Manufacture of Pen Holder for Complex Mechanical Parts</b> .....	95
Zhanbin Gu	
<b>The Design and Implementation of Seismic Hazard Emergency Assessment System of Dongguan</b> .....	101
Ping He, Xiuwu Chen, and Ting He	
<b>Role of Robot Technique in the Manufacture of New Energy Vehicle Engineering</b> .....	108
Juan Shao	
<b>Intelligent Vibration Control Method of Wire Rope Lifting Equipment</b> .....	114
Ye Tian	
<b>Development Path of Energy Internet Industry for Grid Enterprises Based on the Industrial Development Priority Model</b> .....	123
Shanshan Wu and Rui Tang	
<b>Application of PLC Technology in Electrical Engineering and Automation Control</b> .....	131
Meng Wang	
<b>Development of Multifunctional Calculator Based on MCU (Microcontroller Unit)</b> .....	136
Qinzhu Wang	
<b>Innovative Path of IAP Education in Colleges and Universities Under the Background of “Smart Campus”</b> .....	143
Shengli Wang	

**Autonomous Vehicle Control System Based on Mecanum Wheel** . . . . . 149  
 Yanchun Cheng, Yu Liu, Rundong Wang, Yong Liu, and Rui Zhou

**Analysis and System Construction of Information-Based Engineering Management Theory** . . . . . 157  
 Jieyun Yang

**Device for Super Capacitor Constant Power Charging** . . . . . 163  
 Shun Wang and Yixian Chen

**Robust Optimization Model of Island Energy System Based on Uncertainty of Wind and Photovoltaic** . . . . . 171  
 Zhihong Gu, Huiwen Qi, Zhuo Liu, and Rong Zhang

**Exploration and Research on Project Engineering Management Mode Based on BIM** . . . . . 180  
 Dongfeng Li

**Building Optimization Based on Wind Environment Simulation Analysis** . . . . . 185  
 Zhuo Wei, Ningning Xie, and Zhe Jiao

**Feasibility Study of Zero Trust Security in the Power Industry** . . . . . 195  
 Fei Hu, Wei Liu, Danni Wang, and Ran Ran

**Construction of Digital Factory Platform Based on Intelligent Manufacturing** . . . . . 205  
 Ying Kou, Longfei Zhang, and Liang Zhou

**Application of Internet of Things in the Construction of Smart City** . . . 212  
 Ge Guo and Liang Pang

**Adaptive Modeling Algorithm in Distributed Aircraft Intelligent Control System** . . . . . 218  
 Zhang Jinhe, Sun Shujian, Hong Tao, and Du Bin

**Adaptive Control of Wind Power System Based on TMS320** . . . . . 224  
 Zenghui Guo

**The Zynq-7000 SoC on UltraScale Architecture** . . . . . 231  
 Zhiwei Tang

**VHDL Design of Motor Control Module on FPGA** . . . . . 237  
 Zhiwei Tang and Xiaoqing Chen

**Part II: CV Process and Data Mining for Multi-modal Informatics Systems**

**Survey of Computer Vision Synchronous Positioning and Map Construction Technology** . . . . . 249  
 Hong Zhang, Ping Yang, Hongjiao Xue, and Shixia Lv



<b>Application of Conditional Generative Adversarial Network in Image Super-Resolution Reconstruction</b> . . . . .	256
Xiang Wei, Feng Wang, Xi Chen, Yongjie Yan, Ping Chen, and Sheng Liu	
<b>Automatic Visual Inspection System for Injection Molding Parts of Automobile Center Console</b> . . . . .	266
Wenqing Chi, Bin Xue, Xiaofei Li, Yuhang Zhang, and Shuangben Jiao	
<b>Efficient Clustering Algorithm in Dynamic Nearest Neighbor Selection Model</b> . . . . .	274
Jingxin An	
<b>Marketing Strategy of Knowledge-Based Virtual Community</b> . . . . .	280
Zhi Li	
<b>Two-Way Recommendation System for Intelligent Employment of College Students Based on Data Mining</b> . . . . .	286
Yifan Zhang, Qian Liu, and Qingpeng Meng	
<b>Investigation on Knowledge Reduction and Rule Fusion Based on Probability Graph Model</b> . . . . .	293
Yun Duan, Hongbo Ouyang, and Sheng Duan	
<b>Relation Model Between High-Level Athletes' Energy Consumption Mode and Physical Function</b> . . . . .	299
Zhenjun Xu and Weidong Hu	
<b>Face Alignment by Coarse-to-Fine Deep Convolution Network on Mobile Device</b> . . . . .	306
Huaping Liu	
<b>Process Design and Computer Software Simulation of Complex Parts Pen Barrel</b> . . . . .	313
Xiurong Zhu	
<b>Application of CAD Combined with Computer Image Processing Technology in Mechanical Drawing</b> . . . . .	319
Ning Fan	
<b>Scene Merging Technology with High Adaptability</b> . . . . .	325
Jiuchao Li, Liang Zhou, and Ou Qi	
<b>The Relation of Self-efficacy and Well-Being of Primary Managers: The Mediating Role of Hope</b> . . . . .	331
Jun Luo and Yulan Yu	
<b>Image Feature Matching Before Image Fusion</b> . . . . .	336
Dingyun Jin, Ou Qi, and Xiaoyan Gao	
<b>The Role of Drone Photography in City Mapping</b> . . . . .	343
Shiheng Zhao	

**A Cognitive Analysis of Conceptual Metaphors of Color Idioms in English and Chinese Based on Data Mining** . . . . . 349  
 Shiqing Zhou

**Bibliometric Analysis of Benchmarking Literatures at Home and Abroad on the Basis of CNKI Database** . . . . . 356  
 Cheng Wang and Huifan Luo

**Distributed Image Fire Detection and Alarm System Based on Machine Learning** . . . . . 362  
 Yang Du and Yufeng Fan

**Combination of Pre-processing Techniques to Improve the Performance of Target Recognition in SAR Imagery** . . . . . 372  
 Pengju Zhao

**College English Teaching and Testing Based on Data Mining** . . . . . 383  
 Bing Xu

**Information Management Mechanism of Informationization Under Cluster Analysis Algorithm** . . . . . 388  
 Bo Hu, Yangchun Yuan, Yongcai Wang, and Hancong Huangfu

**Development and Application of Video Monitoring System for Poles Based on Ubiquitous Internet of Things Technology** . . . . . 395  
 Hongli Liu, Nan Li, Ye Zhao, Liyun Zhang, and Xuetao Zhou

**Talent Demand Analysis of LIS Based on Python and Apriori** . . . . . 402  
 Xinyu Wu

**Design of Management Learning System Based on SVM Algorithm** . . . . . 409  
 Guo Xiaozhou

**The Application of Improved Genetic Algorithm and Least Square Method in Computer Mathematical Modeling** . . . . . 415  
 Nana Chen and Zhongyu Bai

**Research on Properties of Pore Fissures Based on the CART Algorithm** . . . . . 419  
 Dawei Dai and Ling Zhang

**Recognition Algorithm for Emotion of Japanese Feminine Terms Based on Generalized Semantic Analysis** . . . . . 426  
 Xiaoyu Ge and Chang Liu

**Optimizing Design of College Teaching Based on C4.5 Algorithm** . . . . . 433  
 Gong Sha

**Application of SVM Algorithm in Teaching Process Evaluation** . . . . . 438  
 Guo Jianliang

<b>Design of Enterprise Human Resource Management System Based on Oracle Data Mining Technology</b> .....	444
Qian Liangliang and Yuwei Wang	
<b>Research on Image Feature Processing Based on FPGA</b> .....	450
YuXin Cai, ZhiGuo Yan, Jia Yang, and Bo Zhao	
<b>Design and Application Research of Targeted Persons Control System Based on Big Data</b> .....	459
Jinbo Wu and San-you Zhang	
<b>Part III: Agent-Based and Multi-agent Systems for Health and Education Informatics</b>	
<b>An Innovative Teaching Mode Based on Programming Contest</b> .....	469
Yongjun Luo and Hong Zheng	
<b>The Design of Comprehensive Quality Evaluation System Under the Reform of China's College Entrance Examination</b> .....	478
Xianglin Zhang and Xiaolin Ge	
<b>Efficient Teaching Management Based on Information Technology</b> .....	486
Cuijuan Wei	
<b>Discussion of the Higher Vocational English Teaching in the Informatization Digital Network</b> .....	493
Guolan Yang	
<b>The Construction of Intelligent Classroom System Based on CC2530</b> .....	501
Yue Yang and Dewei Kong	
<b>Development Method of Japanese Translation Teaching Assistant Platform Based on Information Technology</b> .....	508
Xiaoxu Xu	
<b>Thinking and Exploration of Teaching Management in Colleges and Universities Based on Network Information Technology Such as MOOC</b> .....	514
Xin Sui	
<b>Computer Multimedia Technology in the Construction of Classroom Atmosphere in College Ideological and Political Education</b> .....	519
Guoyong Liu	
<b>Application of Speech Recognition Technology in Pronunciation Correction of College Oral English Teaching</b> .....	525
Caiyun Liu	

**Construction of Evaluation-Index System of College Teachers’ Intelligent Teaching Ability Under the Background of Educational Informationization 2.0** . . . . . 531  
 Dongyan Sun

**Construction of the Practical Base of Information Sharing Courses Based on Finance** . . . . . 538  
 Chengwei Zhang and Xinyan Li

**The Application of MOOC in College Students’ Mental Health Teaching** . . . . . 546  
 Fei Wang

**Plan of Physical Education Teaching Platform Based on Campus Network Technology** . . . . . 552  
 Juan Yi and Jie Huang

**Development of Teaching Software for Power Electronic Technology Course** . . . . . 559  
 Hengjuan Liu

**Practice of University Curriculum Construction Under the Background of Informationization** . . . . . 566  
 Wei Cong and Jing Liu

**Course Construction Process of MOOC** . . . . . 573  
 Wei Cong, Hongkun Yu, and Jing Liu

**MOOCs and Developing College English Teaching** . . . . . 579  
 Luqi Li

**Influence of Media Technology on the Development of Contemporary Children’s Literature** . . . . . 585  
 Mingxiu Ding

**Reform and Thoughts of Learning-Centered Classroom Teaching Based on the Cloud Space of World University City** . . . . . 592  
 Jinliang Wang and Xuefeng Xie

**Challenges and Countermeasures of Family Education in the Information Age** . . . . . 598  
 Chaoxi Qian

**New Age MOOCS Teaching in Music Class of College** . . . . . 605  
 Guofeng Liu

**Construction of Behavior-Oriented Smart Teaching Model in Mobile New Media Environment-Take the Course “NC Machine Tool Programming and Operation” as an Example** . . . . . 611  
 Lei Shi

**Innovation and Practice of “1 + N” Compound Design Talents Training Model in Computer Networks: A Case Study of New Higher Education Group Co-founded Undergraduate Program** ..... 617  
 Yuanyuan Li

**College Hotel Management Teaching Mode Based on Computer Information** ..... 624  
 Yuerong Wang

**Design of Calligraphy Online Course in Primary and Secondary Schools Based on K-Means Algorithm** ..... 630  
 Ouyang Xuxia

**Factors Restricting the Quality of Equipment Support** ..... 636  
 Ou Qi, Xiaoyan Gao, Lei Zhang, and Wenhua Shi

**Present Situation, Problems and Countermeasures of China’s Information Industry** ..... 641  
 Qiang Ping

**Application of Information Technology in the Teaching of Art Design Courses** ..... 646  
 Qunying Li

**Sentiment Analysis of Painting Based on Deep Learning** ..... 651  
 Yu Lin

**Informatization of English Teaching and Its Practical Path** ..... 656  
 Yongxin Li

**A Comparative Analysis of Traditional Test of College Oral English and Computer-Based Oral English Test** ..... 662  
 Xuejing Wu

**Customer Satisfaction Evaluation of Airline Based on PLS\_SEM** ..... 667  
 Huali Cai, Xuemei Wei, Yanjun Gu, and Fang Wu

**Image Projection Space Invariant Technology** ..... 672  
 Yibo Wang, Ou Qi, and Xiaoyan Gao

**Secure Network Coding Technology** ..... 677  
 Zhiwei Jin

**A Brief Analysis of the Investigation and Electronic Information Experiment Teaching in Higher Vocational Colleges** ..... 682  
 Jiao Xue, Wei Sai, Feifei Gao, and Guiling Fan

**An Algorithm for Predicting the Optimal Path of Forehand Hitting Long Ball in the Backcourt** ..... 687  
 Ning Zhang and Feng Dong

**Feature Extraction of Basketball Shooting Based on Apriori Algorithm** . . . . . 692  
Wei Zou and Zhixiang Jin

**Innovative Design of Mouse Based on Cloud Computing** . . . . . 697  
Chen Jinxia

**Teaching of Secretary Based on Mobile Phone Teaching Software Application** . . . . . 703  
Yang Jie and Yang Jing

**Design of Teaching System of College Students Based on KNN Algorithm** . . . . . 708  
Hao Yifeng

**Fault Diagnosis System of New Energy Vehicle Based on Hidden Markov Model** . . . . . 713  
Li Taotao

**Evaluation of Tourism Landscape Ecological Environment Based on AHP and Fuzzy Mathematics** . . . . . 719  
Cao Peng and Cui Jing

**Collection and Processing Method of Big Data of Network Public Opinion** . . . . . 724  
Chen Feng, Zhang Dali, and Fu Xianjun

**Internet Finance Innovation and Entrepreneurship Based on Classification Algorithm** . . . . . 729  
Guo Honglei

**Research on Embedded Technology in Industrial Control Networking** . . . . . 734  
Hong Yaoqiu

**Application of Vision Guarding Technique in Intelligent Grasp of Industrial Robot** . . . . . 739  
Lingyan Kong

**K-Means Algorithm in Classical Landscape Design Thought and Modern Landscape Design** . . . . . 745  
Guorui Li

**Optimization Design of Refrigerator Turnover Beam Based on CAE Simulation Technology** . . . . . 751  
Li Qiuli, Li Yan, Zhao Yonghao, Li Hailin, and Luo Hui

**Design College Scores Test System Based on C4.5 Algorithm** . . . . . 756  
Li Tian

**Design of Agricultural Precision Irrigation System Based on Wireless Sensor Network (WSN)** . . . . . 761  
Wensen Lin

**Network Security Situation Awareness Strategy Based on Markov Game Model** . . . . . 766  
Chengfei Lu

**Design of Class Management System Based on Naive Bayes Algorithm** . . . . . 772  
Mao Xu and Haiyan Huang

**Hybrid Development of Teaching and Reading Online Course Based on FA Algorithm** . . . . . 778  
Luo Xiaoli and Liu Wenjun

**Analysis of Rural Tourism Based on C4.5** . . . . . 783  
Meng Na and Li Yan

**Design of Flexible DC Distribution Control System** . . . . . 788  
Xuntao Shi, Qingpai Ke, Hao Bai, Min Xu, Quan Xu, Zhiyong Yuan, and Jinyong Lei

**3D Modeling Technology in 3D Film and Television Animation Production** . . . . . 793  
Sun Wen

**Construction of Real Estate Featured Price Model Based on Massive Transaction Data** . . . . . 798  
Tian Shan

**Enterprise Strategy Management Online Learning with CART Algorithm: Taking an Empirical Analysis of Turnover Management Based on Gray Correlation Model as an Example** . . . . . 803  
Yuwei Wang and Liangliang Qian

**Deep Learning Strategies in Media Teaching System Based on ADABOOST Algorithm** . . . . . 809  
Wang Chang Jiang

**College Online Learning System Based on NLP Algorithm** . . . . . 815  
Xiao Caifeng

**Design and Implementation of Music Online Network Course Based on Cloud Computing** . . . . . 820  
Xuenan Yang

**Conceptual Cognition and Visual Design of Cloud Computing Products** . . . . . 826  
Zhang Jing

**The Application Status and Integration Strategies of Digital Learning Apps for College Students** . . . . . 832  
Jianwu He

**Computer Aided Design of Modern Decorative Pattern** . . . . . 838  
Zhong Jiao

**The Computer-Aided Design of Miao Costume Patterns Based on Big Data** . . . . . 844  
Gao Tao

**Portable Article Management System Based on Wireless Sensing Technology** . . . . . 850  
Bo Zhao, Zhiguo Yan, Jia Yang, and Cheng Cheng

**Author Index** . . . . . 855





# Optimization Design of Refrigerator Turnover Beam Based on CAE Simulation Technology

Li Qiuli<sup>1</sup>, Li Yan<sup>2</sup>, Zhao Yonghao<sup>1(✉)</sup>, Li Hailin<sup>1</sup>, and Luo Hui<sup>1</sup>

<sup>1</sup> School of Mechanical and Electrical Engineering, Guangzhou City Construction College, Guangzhou 510925, Guangdong, China  
enjoily@126.com, xiaolin1600@tom.com,  
935748819@qq.com, yanyan9823@163.com

<sup>2</sup> School of Business, Beijing Institute of Technology, Zhuhai, Zhuhai 519088, Guangdong, China  
aya-z@tom.com

**Abstract.** In the current design of refrigerator turnover beam, it mainly depends on the experience of structural engineers. The overturned beam often has problems such as bending, large assembly gap, large overturning resistance and condensation. The mold needs to be changed repeatedly, extending the product design cycle and increasing the verification cost. It will also bring market complaints and increase the cost of after-sales maintenance. Through the CAE simulation technology, the structure simulation analysis, thermal stress simulation analysis and rotation simulation analysis of the refrigerator turnover beam are carried out, and the targeted optimization design of the refrigerator turnover beam can shorten the design cycle, reduce the design defects of the refrigerator turnover beam, and improve the reliability of the refrigerator turnover beam.

**Keywords:** Refrigerator · Turnover beam · CAE · Structure simulation · Thermal stress simulation · Rotation simulation · Optimization design

## 1 Introduction

At present, the turnover beam of refrigerator is mainly designed according to the experience of structural engineer. The turnover beam designed often has problems such as bending of the turnover beam, large assembly gap, large turnover resistance, inadequate turnover, condensation of the turnover beam, etc. it needs to be repeatedly verified and changed the mold, which prolongs the product design cycle and increases the product development cost. With the increasing sales volume of large volume door-to-door refrigerators, as a key component of door-to-door refrigerators, it is particularly important to improve the design reliability of the flip beam of refrigerators and shorten the design verification cycle of the flip beam. CAE simulation analysis technology is more and more widely used in the field of home appliances, and the technology is becoming more and more mature. CAE technology is used to simulate and analyze the turnover beam of refrigerator. According to the simulation results, the rationality of the structure of the turnover beam is evaluated in advance. The optimization design of the

turnover beam can greatly shorten the design cycle of the turnover beam of refrigerator and the verification cycle of opening mold, and improve the reliability of the design of the turnover beam. 2 Technical flow chart (Fig. 1).

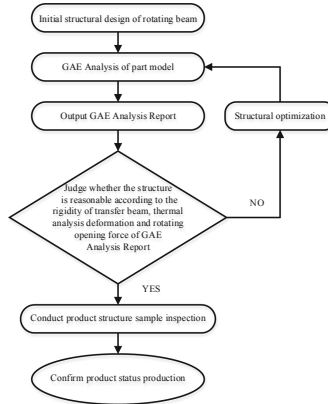


Fig. 1. Technical flow chart

## 2 Structure Simulation

The two ends of the overturned beam are constrained, and the virtual load is applied in the middle to analyze. The results are shown in Figs. 2 and 3.



Fig. 2. Simulated stress cloud chart of turnover beam structure



Fig. 3. Simulation deformation cloud chart of turnover beam structure

### 3 Thermal Stress Simulation

According to the actual use environment of the rotating beam, different temperatures are applied to the inner and outer sides of the rotating beam, and the bending amount of the rotating beam caused by the temperature difference between the two sides of the rotating beam is simulated. The simulation results are shown in Fig. 4 below.



Fig. 4. Cloud chart of thermal stress simulation deformation of turnover beam

### 4 Rotation Simulation

According to the actual use of the turnover beam, the movement process of the rotating beam during the opening and closing of the door is simulated and analyzed, the model is simplified, the contact, constraint and rotation displacement are applied, and the stress nephogram during the opening of the door is shown in Fig. 5 below, and the curve of the opening force with the opening angle during the opening of the door is shown in Fig. 6 below.



Fig. 5. Simulated stress cloud chart of turning beam

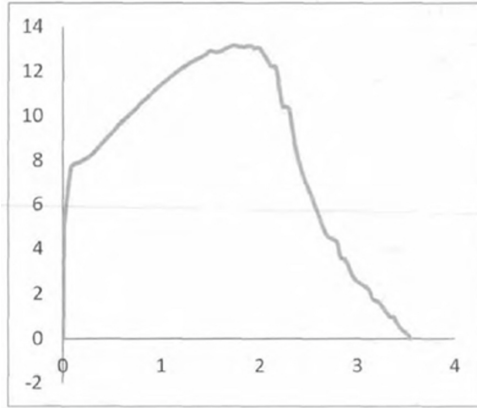


**Fig. 6.** Change curve of simulation door opening force of turning beam

## 5 Structural Optimization

Combined with the structural analysis and thermal stress analysis of the deformation and stress-strain distribution, the structural strength of the rotating beam is improved by optimizing the structure of the notch, increasing the stiffener, increasing the flanging height of the sheet metal, etc., the influence of the residual stress and the shrinkage stress is reduced by optimizing the assembly clearance, optimizing the position of the limit block of the rotating beam, etc., and the change curve of the opening force and the The change of stress and strain in the process of opening the door, optimize the structure of the rotary beam cam, the setting of the spring and the setting of the pulling block. Carry out structural simulation analysis, thermal stress analysis and rotation simulation analysis for the optimized turnover beam again, and get the structural simulation deformation cloud diagram as shown in Fig. 7, the thermal stress simulation analysis deformation cloud diagram as shown in Fig. 8, and the rotation simulation door opening force angle curve of the turnover beam as shown in Fig. 9.

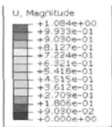


**Fig. 7.** Simulation deformation cloud chart of the optimized turnover beam structure

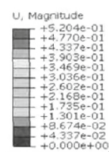


**Fig. 8.** Simulated deformation cloud chart of thermal stress of optimized turnover beam

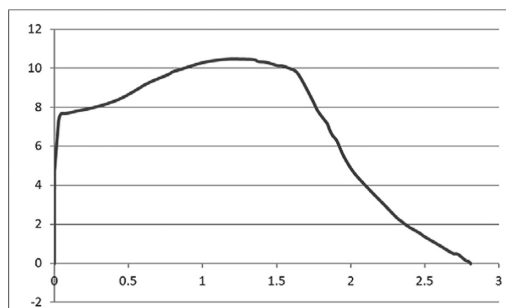


**Fig. 9.** Change curve of opening force with opening angle after optimization of turnover beam

## 6 Result Processing and Analysis

The comparison of simulation data before and after optimization is shown in Table 1. According to the simulation analysis results, the strength of the optimized overturned beam structure is greatly improved, the bending deformation is greatly reduced, and the opening force is also greatly reduced. It can meet the use requirements.

## 7 Conclusion

It can be seen from the simulation and test data that the bending degree of the optimized turning beam is reduced by 53.4% compared with the original turning beam. Under the premise of ensuring the self-locking force and turning force of the rotating beam, the opening force is reduced by 20.5%. The error between simulation results and test results is about 8%, which is acceptable. Under the guidance of CAE simulation analysis results, targeted optimization of the turnover beam structure greatly improves the structural performance and use experience of the turnover beam, shortens the development and verification cycle, improves the design and development efficiency, and ensures the reliability of the turnover beam structure.

## References

- Lei, C., Daihua, W.: Finite element analysis and Simulation of a high axial stiffness triaxial rotating flexible hinge. *Mech. Des.* (1) (2009)
- Guangping, F., Weixiang, Z., Longchun, H.: Optimization of refrigerator product structure and external packaging scheme based on CAE. *Packag. Eng.* (5) (2003)
- Hongjun, W., Jianwei, D., Qiang, S.: Calculation of moment of inertia and moment of inertia by finite element method. *Shijiazhuang Railw. J. Polytech.* (2006)
- Nianjie, W., Yu, L., Lang, G, Ling, P.: Xiangdong refrigerator structure system based on UG secondary development is fast Design. *Mech. Des. Manuf. Eng.* (11) (2013)

# 基于 CAE 仿真技术的冰箱翻转梁优化设计

李秋力 李彦 赵永豪 李海林 罗辉

(广州城建职业学院, 广东广州 510925)

**摘要:** 在目前的冰箱翻转梁设计中, 主要依靠结构工程师的经验。翻转梁经常出现弯曲、装配缝隙大、翻转阻力大、凝露等问题。需要反复更改模具, 延长了产品设计周期, 增加了验证成本。也会带来市场投诉, 造成售后维护成本的提高。通过 CAE 仿真技术对冰箱翻转梁进行结构仿真分析、热应力仿真分析、转动仿真分析, 有针对性的对冰箱翻转梁进行优化设计, 可以缩短设计周期, 减少冰箱翻转梁设计缺陷, 提高冰箱翻转梁的可靠性。

**关键词:** 冰箱; 翻转梁; CAE; 结构仿真; 热应力仿真; 转动仿真; 优化设计

## 1 引言

目前的冰箱翻转梁主要是依据结构工程师的经验进行设计, 设计出的翻转梁经常出现转梁弯曲、装配缝隙大、翻转阻力大、翻转不到位、转梁凝露等问题, 需要反复验证、更改模具, 延长了产品设计周期, 增加了产品开发成本。随着大容积对开门冰箱的销量越来越大, 作为对开门冰箱的关键零部件, 提高冰箱翻转梁的设计可靠性、缩短翻转梁的设计验证周期显得尤为重要。

CAE 仿真分析技术在家电领域的应用越来越广泛, 技术也日趋成熟。利用 CAE 技术对冰箱翻转梁进行仿真分析, 根据仿真分析结果提前评估翻转梁结构的合理性, 有针对性的对翻转梁进行优化设计, 可以极大地缩短冰箱翻转梁的设计周期及开模验证周期, 提高翻转梁设计的可靠性。

## 2 产品设计优化流程

如图 1 所示, 优化流程采用闭环形式, 通过 CAE 仿真模拟, 分析结构缺陷, 优化设计后, 重新进行 CAE 分析, 进行验证, 通过循环递进分析验证, 获得合理结构。

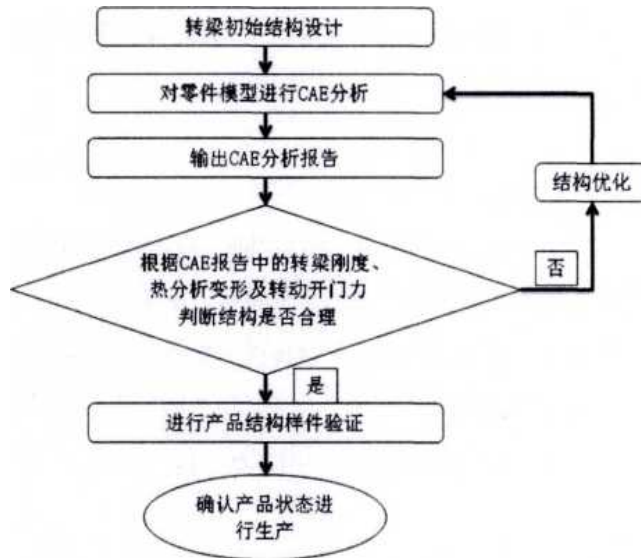


图 1 技术流程图

### 3 结构仿真

翻转梁两端约束，中间施加虚拟载荷进行分析得到结果，如下图 2、图 3 所示。



图 2 翻转梁结构仿真应力云图

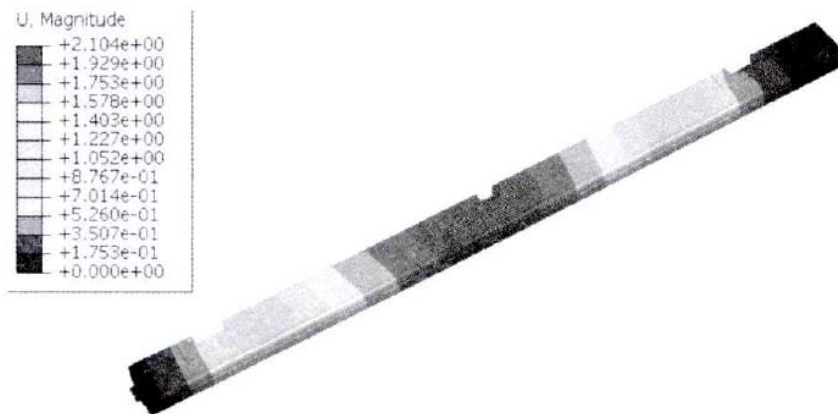


图 3 翻转梁结构仿真变形云图

## 4 热应力仿真

根据转梁实际使用环境，给转梁内、外两侧分别施加不同的温度，仿真翻转梁两面的温度差造成的翻转梁弯曲量，得到仿真结果如图 4 所示。

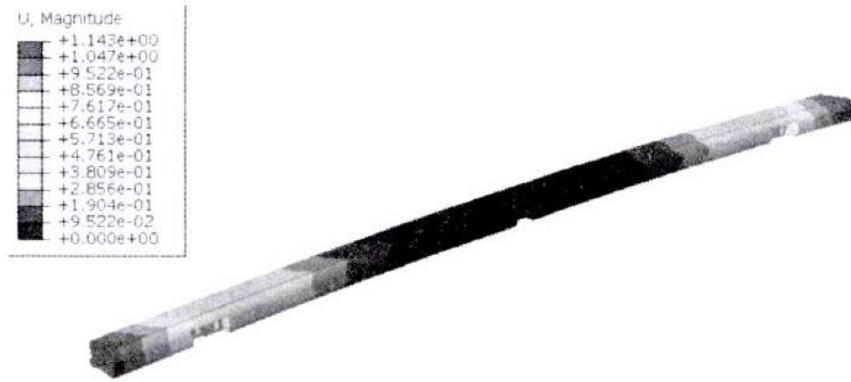


图 4 翻转梁热应力仿真变形云图

## 5 转动仿真

根据翻转梁实际使用情况，仿真分析转梁在开门和关门时的运动过程，简化模型，施加接触、约束、转动位移，得到开门过程中的应力云图如图 5 所示，

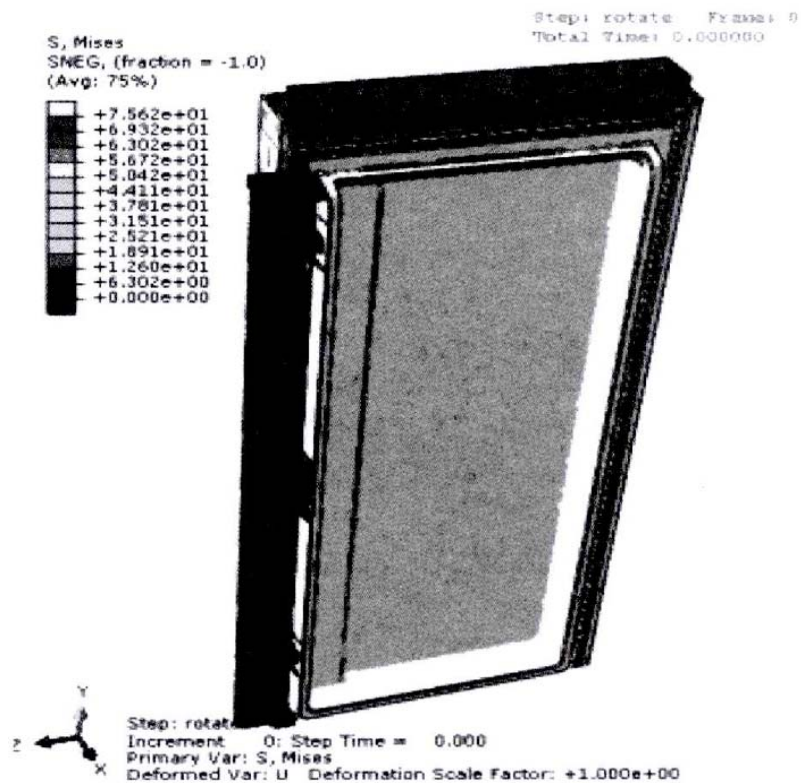


图 5 翻转梁转动仿真应力云图



开门过程中的开门力随开门角度的变化曲线如图 6 所示。

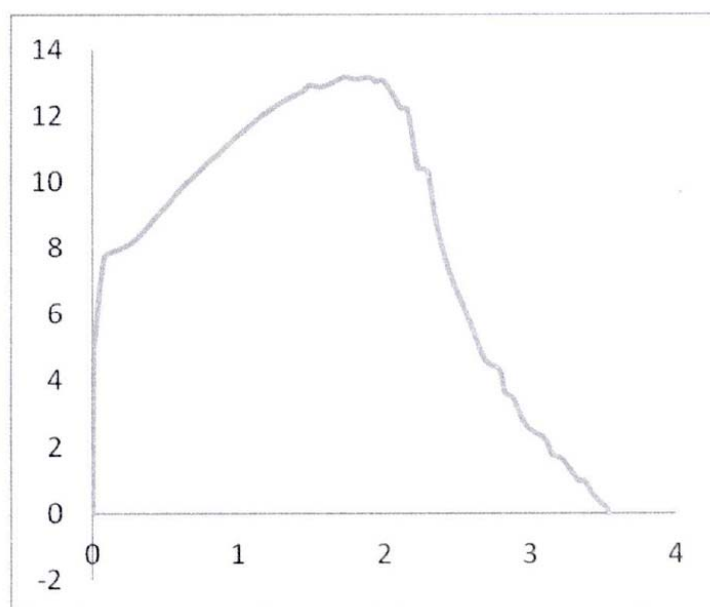


图 6 翻转梁转动仿真开门力变化曲线

## 6 结构优化

结合结构分析和热应力分析变形量及应力应变分布情况,通过优化缺口处结构、增加加强筋、增加钣金翻边高度等方案提高转梁结构强度,通过优化设计装配间隙、优化转梁限位块位置等方案削弱残余应力及收缩应力的影响,结合转动仿真分析的开门力变化曲线及开门过程中的应力应变变化情况,优化转梁凸轮结构、优化 弹簧设置、优化拨动块设置。对优化后的翻转梁再次进行结构仿真分析、热应力分析、转动仿真分析,得到结构仿真变形云图如图 7 所示。热应力仿

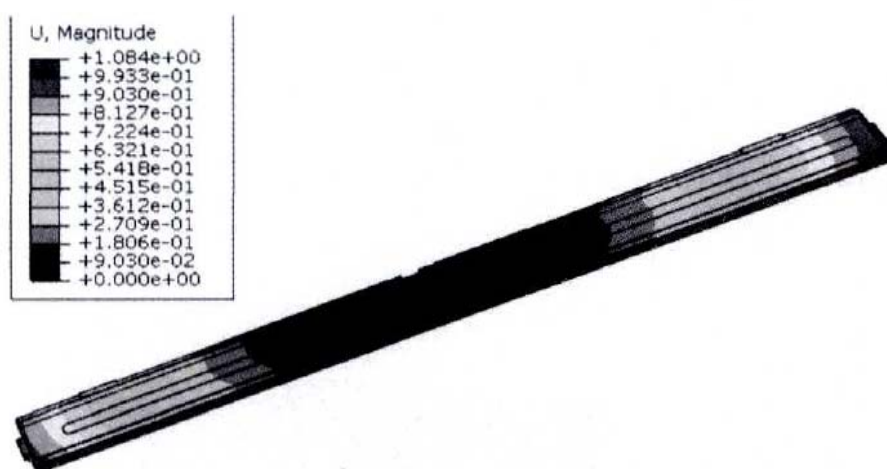


图 7 优化后翻转梁结构仿真变形云图

真分析变形云图，如图 8 所示，翻转梁转动仿真开门力-角度曲线如图 9 所示。

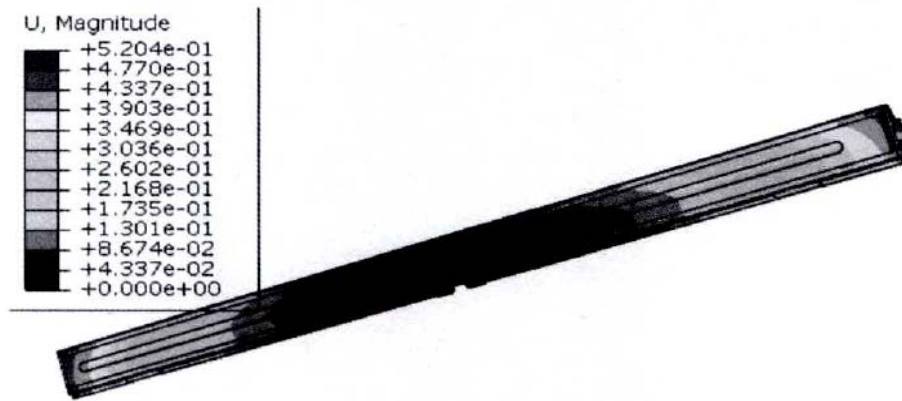


图 8 优化后翻转梁热应力仿真变形云图

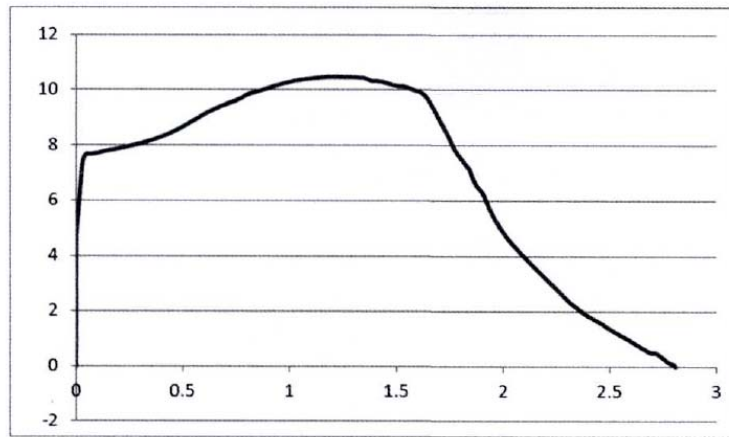


图 9 优化后翻转梁转动仿真开门力变化曲线

## 7 结果处理分析

优化前后仿真数据对比如表 1 所示。

表 1 翻转梁优化前后仿真数据对比

	结构分析变形	对比	热分析变形	对比	转动仿真开门力	对比
原翻转梁	2.1		1.14		13.17	
优化后翻转梁	1.084	降低 48.7%	0.5204	降低 54.4 %	10.47	降低 20.5%

根据仿真分析结果，优化后的翻转梁结构强度比原 翻转梁有了较大幅度的提高，弯曲变形有较大幅度的降低，开门力也有较大幅度的降低，可以满足使用需求。

## 8 结论

由仿真对比数据和测试对比数据可见，优化设计后的翻转梁弯曲度与原转梁

相比减小了 53.4%。在保证转 梁自锁力及翻转力的前提下,开门力降低 20.5%。

通过试验验证,仿真计算结果与试验结果误差在 8%左右,在可接受范围内。在 CAE 仿真分析结果的指导下,有针对性的优化翻转梁结构,大幅提高了翻转梁的结构性能及使用体验, 缩短了开发验证周期,提升了设计研发效率,保证了翻转梁结构的可靠性。

#### 参考文献:

- [1]程磊,王代华.一种高轴向刚度三轴转动柔性铰的有限元分析与模拟[J].机械设计.2017(011)
- [2]冯广平 张伟祥.黄龙春.基于CAE的冰箱产品结构与外包装方案优化[J].包装工程,2018(05)
- [3]王洪军.董建伟,朱强.有限元法计算惯性矩及转动惯量[J].石家庄铁路职业技术学院学报,2016(01)
- [4]汪年结 刘宇 高浪,彭玲 向东基于UG二次开发的冰箱结构系统快速设计[J].机械设计与制造工程,2017(11)



1.

**Accession number:** 20194107524766**Title:** Positioning and grabbing technology of industrial robot based on vision**Authors:** Zhao, Yonghao<sup>1</sup>; Li, Hailin<sup>1</sup>**Author affiliation:** <sup>1</sup> Guangzhou City Construction College, Guangdong Guangzhou, 510900, China**Corresponding author:** Zhao, Yonghao (zhaoyonghaoest1@yeah.net)**Source title:** Academic Journal of Manufacturing Engineering**Abbreviated source title:** Acad. J. Manuf. Eng.**Volume:** 17**Issue:** 3**Issue date:** 2019**Publication year:** 2019**Pages:** 137-145**Language:** English**ISSN:** 15837904**Document type:** Journal article (JA)**Publisher:** Editura Politehnica

**Abstract:** In order to explore the role of machine vision technology in the positioning and grabbing of industrial robots, the application of machine vision image extraction technology in industrial robot positioning and grabbing was studied through experiments and analysis methods. The Gaussian filtering method was mainly used to smooth the image. On this basis, the edge extraction of the target object image was performed by Canny operator edge detection. The robot arm grab point was determined by binocular three-dimensional positioning coordinates, and then the PID (Proportion Integral Differential) position algorithm was used to analyze the dynamic positioning control of the robot. The results showed that the vision-based industrial robot positioning and grabbing technology can improve the recognition efficiency and grasping efficiency of industrial robots, which is superior to the traditional industrial robot positioning and grabbing function. In summary, the introduction of machine vision functions into industrial robot systems and for industrial production can improve the automation, intelligence and efficiency of industrial production, and has good industrial practical use value.  
© 2019 Editura Politehnica. All rights reserved.

**Number of references:** 13**Main heading:** Computer vision**Controlled terms:** Edge detection - Efficiency - Extraction - Industrial robots - Intelligent robots - Proportional control systems - Vision**Uncontrolled terms:** Gaussian filtering methods - Image extraction - Industrial production - Machine vision technologies - Positioning and Grabbing - Recognition efficiency - Robot positioning - Three-dimensional positioning**Classification code:** 723.5 Computer Applications - 731.1 Control Systems - 731.6 Robot Applications - 802.3 Chemical Operations - 913.1 Production Engineering**Database:** Compendex

Compilation and indexing terms, © 2019 Elsevier Inc.

# **ACADEMIC JOURNAL OF MANUFACTURING ENGINEERING**

**VOLUME 17, ISSUE 3**

**Executive Editor:**  
Adrian TRIF

**Desktop publishing:**

Marinela Ința

**Distribution & Publicity:**  
Felicia Veronica Banciu

**ISSN: 1583-7904**



**EDITURA POLITEHNICA**

MANUFACTURING TECHNOLOGY AND MECHANICAL PROPERTIES OF MODIFIED RECYCLED AGGREGATE CONCRETE Yonggui WANG, Haicheng NIU, Yuhui FAN.....	101
MATHEMATICAL REGRESSION MODEL OF UNIDIRECTIONAL GLASS FIBRE REINFORCED POLYMER COMPOSITES Emilia SABAU, Adrian POPESCU, Cristina-Ştefana MIRON-BORZAN, Nicolae PANC.....	108
MODIFICATION DESIGN WITH MINIMAL ROTARY INERTIA FOR THE PITCH CURVE WITH CONCAVE CUSPS OF N-LNG Xin ZHANG, Shuai FAN.....	113
OPTIMIZATION OF ASSEMBLY LINE SCHEDULING BASED ON CROSSOVER OPTIMIZATION ALGORITHM Xiang YANG.....	122
OPTIMIZATION OF HYDRAULIC PERFORMANCE OF AUTOMOBILE COOLING PUMP BASED ON ORTHOGONAL TEST Wang YA-HUI, GE Sai, Yang XING-CHAO, Zhang TAO, Wu JIN-MEI.....	127
POSITIONING AND GRABBING TECHNOLOGY OF INDUSTRIAL ROBOT BASED ON VISION Yonghao ZHAO, Hailin LI.....	137
PRODUCTION SCHEDULING PROBLEM BASED ON MULTI-FACTOR DYNAMIC ANALYSIS ALGORITHM Xiaopin YANG, Yanling GAO.....	146
RESEARCH ON MANUFACTURING FLOW SHOP SCHEDULING METHOD BASED ON MULTI-OBJECTIVE EVOLUTIONARY ALGORITHM Xiaowen YU, Meng LI, Ning DING, Liqing ZHANG.....	153
SHOCK ENERGY CONVERTER FOR ENERGY SUPPLY OF MOBILE LOGISTICS DEVICES Istv á n SZENTMIKLÓSI, B é la ILLÉS.....	159
SIMULATION STUDY ON FLEXIBLE JOB SHOP SCHEDULING OPTIMIZATION OF MULTI-PROCESS PLANNING ROUTES CONSIDERING ENERGY CONSUMPTION Juan GUO.....	164
SIMULATION STUDY ON MULTI-OBJECTIVE BLOCKING LOT STREAMING FLOW SHOP SCHEDULING BASED ON IMPROVED ARTIFICIAL BEE COLONY ALGORITHM Gaizhen YANG.....	173
SIMULATION STUDY ON THE INFLUENCE OF VARIABLE FREQUENCY AND INPUT QUANTITY ON FEEDING ABILITY OF VIBRATORY FEEDER Lingling LI, Yuanpeng LI, Jinlong WANG, Xuedong MA.....	183
SOLUTION FOR PROCESSING PROBLEMS IN PRODUCTION WORKSHOP BASED ON FUZZY IMPROVED OPTIMIZATION ALGORITHM AND FUZZY WORKING HOURS Peng ZHANG, Xiaoyu GUO.....	191

# POSITIONING AND GRABBING TECHNOLOGY OF INDUSTRIAL ROBOT BASED ON VISION

Yonghao Zhao<sup>\*</sup>, Hailin Li

Guangzhou City Construction College, Guangdong Guangzhou, 510900, China.

Corresponding author: Yonghao Zhao

Email: zhaoyonghaobest1@yeah.net

**ABSTRACT:** In order to explore the role of machine vision technology in the positioning and grabbing of industrial robots, the application of machine vision image extraction technology in industrial robot positioning and grabbing was studied through experiments and analysis methods. The Gaussian filtering method was mainly used to smooth the image. On this basis, the edge extraction of the target object image was performed by Canny operator edge detection. The robot arm grab point was determined by binocular three-dimensional positioning coordinates, and then the PID (Proportion Integral Differential) position algorithm was used to analyze the dynamic positioning control of the robot. The results showed that the vision-based industrial robot positioning and grabbing technology can improve the recognition efficiency and grasping efficiency of industrial robots, which is superior to the traditional industrial robot positioning and grabbing function. In summary, the introduction of machine vision functions into industrial robot systems and for industrial production can improve the automation, intelligence and efficiency of industrial production, and has good industrial practical use value.

**KEYWORDS:** Industrial Robot; Positioning and Grabbing; Vision; Edge Detection; PID

## 1 INTRODUCTION

Industrial robots are machine devices that perform work tasks according to pre-programmed program codes, and have been widely used in the industrial field [1]. For example, it is applied in product line assembly, parts sorting, welding, loading and unloading, etc. Industrial robots can replace humans in some dangerous environments, repetitive high-tech scenes, reducing labor costs while improving the quality and efficiency of production. However, with the increasing complexity of the production environment, the requirements for the use of robots are also increasing. When positioning and grasping, in order to achieve the production tasks that are difficult and difficult to successfully complete the process, it is necessary to improve the industrial robot process system and design to add more automated processing functions [2]. The positioning and grabbing process requires the use of visually relevant techniques such as detection recognition, positioning, and dynamic tracking.

Vision-based industrial robot positioning and grabbing technology is a new functional technology application that combines machine vision technology with robot motion technology [3]. If make robots to replace human work well, the first thing to do is to let them be able to "see". Machine vision is the eye of an industrial robot. It processes

and analyzes the image information acquired by the camera [4] to form the position of target object, and then leads the industrial robot to operate the corresponding tracking and grabbing actions. For robots, machine vision gives its sophisticated computing system and processing system [5], simulating the way of bio-visual imaging and information processing, allowing robot arm to perform more anthropomorphic and flexible operations [6] while simultaneously identifying, comparing, and processing scenes, to generate execution instructions, and then complete the action in one go. Machine vision is decisive for the flexibility and operability of robots.

In summary, this paper took the promotion of the grabbing efficiency of industrial robots as the direction of efforts, and increased the application function of industrial robots by using machine vision technology, which makes industrial robots have better flexibility and can further improve the working efficiency, application range and intelligent automation level of industrial robots.

## 2 RESEARCH STATUS

### 2.1 Extraction of vision system images

The machine vision system refers to extracting an image through machine vision, and then digitizing the image in a system processing unit, and determining the size, shape, and the like according to information such as pixel distribution

and brightness, and then controlling the device operation at the site based on the result of the determination. In order to realize the machine eye function similar to the human eye function, it is necessary to optimize the image clarity and integrity. After all, the main information data is derived from the original image [7]. The filtering processing technology is to weaken the noise in the image obtained by camera, so that the image retains more key information, and the image quality is improved, and the validity and reliability of the image as a basis for subsequent technologies are guaranteed [8]. The Gaussian filtering method was used to eliminate interference in the image in this study. In addition, gray processing needs to be carried out for the image, that is, image enhancement, the color photo was converted into black and white grayscale display. This method can enhance the contrast ratio of the selected object, so that the target object has a stronger layering and highlighting. The edge-based image detection method mainly uses the difference value between the pixel value of the edge of the target object and the pixel value of the background image to extract.

Machine vision is widely used in industrial manufacturing. The characteristics of machine

vision mainly include: firstly, high precision, which means that it can adapt to complicated processes and mass of fine processing steps, and there is no wear and tear on fragile components; secondly, flexibility, which means that it can capture a variety of different images and adapt to different functions. Thirdly, the cost is low, and as the price of computer processors decreases, the cost of machine vision systems also decreases. The fourth is high continuity. It can be used in place of people for continuous operation.

The application process of machine vision includes image acquisition, image processing, feature extraction, decision and control. Among them, image acquisition is to use the camera to acquire the image of the measured object [9], and convert the image and the intrinsic features into data that can be processed by the computer. Image processing is the processing of image enhancement, smoothing, edge sharpening, segmentation and other content. Feature extraction is a key feature that the processor recognizes and quantifies image, and then passes the data to the control program. Decisions and controls are based on data received by the processor. The application process is shown in Figure 1.

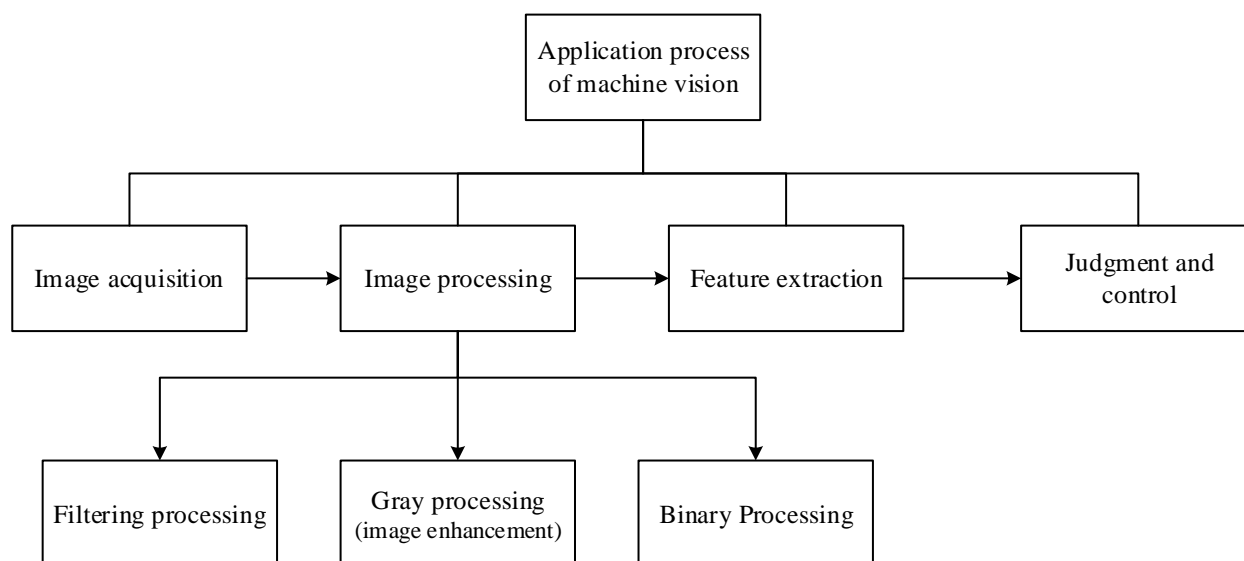


**Figure. 1 Machine vision application process**

Image preprocessing technology can reduce the noise in the image and maintain the image with clear quality [10]. Gaussian noise is one of the common noises. There are many ways to remove noise. The elimination effect of various methods is not the same. Gaussian filtering was used to denoise in this study. Gaussian filtering is a linear smoothing filter that is suitable for eliminating Gaussian noise and is widely used in the noise reduction process of image processing. In fact,

Gaussian filtering is a process of weighting and averaging the entire image through a Gaussian function. The value of each pixel is obtained by weighted averaging of itself and other pixel values in the neighborhood [11]. Gaussian filtering is performed by using a Gaussian filter, which converts the noise signal in the image into a high-frequency signal, calculates the weight and performs denoising by linear convolution. The specific operation of Gaussian filtering is to scan



each pixel in the image with a template and replace the value of the center pixel of the template with the weighted average gray value of the pixels in the neighborhood determined by the template. Gaussian filtering is a signal filter whose purpose is to smooth the signal. The filter is a mathematical model that is used to transform the image data into energy. The noise belongs to the high frequency part, and the Gaussian filter smoothes the noise to reduce the effect.

$$P(z) = \frac{1}{\sqrt{2\pi}\sigma} e^{-\frac{(z-\mu)^2}{2\sigma^2}} \quad (1)$$

Equation (1) is an expression of Gaussian noise, in the equation the parameters include:  $\mu$  represents the expected value,  $\sigma$  represents the standard deviation, that is, the Gaussian radius,  $\sigma^2$  represents the variance value.  $P(z)$  represents the probability.

$$g(x, y) = \frac{1}{2\pi} \exp\left(-\frac{x^2 + y^2}{2\sigma^2}\right) \quad (2)$$

Equation (2) is an expression of image Gaussian filtering. Combined with the actual processing of the image, the Gaussian filtering method can remove the image interference noise on the basis of ensuring the original image feature as much as possible, and has a small image edge ambiguity.

The edge of the image is composed of some discontinuous gray values of the pixel. The edge of the image is the basic feature of the image. It is a collection of pixels that are not continuous with the grayscale of the neighborhood or have a sharp change in grayscale. It contains most of the key information of the image. The purpose of edge detection is to identify points in the digital image where the brightness changes significantly, and edge detection can effectively reduce the total amount of computation during image processing. Therefore, edge detection is a crucial part of image analysis processing and target recognition systems [12]. The edge detection technique generally detects the features by solving the first-order, second-order derivatives or gradients of the gray values of the pixels in the neighborhood, and analyzes whether the gray level of the image has a large variation to detect the edge of the image. The edge detection of the image is to weaken the background part and highlight the edge features of the target object [13]. There is a large gray value gradient amplitude at the edge of the image, so the maximum local amplitude of the gray gradient can be calculated to extract the edge points. Further, the contour of the target is obtained by tracking the straight edge of the pixel. The Canny edge detection operator is a multi-level edge detection algorithm. It is a multi-stage optimization operator with filtering, enhancement

and detection. The implementation steps are as follows: first input the image, then perform Gaussian smoothing, then the gradient calculation, non-maximum suppression, finally double threshold detection, edge image. In order to satisfy the algorithm to identify the actual edges in the image as much as possible, and the identified edges should be as close as possible to the actual edges, Canny uses a variational method that closely approximates the first derivative of a Gaussian function for the possibility of image noise that may not exist to identify edges. Gaussian filtering smoothing is required in the Canny operator. The edge gray level change of the two-dimensional image can be represented by a gradient, and the first derivative also corresponds to the gradient operator. The two-dimensional image  $f(x, y)$ , the gradient operator of the pixel at  $(x, y)$  can be represented by a vector, and the expression is expressed as equation (3):

$$\nabla f(x, y) = [f'_x f'_y] = \left[ \frac{\partial f}{\partial x} \frac{\partial f}{\partial y} \right]^T \quad (3)$$

The gradient is used as the edge detection operator, the mode of the gradient is the edge intensity, and the direction angle of the gradient is the direction of the edge. Equation (4) is the direction angle of the gradient.

$$\theta(x, y) = \arctan\left(\frac{f'_x}{f'_y}\right) \quad (4)$$

After Gaussian filtering was used to smooth the image, noise interference was removed, image enhancement was realized, image and background values were separated, and then Canny edge detection operator was used to extract image edges and highlight image edge features. The Canny operator can be approximated by the first derivative of the Gaussian function and is the optimal solution of the product of the localization and the signal-to-noise ratio. This operator subtly converts the edge detection problem into the problem of finding the extreme point of the unit function. The five steps of the processing flow of the Canny edge detection algorithm are as follows;

First: Use a Gaussian filter to smooth the image and filter out noise.

Second: Calculate the gradient strength and direction of each pixel in the image.

Third: Apply non-maximum suppression to eliminate spurious responses from edge detection.

Fourth: Apply dual threshold detection to determine real and potential edges.

Fifth: Edge detection is finally completed by suppressing the weak edges of isolation.

The Canny operator edge detection method has obvious effect on image edge extraction, which

makes the target object different from other parts of the color, and the extraction of weak edge information is relatively complete and obvious. The Canny operator is less affected by noise, and the detected edges are continuous and the edges are clear.

### 2.2 Target tracking position control

The three-dimensional positioning directly determines the accuracy in the grabbing. The binocular stereo vision can obtain the three-dimensional geometric coordinate information of the target object in the stereoscopic scene, which is equivalent to positioning the target object and providing the machine coordinate basis for the subsequent grabbing. Compared with two-dimensional image information, the three-dimensional positioning coordinate technology is suitable for large and complex production requirements in the industry, and realizes object

grabbing of various types of shapes and sizes. The left and right cameras respectively collect image of the target object at different angles, and extract the feature according to the acquired image information and image library generation information. Then, the matching and recognition of the two are performed, and then the contour extraction is performed, and then the parallax calculation of the left and right camera images is performed, and the left and right double targets are determined, and finally the target positioning is achieved. And the left and right camera coordinates of the object were obtained. The binocular visual image plane forms a triangle with the target object image plane. On the basis of the known left and right camera image position information, the three-dimensional coordinate size of the target object can be obtained, as shown in Table 1 below:

**Table 1 3D coordinates of the target object**

No.	Left camera	Right camera	Three-dimensional coordinates
1	254,104	155,107	1.63,92.11,38.95
2	198,127	94,122	65.45,82.41,38.98
3	239,156	161,152	11.13,50.24,11.46
...	...	...	...

After obtaining the three-dimensional coordinates of the target object, the end effector of the robot performs a movement process from one point to another. The four-degree-of-freedom robot can control the position and speed requirements of the robot by controlling the joints of the robot arm. Joint motion control is accomplished in two steps, first with the completion of the joint motion servo command, transforming the motion of the position and posture of the end effector in the workspace into a time series represented by the joint variable or as a function of the joint variable as change of time. The servo control of the four joint motions is

then completed, that is, the joint variable servo command generated in the first step is followed. The computer sends a control command, and the four joint axes can independently set parameters to exchange data with the motion controller and form a bridge of communication between the two. And the motion controller transmits the current motion position, velocity and acceleration information to the digital servo motor, then a control signal is generated in comparison with the actual position to initiate accurate position control. The structural parameters of the robot arm are shown in Table 2 below:

**Table 2 Structural parameters of the robot arm**

Parameters	Symbol
Motor frequency per revolution	P Value
Screw pitch	L(mm/r)
Ratio of transformation	n (When the motor is directly connected to the lead screw, n=1)
Target location	Pos(plusc)
Target speed	Vel(Pluse/ST)
Target acceleration speed	A.cc(Pluse/ST <sup>2</sup> )
Control cycle ST	T(/μs)

The joint of the robot arm and the end position of the robot arm of industrial robot were taken as the starting point for positioning and grabbing. In the robot arm motion control, the inversion motion

is performed according to the three-dimensional coordinate data, the target position of each joint is obtained, and the joint motion is controlled, so that the end effector of the robot obtains the trajectory of

the motion route according to the joint, and the positioning and grabbing of the robot is ensured. The robot end point error and the rotation angle

error of the arm joint are all declining, as shown in Figure 2.

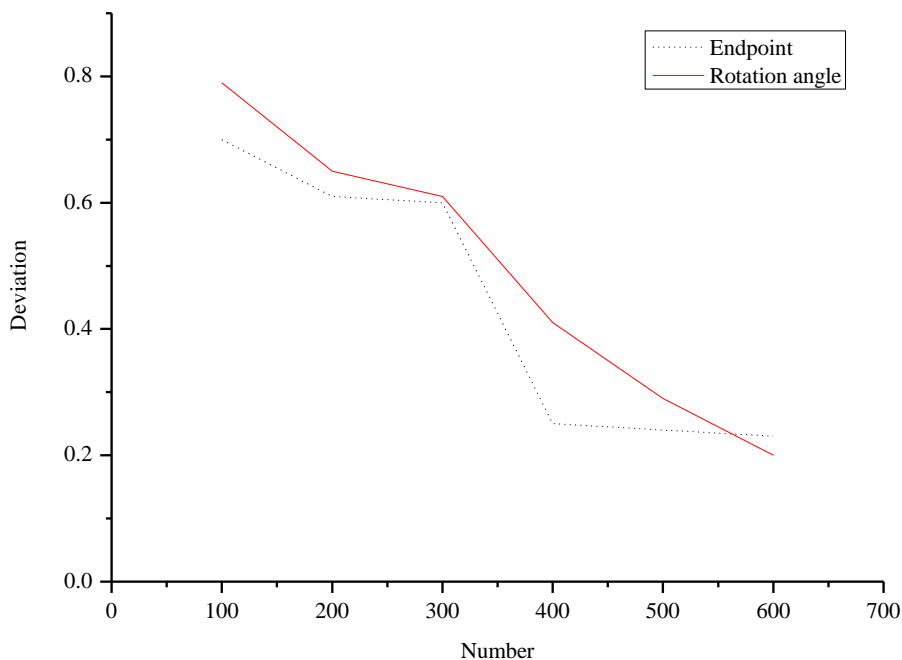


Figure. 2 End point and rotation angle error of robot arm

When the object is dynamically tracked, the PID algorithm can be used to realize dynamic tracking of the conveyor belt and dynamic monitoring of the target. The PID (Proportion Integral Differential) controller is the most widely used industrial controller. In the controller, the unit P is the basis of PID control; the unit I plays the role of eliminating the steady state error, but may increase the overshoot; unit D can increase the inertial response speed and weaken the overshoot. In the industrial automation production, according to the position information of the target, the robot arm trajectory is planned to realize dynamic and effective grabbing. After determining the grabbing position of the target, it is necessary to adjust the position between the robot arm and the conveyor belt target in real time. The conveyor belt is arranged in the XOY plane of the robot arm coordinate system, and the dynamic grabbing process only needs real-time tracking in the XY direction.

After the camera captures the image of the target object and then performs image pre-processing, since the target object is dynamically moving on the conveyor belt, the target has two positions, one is the current initial position Z1 of the target object, and the other is the intended grab position Z2 after the dynamism. The coordinates of the robot arm and the target object are calculated, and the X and Y components of the coordinate are used as the basis for controlling the grasping position Z2 of the

industrial robot arm. By continuously adjusting the speed, position and other elements of the robot arm and the conveyor belt, the error between the robot arm and the conveyor belt is reduced, and according to the real-time situation, the difference between the coordinate Z2 of the intended grabbing position and the coordinate of the robot arm in the XOY plane is continuously reduced, so that The square is more matched, and when the position and speed of the robot arm and the target are agreed upon, the accurate grasping action is completed. The PID algorithm can be used to reduce this error.

$$m(t) = k_p \left[ \varepsilon(t) + \frac{1}{T_i} \int_0^t \varepsilon(\tau) d\tau + T_d \frac{d\varepsilon(t)}{dt} \right] \quad (5)$$

In the PID time domain control expression equation (5) of PID control algorithm, m (t) refers to the control output, k<sub>p</sub> refers to the proportional coefficient, T<sub>i</sub> and T<sub>d</sub> refer to the integral time constant and the differential time constant, respectively, and the addition in braces represents the proportional control term, the integral control term and the sum of the differential control terms.

Proportional P control is one of the simplest control methods, which makes the output of the controller proportional to the input error signal. When there is only proportional control, the system output has a steady-state error. Both the integral I control and the differential D control are the control of the deviation. In the I control, the output of the controller is proportional to the integral of the input

error signal. In order to eliminate the steady-state error, the “integral term” must be introduced. The relative error of the integral term depends on the integral of time, and the integral term will increase with time. It pushes the controller's output up so that the steady-state error is further reduced until it equals zero, leaving the system with no steady-state error after entering steady state. The D control makes the output of the controller proportional to the differential of the input error signal (the rate of change of the error). It can predict the trend of error variation, adjust the mutation in advance, solve the lag problem, and improve the dynamic response speed. The P+D controller can make the control effect of the suppression error equal to zero or even a negative value in advance, thereby avoiding the serious overshoot of the controlled quantity and improving the dynamic characteristics of the system during the adjustment process.

During the dynamic grabbing process of the robot arm, the robot arm and the target object will change in the XOY plane of the conveyor belt. The dynamic response change is made according to equation (5). The system response error during the dynamic grabbing process is as shown in Figure 3, indicating that the previous error margin is concentrated. As time increases, the displacement error of the robot arm and the target object tends to zero, which realizes the unification of the two positions and facilitates subsequent grabbing. PID

position control technology is used for dynamic tracking and dynamic monitoring of target objects, which can adjust parameters to achieve dynamic response of moving targets, and improve dynamic picking efficiency in industrial production and manufacturing.

### 3 RESULTS AND DISCUSSION

As can be observed from Figure 2, the end error of the arm and the rotation angle of the joint are both declining, and the end point error directly affects the result of the grab. The decrease of the error indicates that the visual-based industrial robotic robot arm has higher grabbing accuracy.

It can be observed from Figure 3 that in the dynamic grabbing process, at the early stage of positioning and tracking of industrial robots and target objects, the displacement error between the robot and the target object is large, and the error amplitude fluctuates greatly. As time increases, the actual distance between the two is reducing, and the displacement error gradually approaches 0, which means that the position of the robot and the target object is unified, and then the positioning and grabbing is completed, indicating that the industrial robot based on PID position control under machine vision can achieve accurate positioning and tracking and grabbing in dynamic.

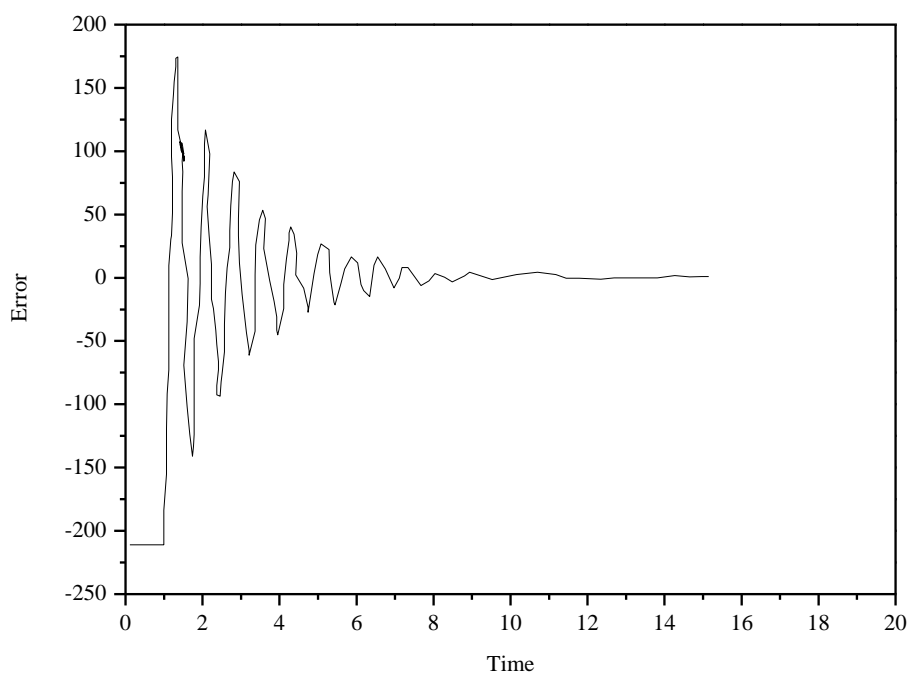


Figure. 3 Response error of dynamic grabbing process system

In Figure 4 is an error diagram after adjusting the differential time constant parameter in Figure 4 twice. It can be observed from the figure that after a

small amplitude adjustment, the position error tends to approach 0 faster. The application of PID position algorithm control reduces the range of the

fluctuation range of the error value and reduces the time taken for the fluctuation, which can tend to be stable more quickly and enhance the system response performance. It is shown that the vision-

based industrial robot can reduce the coincidence time with the target object during dynamic positioning and grabbing, which is beneficial to the positioning and grabbing.

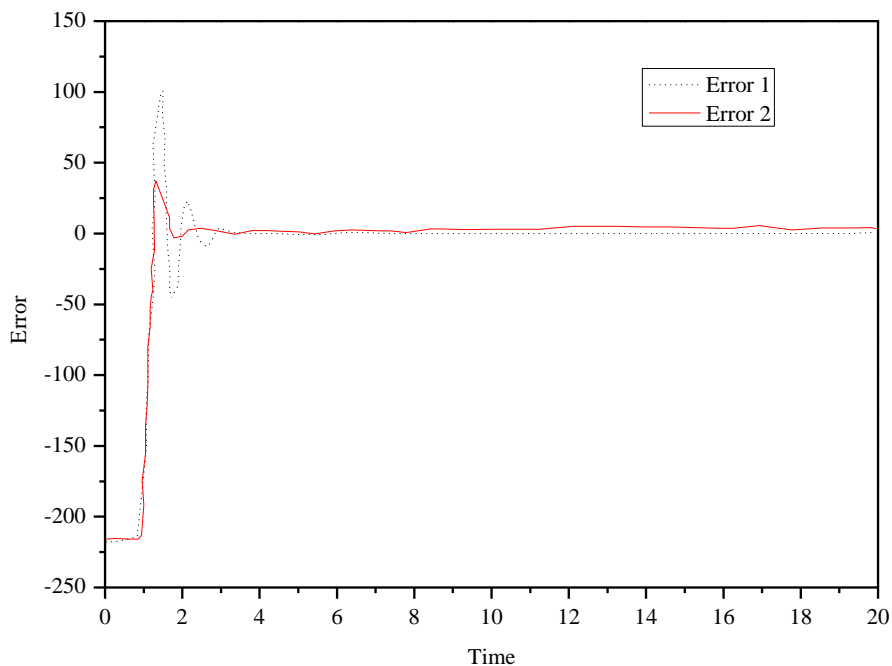


Figure. 4 Position error after adjusting parameters in the dynamic grabbing process

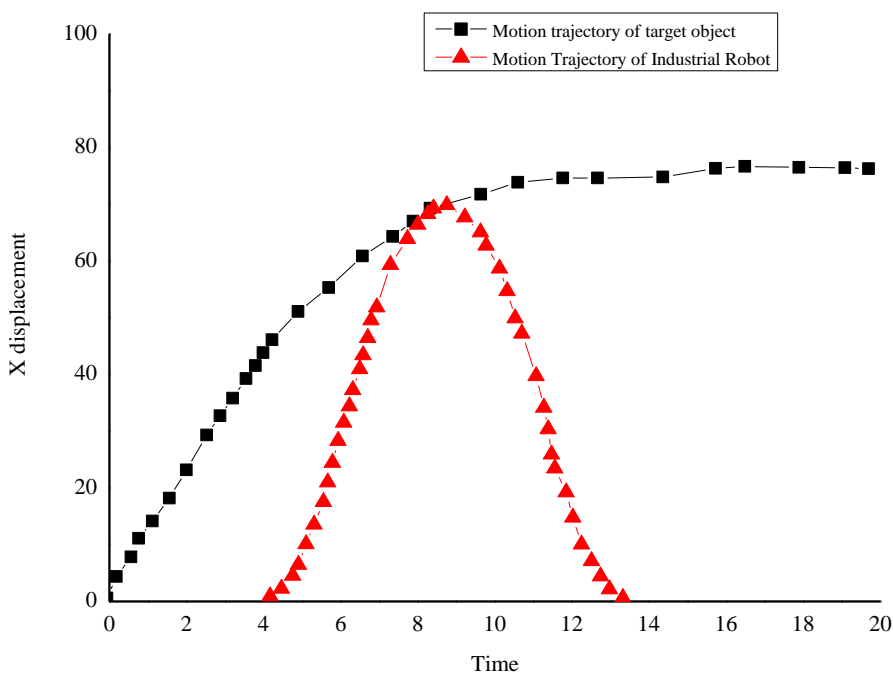


Figure. 5 PID tracking and grabbing of dynamic targets

As shown in Figure 5, in the PID dynamic target tracking, the black square curve and the red triangle curve table represent the motion trajectory curve of the target object and the motion trajectory curve of the robot. The two intersect at a time position of 0.9s, indicating that the robot arm of the industrial robot meets the target object at this time, which is also the time point for performing the positioning

and grabbing. When the motion state of the target object changes with time, the distance between the robot arm and the target object in the position direction and speed is unified by continuously adjusting the distance between the robot arm and the target object, and then the grabbing action is performed. It shows that the dynamic position

tracking of PID based on machine vision has a good effect.

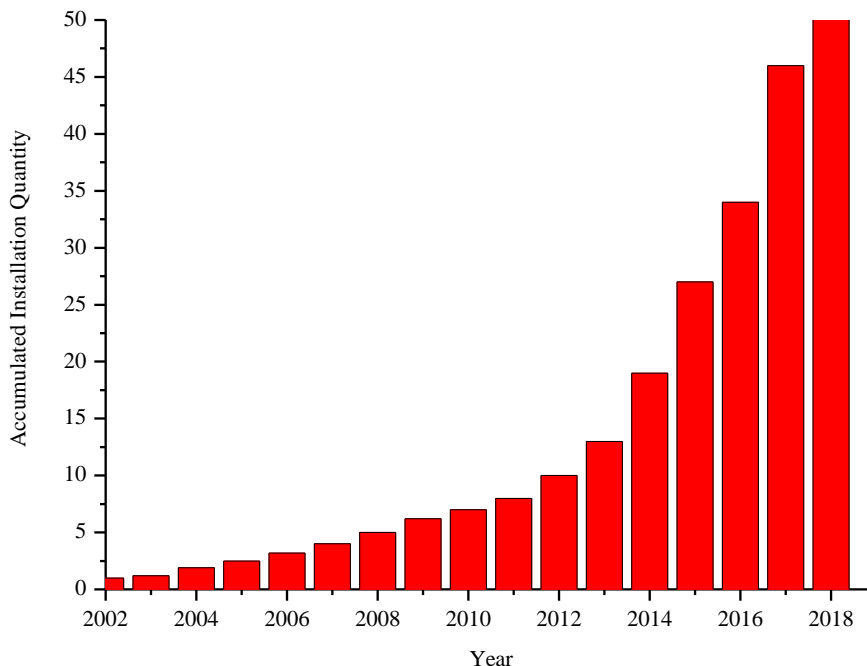


Figure. 6 Accumulated installation capacity of industrial robots in China in recent years (10,000 units)

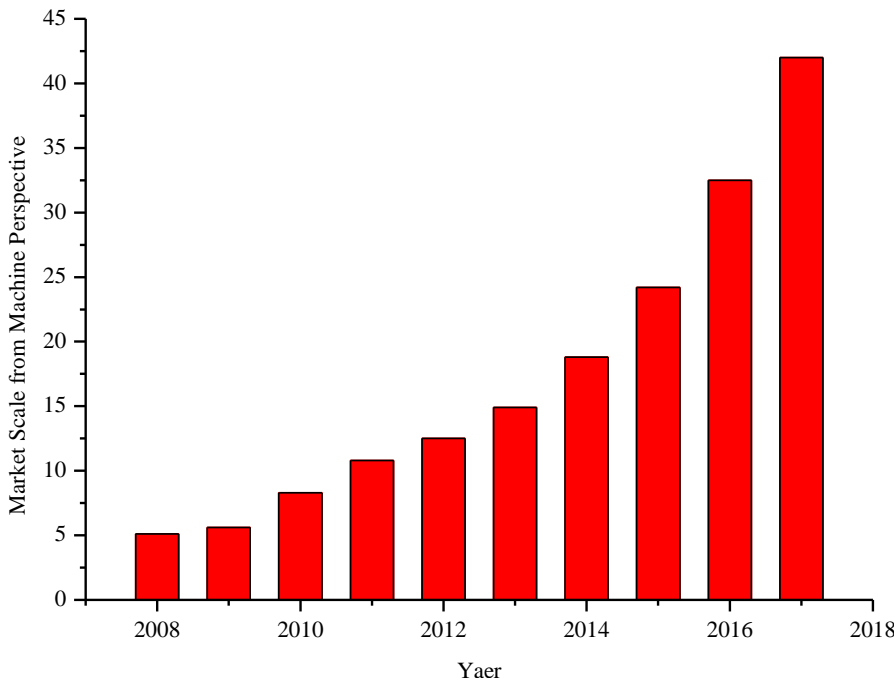


Figure. 7 China's machine vision industry market scale (100 million CNY)

Figure 6 shows the cumulative installation capacity of industrial robots in China in 2002-2018. Since 2003, the market share of industrial robots in China has risen linearly and is expected to maintain rapid growth, indicating that the use of industrial robots in China will increase.

As shown in Figure 7, the scale of China's machine vision market has shown an upward trend in recent years. In 2014, it was about 1.88 billion CNY. In 2015-2017, the industry entered a stage of

rapid development, and in 2017 it reached 4.2 billion CNY. From 2016 to 2020, the growth rate of China's machine vision market is expected to remain above 20%, and the market space is growing.

The application of machine vision technology to industrial robots is necessary to optimize the function of robots. The market-oriented industrial robot positioning and grabbing technology has a

large market demand and maintains a rapid growth trend.

It has good practical effects in industrial production, low cost of use and high production efficiency, which further meets the intelligent manufacturing needs of industrial automation production lines.

#### 4 CONCLUSION

This study tries to solve the limitation of robot positioning and grabbing, and proposed a vision-based robot positioning and grabbing method. By combining the machine vision system image processing technology with the industrial robot control technology, and pre-processing the acquired image to optimize the quality, the three-dimensional positioning of the target object was then realized. The Canny detection was then used to obtain good edge features of the target object, and then the PID position control was used to acquire the motion tracking of the target object. The results showed that the vision-based robot system had fast and accurate image recognition, and the positioning was smart and precise, and it had high industrial application value. This technology is an important symbol of industrial modernization and automation development, and is also a technical support for industrial enterprises to improve production efficiency. This technology not only expands the range of applications of industrial robots, but also enhances the adaptability and working ability of robots in the industrial field. The scale of machine vision industry and the cumulative installation capacity of industrial robots in China are growing rapidly. In actual production, visual-based industrial robots are needed to complete the positioning and grabbing work. Faced with the increasingly complex production requirements in the intelligent manufacturing process of industrial robots, further expanding the integration of various functions can be considered. In the subsequent optimization design, it is feasible to start from the robot multi-arms and study the coordination of multiple arms to achieve better production efficiency of industrial robots.

#### 5 REFERENCES

[1] Tae-jae Lee, Chul-hong Kim, Cho D I D. A Monocular Vision Sensor-Based Efficient SLAM Method for Indoor Service Robots. *IEEE Transactions on Industrial Electronics*, 2018, 66(1): 318-328.

[2] Wang X, L. He, T. Zhao. Mobile Robot for SLAM Research Based on Lidar and Binocular Vision Fusion. *Chinese Journal of Sensors & Actuators*, 2018, 31(3): 394-399.

[3]. Li L, Liu, Y, Jiang T, et al. Adaptive Trajectory Tracking of Nonholonomic Mobile Robots Using Vision-Based Position and Velocity Estimation. *IEEE Trans Cybern*, 2018, 48(2): 571-582.

[4] Fang, Ge, Wang, Xiaomei, Wang, Kui, et al. Vision-based Online Learning Kinematic Control for Soft Robots using Local Gaussian Process Regression. *IEEE Robotics and Automation Letters*, 2019, 4(2): 1194-1201.

[5] Colmenero-Martinez J T, Blanco-Roldán Gregorio L, Bayano-Tejero Sergio, et al. An automatic trunk-detection system for intensive olive harvesting with trunk shaker. *Biosystems Engineering*, 2018, 172: 92-101.

[6]. Eisenbruch M. The cloak of impunity in Cambodia I: cultural foundations. *International Journal of Human Rights*, 2018: 1-17.

[7] Zhang Z, Dequidt, Jeremie, Duriez, Christian. Vision-Based Sensing of External Forces Acting on Soft Robots Using Finite Element Method. *IEEE Robotics & Automation Letters*, 2018, 3(3): 1529-1536.

[8]. Calli B, Caarls, Wouter, Wisse, Martijn, et al. Active Vision via Extremum Seeking for Robots in Unstructured Environments: Applications in Object Recognition and Manipulation. *IEEE Transactions on Automation Science & Engineering*, 2018, (99): 1-13.

[9] Kudryavtsev A V, Chikhaoui, Mohamed Taha, Liadov, Aleksandr, et al. Eye-in-Hand Visual Servoing of Concentric Tube Robots. *IEEE Robotics & Automation Letters*, 2018, 3(3): 2315-2321.

[10] Omisore O M, Han, Shi Peng, Ren, Ling Xue, et al. Towards Characterization and Adaptive Compensation of Backlash in a Novel Robotic Catheter System for Cardiovascular Interventions. *IEEE Transactions on Biomedical Circuits & Systems*, 2018, (99): 1-15.

[11]. Mingmei Cheng, Yigong Zhang, Yingna Su, et al. Curb Detection for Road and Sidewalk Detection. *IEEE Transactions on Vehicular Technology*, 2018, 67(11): 10330-10342.

[12] Fan Z, Tang H, Liu Y H. Odometry-Vision-Based Ground Vehicle Motion Estimation With SE(2)-Constrained SE(3) Poses. *IEEE Transactions on Cybernetics*, 2018, (99): 1-12.

[13] Ikeuchi, Katsushi, Ma, Zhaoyuan, Yan, Zengqiang, et al. Describing Upper-Body Motions Based on Labanotation for Learning-from-Observation Robots. *International Journal of Computer Vision*, 2018, 1-15.

# ACADEMIC JOURNAL OF MANUFACTURING ENGINEERING

## EDITORIAL BOARD

### Editor

Petru Berce *Universitatea Tehnică din Cluj-Napoca, Romania*

### Associate Editors

Paul Dan Brîndașu *Universitatea "Lucian Blaga" din Sibiu, Romania*  
Cristian Doicin *Universitatea POLITEHNICA din București, Romania*  
Gheorghe Oancea *Universitatea "Transilvania" din Brașov, Romania*  
Laurențiu Slătineanu *Universitatea Tehnică "Gheorghe Asachi" din Iași, Romania*  
Dănuț Șoșdean *Universitatea Politehnica Timișoara, Romania*

### Editor in charge

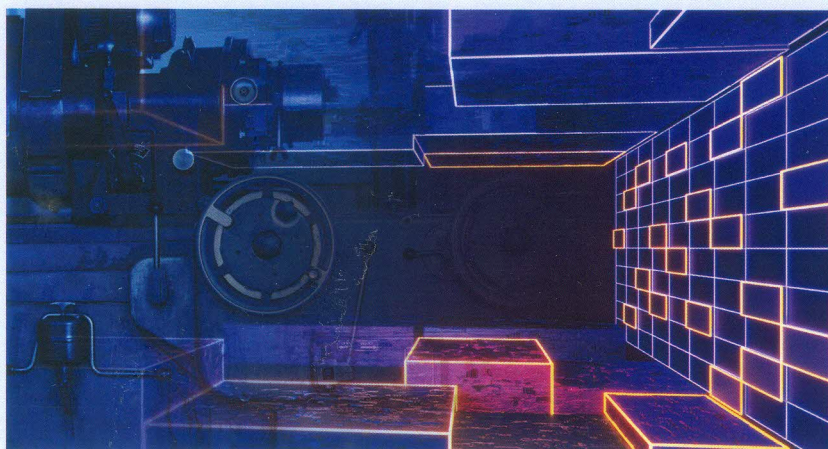
Paul Dan Brîndașu *Universitatea "Lucian Blaga" din Sibiu, Romania*

## International Editorial Board

Michael Abramovici *Ruhr-Universität Bochum, Germany*  
Gheorghe Amza *Universitatea POLITEHNICA din București, Romania*  
Nicolae Bâlc *Universitatea Tehnică din Cluj-Napoca, Romania*  
Alain Bernard *Ecole Centrale Nantes, France*  
Florin Blaga *Universitatea din Oradea, Romania*  
Octavian Bologna *Universitatea "Lucian Blaga" din Sibiu, Romania*  
Daniel Brissaud *Institut National Polytechnique de Grenoble, France*  
Ian Campbell *Loughborough University, United Kingdom*  
George Drăghici *Universitatea Politehnica Timișoara, Romania*  
Igor Drstvenšek *University of Maribor, Slovenia*  
Cătălin Fetecău *Universitatea „Dunărea de Jos” din Galați, Romania*  
Uwe Heisel *Universität Stuttgart, Institut für Werkzeugmaschinen, Germany*  
Fred J.A.M. van Houten *Universiteit Twente, Nederland*  
Tudor Iclănzan *Universitatea Politehnica Timișoara, Romania*  
Nicolae-Valentin Ivan *Universitatea "Transilvania" din Brașov, Romania*  
Valeriu Jinescu *Universitatea POLITEHNICA din București, Romania*  
Panagiotis Kyratsis *Technological Institute of West Macedonia, Greece*  
Stanislaw Legutko *Poznan University of Technology, Poland*  
Mathias Liewald *Institute for Metal Forming Technology, Stuttgart, Germany*  
Chris McMahon *University of Bath, United Kingdom*  
László Monostori *MTA SZTAKI & BME, Hungary*  
Gavril Muscă *Universitatea Tehnică "Gh. Asachi" din Iași, Romania*  
Slobodan Navalusic *University of Novi Sad, Serbia*  
Herbert Osanna *Technische Universität Wien, Austria*  
Liviu Iulian Palade *Universite de Lyon, France*  
Eugen PĂMÎNȚAȘ *Universitatea "Politehnica" din Timișoara, Romania*  
Loredana Santo *University of Rome „Tor Vergata”, Italy*  
Moshe Shpitalni *Technion, Israel Institute of Technology*  
Serge Tichkiewitch *Institut National Polytechnique de Grenoble, France*  
Engelbert Westkämper *Institut für Industrielle Fertigung und Fabrikbetrieb, Germany*  
Paul Xirouchakis *Ecole Polytechnique Fédérale de Lausanne, Switzerland*



# Journal of Physics Conference Series



# 1605

Volume 1605

Online ISSN: 1742-6596 Print ISSN: 1742-6588

[jpcs.iop.org](http://jpcs.iop.org)

**IOP** Publishing

- 012100 Research about a Kind of Gantry Type Single-side Drive Straight Line Motion Mechanism**  
*Fu Jieqiong, Bu Leping, Li Hailin and Zhang Yong*
- 012101 Research on Pure Mechanical Lifting Pedal Applied to Rail Transit Vehicles**  
*Yingyong Zhang, Zhaozhan Hou, Xiangli Lin, Changkai Xia, Dongjun Yang and Jianwei Song*
- 012102 Error Prediction of CMM Using a Hybrid Model Based on Neural Network Quantile Regression and Kernel Density Estimation**  
*Haiting Wu, Mei Zhang, Guihua Li, Haifeng Zhao and Xiaoping Wu*
- 012103 Analysis of CMM Dynamic Measurement Error Based on Decision Regression Tree**  
*Xiaoping Wu, Mei Zhang, Guihua Li, Haifeng Zhao and Haiting Wu*
- 012104 Study on Topology Optimization Design of Screw Extrusion Filter**  
*Yuanlong Chen, Qianqian Cheng and Rongna Chen*
- 012105 Profile imitation algorithm research for the cam contour**  
*Xu Qinglu*
- 012106 Research on Multi-Order Anti-Aliasing Filter in Bearing Profile Detection**  
*He Gaoqing, Han Jiang, Liang Leilei and Xiao Jian*
- 012107 Measurement of mechanical properties of carp scales based on digital image correlation method**  
*Zhongnan Fu, Wanlong Ma, Tiantian Zhu, Pei Ye and Guihua Li*
- 012108 Application of 3D printing technology in equipment structure teaching**  
*Bai Xiaotao and Li Jie*
- 012109 A research on evaluation and development of single-pedal function for electric vehicle based on PID**  
*Zhao Yongqiang, Zhang Xin, Li Jiashi, Huo Haitao, Ma Teng and Zhou Chunyu*
- 012110 Study on vibration characteristics of plastic helical gear assembly with prestress**  
*Wu Baogui, Du Zaiyou and Huang Ruchen*
- 012111 Deduction of gear system proportion in any leaf rose line drawing**  
*Li'an Ma, Jixiang Yue and Guodong Wang*
- 012112 Study on the forward slip of cup with variable wall thickness during roll forming**  
*Baohong Zhang, Bin Hu, Zhimin Zhang and Xi Zhao*

## Research about a Kind of Gantry Type Single-side Drive Straight Line Motion Mechanism

Fu Jieqiong<sup>1a</sup>, Bu Leping<sup>1b, 2a</sup>, Li Hailin<sup>1c</sup>, Zhang Yong<sup>2b</sup>

<sup>1</sup> Guangzhou City constructing College, Guangzhou 510925

<sup>2</sup> College of Mechanical and Electrical Engineering, Inner Mongolia Agricultural University, Hohhot 010018

Corresponding author Bu, Leping: Male, born in 1958, professor, Doctor of Engineering, graduate student tutor, research direction: material processing technology and equipment, E-mail:buleping1958@126.com

First author Fu, Jieqiong: Female, born in 1982, associate professor, Master of Engineering, research direction: mould designing and manufacturing as well as numerical control, E-mail:332460235@qq.com

**Abstract:** The article mainly has conducted comparison to three kinds of frequently-used long-span gantry type mechanism that do straight line motion, which thereby has obtained that the gantry type single-side drive mechanism had possessed relatively prominent advantage in the smoothness, assembly debugging, reliability and maintenance aspects of the motion and it has conducted reason analysis and structural improvement to problems existed in occasions of its application in large scale equipment, long span or heavy load with impact, which therefore has guaranteed the need for high precision and high stability in practical application.

### 1. Advantage and Existing Problem of Gantry Type Single-side Drive Straight Line Motion Mechanism

In the automation equipment structural design, it often has adopted gantry mechanism as the mechanism to execute round-trip of the rectistraight line motion, which can complete motion and position required by processing, assembly, detection, etc<sup>[1]</sup>. This kind of mechanical engineering generally has three kinds of driving methods, below table will conduct comparison from stability of mechanical structure, assembly debugging, reliability of the mechanism, maintainability as well as cost, etc aspects.

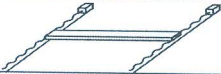
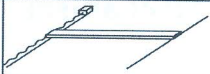

From analysis and comparison of the above table, it has obtained that the gantry type single-side drive mechanism has possessed rather prominent advantages in smoothness of the motion, assembly debugging, mechanical reliability and maintenance aspects, which is optimal among the three design schemes. But in the actual application, as the load end of the single-side drive mechanism has existed effect of rotating the torque by winding the Z axis, the range that limits its application has mainly lied in gantry structure or small span gantry (ie., gantry whose width of guiding structure at both sides is no bigger than 600mm) or occasions whose heavy load has had impact cannot fall down on its job, which has mainly existed effects of below two aspects.



I. When the mechanism is in non-motion static status, if the span or the load is too big, it has higher and harsher requirement to the rigidity as well as installation precision of the guiding system at both sides of the gantry, especially the guiding precision and rigidity of the drive side<sup>[3]</sup>.

II. When the mechanism is in motion status, if the span is too big, as the driving power is only designed at the single-side, the cantilever domino effect of its load to the driving system will be very obvious, the pulsation of its moving speed as well as impact acting force of the load will generate

Table 1 Three Kinds of Frequently-used Long Span Gantry Type Straight Line Motion Mechanism

Type	Double-drive of dual-motor	Single-side drive	Transmission synchronous drive
Schematic diagram			
Explanation	Two sides of the gantry all have designed drive motor and transmission-guide mechanism to realize synchronous movement via the control.	One side of the gantry has designed the drive motor and transmission-guide mechanism; the other side has designed support and guide structure, the power is provided by the single-side.	One side of the gantry has designed the drive motor and transmission-guide mechanism, the other side has designed the transmission-guide mechanism, there is no drive motor, the power has guaranteed the drive synchronization of two sides, with method of power synchronous transmission.
Smoothness analysis for motion of the mechanism <sup>[2]</sup>	Smoothness of the motion is mainly decided by below factors: ①Guiding precision of two sides; ②Precision of mechanical transmission in two sides; ③Smoothness and synchronization of dual-motor motion in two sides; ④Kinematic accuracy of bilateral drive motor, especially the synchronization of bilateral drive motor motion.	Smoothness of the motion is mainly decided by below factors: ①Guiding precision of two sides; ②Mechanical precision of transmission in driving side; ③Motion degree of the driving motor, especially the rigidity and intensity of guiding structure in two sides.	Smoothness of the motion is mainly decided by below factors: ①Guiding precision of two sides; ②Precision of transmission gearing in two sides; ③Precision and rigidity of synchronous drive transmission structure in two sides; ④Motion precision of the drive motor, especially the precision and rigidity of the synchronous motion structure in two sides.
Assembly, debugging of the mechanism	Quantity of the structural parts are very large, mechanical assembly and precision debugging difficulty is common, but two sides are two power and drive system, debugging difficulty of electric control is relatively high.	Quantity of the structural parts are very small, mechanical assembly and precision debugging is very easy, at the same time, its transmission is only a set of system, debugging of electric control is also very easy.	Quantity of the structural parts are very large, in order to guarantee the synchronism and stability of motion in two sides, debugging difficulty of its overall motion system is very big, but the debugging of electric control is relatively very easy.
Reliability and maintainability of the mechanism	In order to guarantee the synchronism of motion in two sides, it needs corresponding detectors, if the reliability has extent guarantee, it needs to periodically maintain the electric control and two sets of drive transmission structures, the maintaining difficulty is general.	In order to guarantee the motion precision and reliability of the single-side drive, the guide precision and rigidity requirement of its driving side is very high, which needs to periodically maintain the drive transmission structure and the rigidity of the guiding, the maintenance is relatively very easy.	In order to guarantee the synchronism of motion in two sides, it has had extent transmission precision and rigidity requirement to the power transmission structure, at the same time, if it is to guarantee the precision of the drive and transmission position, the periodical maintenance it needs are synchronous transmission structure, drive transmission structure, especially the maintaining frequency of the transmission structure is very high, which relatively is the most difficult.
Cost	Very high	Rather low	Rather high

-torque on the beam, therefore rigidity of the beam as well as the smoothness of the operation are problem that must be solved.

## 2. Optimal Design of Large Span Gantry Type Single-side Drive Straight Line Motion Mechanism

### 2.1. Countermeasures of the Guide Precision and Rigidity

There are generally two sets of guiding structure in the gantry type single-side drive straight line motion mechanism, among which structure of the driving side has mainly played the guiding role, whose precision and rigidity has played important role in the overall gantry motion system. However, the other side has mainly provided support for the end of the beam and has strengthened the guidance quality of the beam. As is shown by below figure 1, when the span  $L$  of the gantry increases, however effective guiding length  $k_1$  of the two sliding blocks does not increase, which has directly lead to the decline of specific value for guiding rigidity coefficient  $k_1/L$ , when specific value of rigidity coefficient  $k_1/L$  is no bigger than 0.5, rigidity variation of the guiding system will be magnified in multiple by the gantry beam<sup>[4]</sup>. This means the deviation in rigidity and stability of the system. In order to enhance the stability of the gantry type single-side drive straight line motion mechanism, except by increasing the pre-pressing grade of the ball straight line guideway sliding block, it also must enhance the guiding rigidity coefficient  $k/L$ . The most frequently-used practice is to increase the space between two sliding blocks in the straight line guideway, ie., to directly increase  $k_1$ . Aiming at defects of gantry type single-side drive straight line motion mechanism in large span occasions, except for method of directly increasing space  $K_1$  between two sliding blocks, it has additionally had method of adding one sliding block and strengthening block (As parts expressed by imaginary line in figure 1), via this optimal design, it can directly increase the original effective guiding length  $k_1$  to  $k_2$ , which therefore has enhanced the specific value  $k/L$  of guiding rigidity coefficient. At the same time, when in installation debugging, the optimal design of this kind of structure can firstly assemble and debug in place via two sliding blocks (as is shown by 2 full line sliding block and beam parts of left side in figure 1), then it has assembled the third sliding block and it has added the guiding ability of the sliding block onto the gantry structure component via the strengthening component, which therefore has strengthened the load ability and motion rigidity of the gantry type single-side drive straight line motion mechanism.

### 2.2. Power design Countermeasures of the Drive and Transmission

As is shown by the above figure 2, for gantry type single-side drive straight line motion mechanism, the general power design can be distributed at three points, which respectively are ①②③ three points. In order to lower the cantilever beam effect of the large gantry span load to the driving system, via force analysis, it is better to design the application point of transmission and drive onto position <sup>[5]</sup> ③.

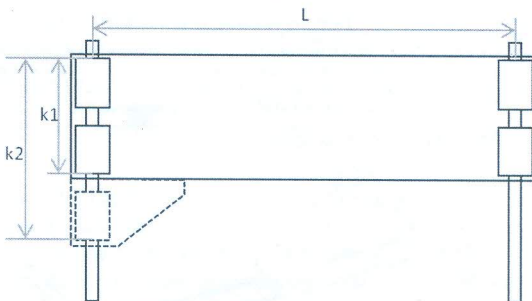


Figure 1 The Guiding Rigidity and Stability of the Strengthening Driving Side

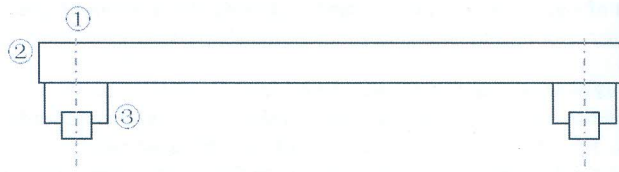


Figure 2 Lower Design Schematic Diagram of Gantry Power Side

### 2.3. Design of the Beam Structure

Integrating above analysis to structure, rigidity, loading form, etc of the gantry type, under the premise of guarantee the intensity of beam, for beam plate, the Y direction motion of the loading motion on the Z axis is the impact acting force of Y axis, however, for beam plate, X direction motion of the loading motion on Z axis is the impact acting force of X axis direction and the positive and negative twisting force winding Z axis for rotation. Therefore, when designing the beam, the key point is to increase the ability of beam plate's resisting Z axis torque, i.e., the intensity and rigidity of XY plane. Therefore, it has designed the beam into the flat plate type, whose two dimensional diagram is shown as figure 3:

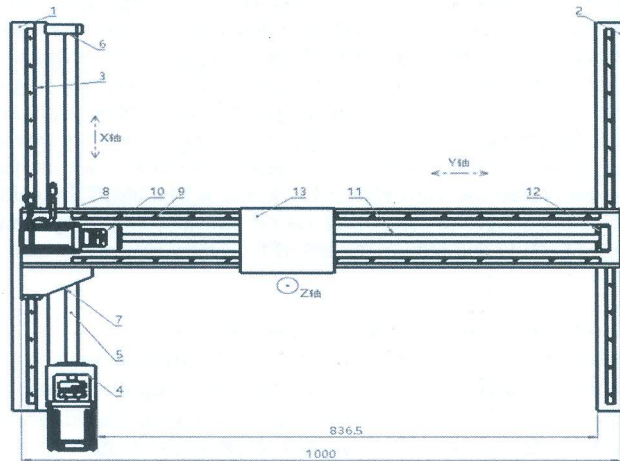


Figure 3 Structural Design Drawing of Large Span Single-drive Gantry

1. Gantry frame at power side, 2. Gantry frame at support side, 3. Guiderail of Y axis, 4. Motor as well as fixed seat of lead screw on Y axis, 5. Lead screw on Y axis, 6. Supporting seat of lead screw, 7. Strengthening block of the gantry, 8. X arm of the gantry, 9. Guiderail of X axis, 10. Motor as well as fixed seat of Y axis, 11. Lead screw of X axis, 12. Supporting seat of lead screw on X axis, 13. Moving plate on X axis

Finally, its 3D diagram after the design is as follows:

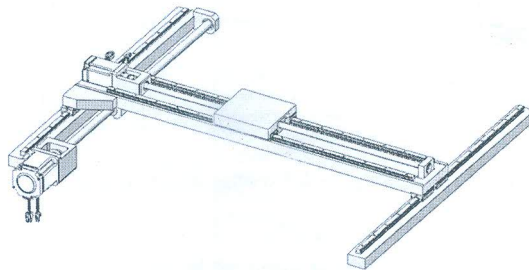


Figure 4 3D Diagram of Large Span Single-drive Gantry Structure

### 3. Practical Application Cases of Gantry Type Single-side Drive straight line Motion Mechanism

In one set of mechanical equipment, the needed gantry span is 1200mm, by adopting above design method, it has designed the guide of the drive side into three sliding blocks, among which it has strengthened one sliding block onto the gantry structure. Then it has installed the power design onto the position of point ③ of the gantry system, in order to reduce that the weight of beam plate will bring excess loading for the large span gantry type single-side drive straight line motion mechanism and in order to guarantee its intensity and rigidity, it needs to conduct weight losing optimal designs<sup>[6]</sup> to the beam plate, whose design diagram is shown as figure 5:

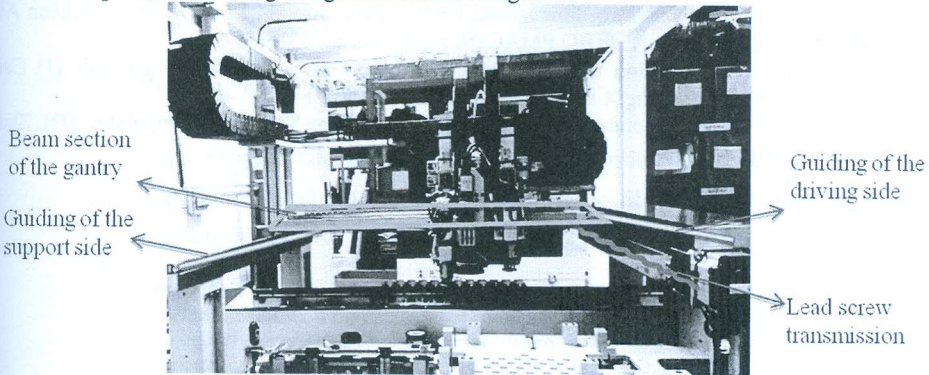


Figure 5 Application Drawing after the Actual Manufacturing a Finished

Table 2 Using of the field, test as well as testing data  
(Test the average value for 30 times) after the equipment runs in vain for 48H

No	Item	Measuring apparatus	Data after the debugging	Data after 48H's running in vain
1	Repeatability of guide point on left side of the gantry	Dial test indicator	0.0012 mm	0.0015 mm
2	Repeatability of guide point on left side of the gantry	Dial test indicator	0.0016 mm	0.0017 mm
3	Gantry left load is 20kg, positional accuracy	Machine vision	0.0032 mm	0.0042 mm
4	Gantry left load is 20kg, positional accuracy	Machine vision	0.0037 mm	0.0044 mm

### 4. Conclusion

The article has intensified the rigidity and intensity of the large span gantry type single-side straight line motion mechanism via reasonable design and it has got verification and application in practical application, at the same time, via these two kinds of methods, it has effectively enlarged such simple, practical and stable structure as large span gantry type single-side drive straight line motion mechanism, which has made it to have larger application space.

### Research project

Scientific research task of Guangzhou City Construction College (Y201909)

Inner Mongolia Natural Science Funds (2009MS0802), Inner Mongolia Office of Personnel Services Talent Funds, National Natural Science Foundation of China (61563042)

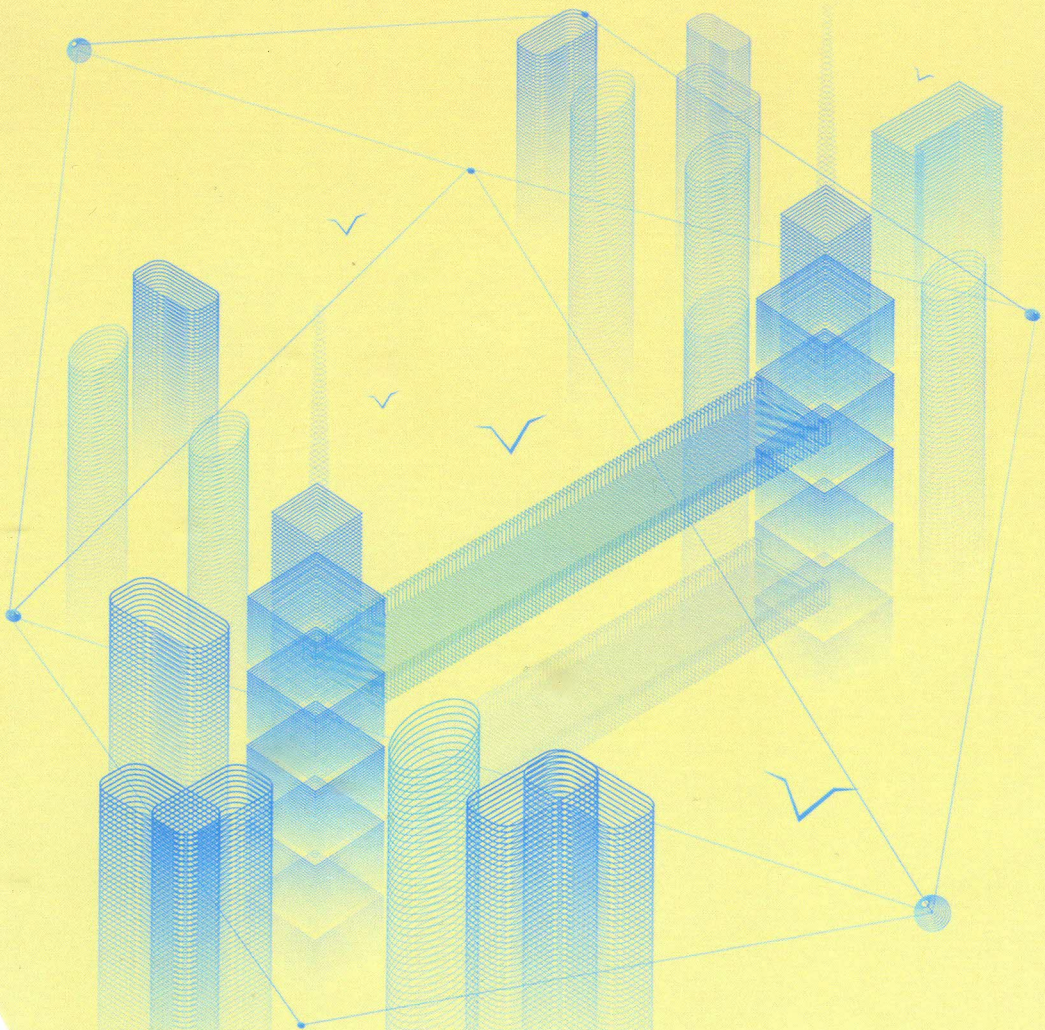
**References**

- [1] Trajectory Tracking Controller Design of Straight Line Motor Precise Motion Platform [J]. Zhang, Gang, Liu, Pinkuan, Zhang, Bo, Ding, Han. Optics Precise Engineering. 2013(02)
- [2] Vibration Performance Research of Bilateral Drive Precise Motion Platform [J]. Jia, Songtao, Zhu, Yu, Yang, Kaiming, Xu, Dengfeng, Wang, Chunhong. Mechanical Science and Technology. 2009(05)
- [3] System Modeling and Analyzing Research of Coarse, Fine, Dynamics and Ultra-precision Motion Platform [J]. Yang, Yibo, Yin, Wensheng, Zhu, Yu, Wang, Chunhong. China Mechanical Engineering. 2008(23)
- [4] Track Precision Research of Two-dimensional Gantry Type Straight Line Driving Precision Air Bearing Table Based on TURBO PMAC2[D]. Lu, Xinhui. 2015(34-35)
- [5] Welding Precision Optimization and Simulation Control of Gantry Type Welding Robot [J]. Cai, Yuqiang, Zhu, Dongsheng. Computer Simulation. 2018(09)
- [6] Design and Main Girder Structure Optimization of Gantry Type Vac-sorb Manipulator [D]. Zhu, Jianguo. 2016(13)



Online ISSN: 1742-6596 Print ISSN: 1742-6588  
Journal of Physics: Conference Series Vol.1605  
Electronically available at <http://iopscience.iop.org>

# WOP in Engineering and Science Research



Francis Academic Press, UK

---

**2020 7th International Conference on Civil  
Engineering, Materials and Chemistry (ICCEMC 2020)**

---

**April 14-16, 2020. Ankara, Turkey**

**Francis Academic Press, UK**

# Table of Contents

<b>Research on rapid qualitative detection of bismuth in pyrotechnic powder used for fireworks and firecrackers</b>	<b>1</b>
<i>Wu Junyi</i>	
<b>The Discussion on Quality Control Measures for Municipal Engineering Construction</b>	<b>6</b>
<i>Shufang Li</i>	
<b>Exploring the Influence of Landscape Architecture Design on the Reduction of Atmospheric Pollution</b>	<b>11</b>
<i>Yanrong Bai</i>	
<b>Analysis on Preparation and Properties of Waterborne Epoxy Emulsified Asphalt Mixture</b>	<b>16</b>
<i>Jianguo Sun, Yujie Chen, Hongyan Yin, Qiuyun Wang</i>	
<b>Discussion on the Application of Instrumental Analysis Technology in Environmental Inorganic Analytical Chemistry</b>	<b>21</b>
<i>Hou Fang</i>	
<b>Research on Construction Technology Control of Concrete Permeable Pavement in Sponge City Construction</b>	<b>27</b>
<i>Zhao Junjie, Zhu Yuanli</i>	
<b>Research on Sequentially Controlled Hot Runner Injection Molding for Led Tv Rear Panel</b>	<b>31</b>
<i>Qiuli Li, Yan Li, Hailin Li, Hui Luo, Yonghao Zhao</i>	
<b>Study on the Safety Evaluation of Prefabricated Building Construction</b>	<b>38</b>
<i>Chao Fan</i>	
<b>Study on the Construction Period Risk of Long-Span Bridge</b>	<b>42</b>
<i>Xiuyong Ni</i>	
<b>Study on Energy Conservation of Urban Buildings and Green Development Strategy in Lanzhou</b>	<b>46</b>
<i>Yang Linping, Liu Hao</i>	
<b>Discussion on Construction Management and Progress Control of Building Engineering</b>	<b>50</b>
<i>Wei Xi, Zicheng Zhang, Bing Zhou</i>	
<b>The Embodiment of Regional Culture in the Planning and Design of the Scenic Spot of the Nujiang Grand Canyon Bathhouse</b>	<b>55</b>
<i>He Jin, Nan Zhang</i>	

## Research on Sequentially Controlled Hot Runner Injection Molding for Led Tv Rear Panel

Qiuli Li<sup>1</sup>, Yan Li<sup>2\*</sup>, Hailin Li<sup>1</sup>, Hui Luo<sup>1</sup>, Yonghao Zhao<sup>1</sup>

<sup>1</sup> School of Mechanical and Electrical Engineering, Guangzhou City Construction College, Guangzhou Guangdong, China

<sup>2</sup> School of Business, Beijing Institute of Technology, Zhuhai, Guangdong, China

\*Corresponding Author

**Keywords:** Cae, Injection molding, Hot runner technology, Sequence control, Svg

**Abstract:** The traditional injection molding method for large-scale thin-shell plastic parts is realized by multi-gate hot runner technology. Due to the simultaneous injection of multiple points, defects such as bubbles, shrink marks, and more weld marks on the product are likely to affect the appearance of the plastic part. Quality, strength and effect of subsequent painting. This article takes LED TV rear panel products as an example, and uses CAE mold flow analysis technology and hot runner sequence control technology to optimize the injection molding process and mold through the three steps of process condition presetting, molding scheme analysis and estimation, and test mold verification. Design, the purpose of obtaining good plastic parts. It provides an efficient and stable injection molding process method for the development of such large-sized, thin-shelled, and high-demand product products to solve and improve their molding defects.

### 1. Introduction

For large-scale thin-shell injection-molded products, due to their large size and thin wall thickness, the problems of injection molding filling and narrow process range are caused. The mold structure often adopts a multi-gate design, which makes it difficult to balance the filling of the mold cavity, and the number of weld marks increases, which seriously affects the appearance quality and mechanical properties of the product.

At present, the use of full hydraulic secondary compression injection molding technology [1] can solve the problem of difficult filling of such injection molded products, and at the same time solve the problem of light refraction of high-gloss products or transparent materials. The use of electric heating injection molding technology and high-gloss injection molding (RHCM) technology [2] can control the temperature field balance during molding, and reduce the effects of surface welding and other defects. However, these methods can achieve the molding process only through special process equipment or molds, and the process control is difficult, the waste rate is high, the energy loss is large, and the production cost is high.

Hot runner sequential control (Sequential Valve Gating, SVG for short) pouring technology [3], which uses gas / hydraulic devices and time control devices to control the movement and stop of the valve needle at a predetermined position and time, and cooperates with the nozzle valve to achieve sequential opening and closing. The melt flow achieves an orderly "relay" flow, and achieves "dynamic" control of the material flow [4]. Provides new ideas for solving the above problems.

This article will take the LED TV rear panel as the research object, based on the CAE mold flow analysis technology and sequential control hot runner technology, explore the product hot runner valve gate opening and closing control law, and study the optimization of the product injection process scheme under different process conditions. Inferior, and through the test experiment, verify the CAE mold flow analysis results to optimize the injection molding process.

## 2. Sequence Control Principle and Characteristics of Hot Runner Structure

The sequential control of the hot runner is the opening and closing of the nozzle gate by the valve needle driven by the gas / hydraulic device. However, the control of the gas / hydraulic device is no longer only mechanical, but a time sequence control device is introduced. The time setting sequence opens and closes the valve, so that the material flow flows sequentially and sequentially, and the filling process is balanced and controllable.

As shown in Figure 1, the interior of the SVG hot runner mold structure is mainly composed of ① positioning ring, ② nozzle, ③ heating wire, ④ hydraulic cylinder, ⑤ plunger, ⑥ heating rod, ⑦ manifold, ⑧ valve needle, ⑨ thermocouple, ⑩ Nozzle and other components, there are temperature control device, pneumatic / hydraulic drive device, needle valve time control device and so on.

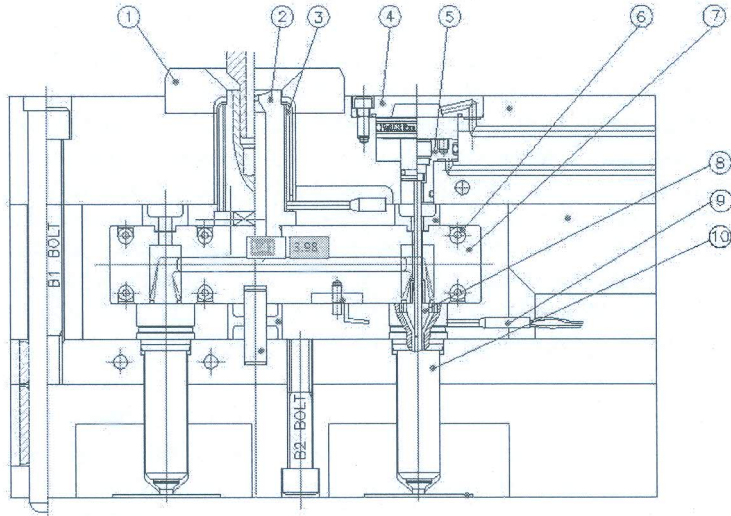


Fig.1 Svg Hot Runner System Structure

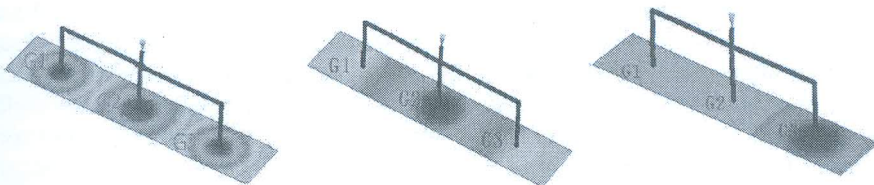
## 3. Sequential Valve Hot Runner Features

Compared with other types of hot runners, SVG has the following advantages in engineering applications: during the injection molding process, the materials in the runners will not always melt, the runners will not form, and there is no need to design the device to discharge materials. Compared with other systems, it has a larger nozzle gate channel, which can effectively reduce the filling time, reduce the molding cycle, and obtain higher production efficiency. The valve-controlled gate and the design of the return groove ensure the gate. When closed, no resin will remain on the surface, ensuring no casting marks on the surface of the product; it can effectively improve defects such as welding marks and shrink marks on the surface of large thin-walled plastic parts, and improve the surface quality of the product; it can also effectively reduce the clamping force and maintain the mold Filling balance, reducing process characteristics such as warpage of the product.

Of course, SVG hot runner also has some shortcomings that are not easy to solve: the implementation of technology requires precise regulation, such as the time sequence of gas / hydraulic devices, motion control; the effective control of the temperature of each section of the hot runner, and the cooperation between the gate valve needles Accuracy and other factors are the key factors that affect the molding. Therefore, there are very high requirements for operation and maintenance personnel; the pressure loss along the hot runner is relatively large, and a large injection pressure is required as a support, which places higher requirements on the injection molding equipment.

The molding CAE numerical simulation technology, through computer simulation of the plastic product molding process, provides a good basis for the subsequent design of high-quality molds and molding process parameters. CAE software is used to perform finite element modeling of the product, build product models, mold casting, and cooling structure models. Through flow simulation in the cavity, it can analyze and predict surface defects after injection molding of the product; through cooling simulation, it can analyze Predict the shrinkage and warpage of the product. These analysis results will guide the design and optimization of the product and mold structure. After the optimization, the improvement of the predicted defects will be further analyzed until the expected good product is obtained [5].

Take a long plastic piece as an example, as shown in Figure 2, using three-point hot nozzle injection, mold flow numerical simulation and simulation experiments using Moldflow software, first finite element modeling, hot runner process parameter settings and other operations Through the simulation of filling, understand the principle of sequential control of valve needle opening and closing in the hot runner.



(a) Simultaneous hot runner injection (b) SVG central diffusion sequential injection (c) SVG linear progressive injection

Fig.2 Moldflow Simulation Principle of Sequential Control Hot Runner

As shown in Figure 2 (a), in the conventional hot runner structure, three nozzle gates G1, G2, and G3 are injected at the same time. According to the filling simulation, the plastic flow front between gates G1 and G2 and G3 and G2 form a large Welding angle is expected to form welding mark defects. As shown in Figure 2 (b), the SVG structure is center-diffusion sequential injection. First open the G2 gate valve pin. When the plastic melt front passes through the G1 and G3 gates, open the G1 and G3 valve pins, and the G2 melt is integrated into the G1 and G3 interiors and pushed forward together until it fills the cavity. During the entire pouring process, no cold stream fusion will be formed, and no fusion mark defects are expected, which is suitable for forming large plastic products.

As shown in Figure 2 (c), the SVG linear progressive type, first open the G3 gate valve pin, when the melt front flows through G2, open the G2 valve pin instantly, G2, G3 melt flow to G1. When the leading edge of the melt flows through G1, the G1 valve pin is opened momentarily until the cavity is filled. The whole process, such as a relay race, sequentially opens the needle valve, and the material flow is transferred to complete the filling. No weld marks are produced. Suitable for forming long plastic parts.

#### 4. Optimization of Injection Molding Process Based on Cae Numerical Simulation of Hot Runner Sequence Control

The appearance of the rear panel of this LED TV is a thin and shallow box structure with a thickness of 1.6 ~ 3.5mm, and its outer dimensions are: 920mm \* 430mm \* 73.8mm. It is selected from Taiwan Chi Mei's universal grade ABS, POLYLAC (ABS + PC). Model PA757 is a commonly used material for electrical enclosures. The main processing performance is shown in Table 1. The injection molding machine of China Haitian Company is selected, model: HTF3300X-B.

Table 1 Pa757 Material Performance Parameters

PROPORTIONg/c m3	SOLUTION TEMPERATU RE °C	MOLD TEMPERATU RE °C	DEMOLDING TEMPERATU RE °C	SHEAR RATE [1/s]	MAXIMUM SHEAR STRESSMPa	MOLDING SHRINKAG E %
1.05	180~240	30~70	84	100000	0.5	0.4~0.7

Table 2 Working Parameters Of Haitian Htf3300x-B Injection Molding Machine

SCREW DIAMETER (mm)	MAXIMUM INJECTION VOLUME (g)	INJECTION SPEED (g/S)	INJECTION PRESSURE (MPa)	CLAMPING FORCE (KN)	MOLD HEIGHT (mm)	EJECTION STROKE (mm)
215	39612	2121	135	33000	900~1900	500

According to product structure and process requirements, Moldflow geometry tools are used to create valve nozzles and runner structures. By determining the optimal gate and quantity, the initial plan determined to use 6-point glue. In order to ensure the pouring balance, the distance from the 6 gates to the entrance of the mainstream channel is consistent and arranged in parallel. As shown in Figure 2, the nozzles Structural modeling should be different from ordinary hot runners, because the valve nozzle has a valve needle in the middle, and the vertical runner section is a “ring” structure. First set the nozzle valve gate as the hot gate attribute. According to the actual hot runner selection, the shape is circular  $D1 = 5\text{mm}$ , named in order:  $G1 \sim G6$ . Set the vertical hot runner attribute and set the inner and outer diameter of the annular runner. It is:  $D = 16\text{mm}$ ,  $d = 5\text{mm}$ ; set the properties of the hot runner, with a diameter of  $16\text{mm}$ ; set the properties of the hot runner, the dimensions of the two ends of the cone are  $d = 8$ ,  $D = 16$ ; the length of each section is set according to the selected hot runner structure set.

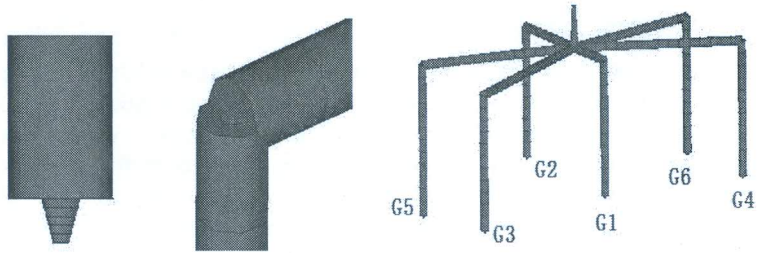


Fig.3 Svg Valve Gate Location and Runner Structure Modeling

By studying the results of the isotherm analysis of the filling, it was found that the initial design scheme was in the molding. When the gate of the  $G1$  valve was opened, the plastic melt did not reach  $G5$  during the injection process, and the isotherm was dense, indicating the flow resistance there Larger, the front melt stays, it is expected that when the  $G5$  valve gate is opened, it cannot reach the position as scheduled, causing the melt to flow backwards and causing welding defects. As shown in Figure 3 (a).

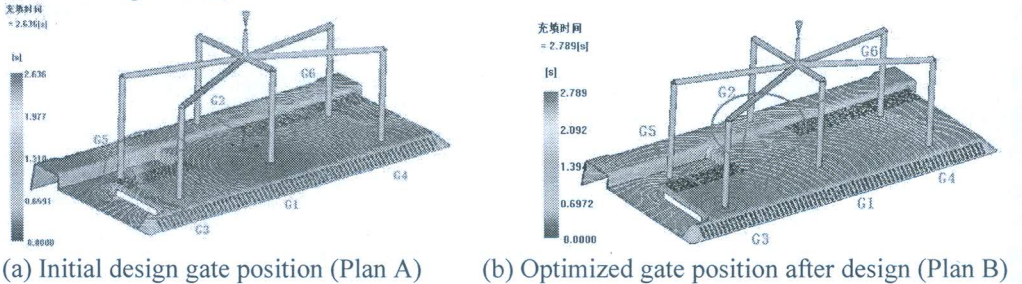


Fig.4 Analysis Results of Filling Time Isotherms

The reason is that the design concept of this runner system is the balance of the gates. When using the hot runner to sequentially control the pouring, the nozzles are opened sequentially and the relay is completed. It is necessary to maintain a close distance between the nozzles. The first



opening gate is too far away from the lower gate, which causes the material flow distance to be too long, leading to the stagnation of the front melt. In addition, the complexity of the structure of the plastic product itself will also lead to the complexity of the melt flow. The solution is to calculate the approximate melt flow distance between valve gates by calculating the melt flow rate, and then through CAE filling experiments, adjust the distance between the nozzles, and set a reasonable pouring position [6]. According to the above method, the gate position is adjusted as shown in Table 3.

Table 3 Svg Nozzle Position Adjustment Table

Gate	G1,G2	G3	G4	G5	G6
initial position (X,Y,Z)	initial position	(305,-175,0)	(290,-150,0)	(300,80,-25)	(280,30,0)
Adjust position (X,Y,Z)	No Adjust	(-200,-60,0)	(-225,-95,0)	(-200,-90,-25)	(-215,25,0)

After the gate position is optimized, the filling analysis is performed again to obtain a stable melt flow state. Based on this, the design and optimization of the structure of the SVG system and the mold runner are carried out.

Based on the hot runner valve gate 6-point injection, two valve gate opening schemes can be formed. Solution A adopts the center diffusion method, that is, the central gate G1 is opened first, and the plastic melt flows toward the other five gates at the same time. When the melt flows through a gate, the gate should be opened instantaneously, and then injected until fill the cavity. As shown in Fig. 3 (a); Solution B: Linear progressive type, that is, the gate G3 on one side is opened first, the plastic melt flows to the gates G1, G2, G5 at the same time, and the plastic melts after the gates of G1 and G2 are opened. The body continues to flow to G3 and G4, and then the gates of G3 and G4 valves are opened until the cavity is filled.

The Moldflow valve gate controller is used to set the opening and closing time of each gate in the A and B schemes. Generally, the initial setting is that the plastic melt front reaches the valve gate, and the delay is 0.2 seconds to open. When numerical simulation is performed, the specific time of valve gate opening and closing is analyzed based on the flow state and displayed on the analysis log. Analysis of the main appearance indicators of the weld line results. It is expected that the location of the larger weld defects will be in the red line area, which will affect the surface quality and structural strength of the plastic parts. The remaining weld lines are small and distributed in the frame and the grille, without affecting the product. Surface aesthetics and strength. Compared with the common hot runner scheme, the two schemes A and B have significantly improved the weld mark defects, and the scheme B is slightly better than the scheme A, so the scheme B is preferred. As shown in Figure 4.

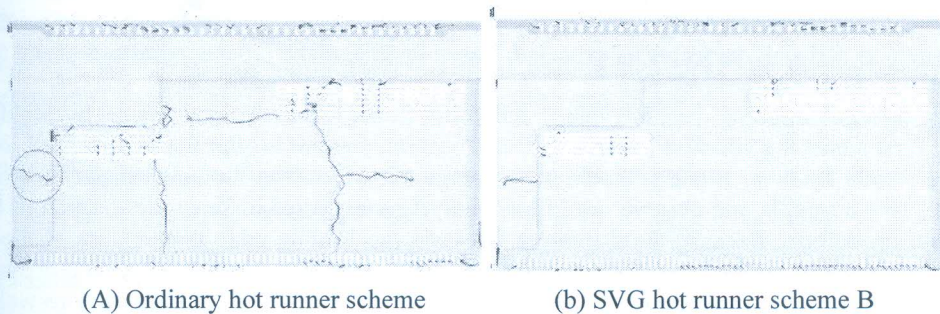


Fig.5 Comparison of Expected Fusion Lines of Various Schemes

Based on Figure 5, the melt flow trend is analyzed. The stream reaches this area and is divided into three streams, A, B, and C. As shown in Figure (a), after each flow, the branches A of A and B merge, and A2 and C fusion will form a weld line at the position shown in Figure (b). The flow diversion caused by the plastic part structure in this area is the main reason for the formation of weld lines. In scheme B, the first nozzle opened is G3 in this area, and the subsequent opening is G5,

so the welding line at 1 position is effectively eliminated, but the welding line at 2 positions cannot be avoided.

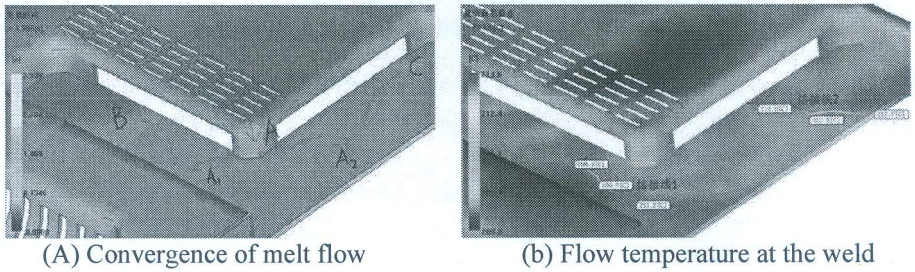


Fig.6 Analysis of Weld Line Formation

The method to solve the welding defects here is ① No treatment is performed. In the analysis, the welding line is only the appearance of the fusion of the melt angles. In the case of the high melt temperature at the front, as shown in (b), the melt temperature at the fusion is about 210°C, The melt temperature is close, which can ensure the effect of stream fusion, and theoretically no welding defects will occur. ② Locally heat the expected welding position. At present, local steam heating is often used for processing, but the mold design is difficult, and additional equipment needs to be added to increase production costs. ③ Start with the design of the cooling system, strictly control the cold water supply time in the area, and do not cool at the fusion time. This method can be used to adjust the waterway during the test.

Based on the above analysis ideas, the relevant time and sequence are continuously fine-tuned, and then Moldflow analysis is used to verify and obtain the optimal time control scheme, as shown in Table 4.

Table 4 Moldflow Needle Valve Opening Time Optimization

	G1(s)	G2(s)	G3(s)	G4(s)	G5(s)	G6(s)
Valve opening time (s)	0.93	1.71	0	1.61	0.90	1.76
Injection time(s)	5	4	5.5	4	5	4

## 5. Tryout Verification

In view of the properties of the household appliance of the rear panel of the LED TV, the requirements for the appearance and dimensional accuracy of the product

High, verify the improvement of the appearance quality of the rear panel of the LED TV after using the SVG control technology, and check whether the location and number of defects such as welding defects and sink marks are as expected. Based on this, make process adjustments and retest the mold.

On the injection molding machine, debug according to the process parameters set by Moldflow analysis. First adjust the injection balance by trial injection, pressurize after the balance, and set the flow rate to 600 cm<sup>3</sup> / s, which is stable in the range of ± 10. After the injected plastic product stabilizes, take a sample and observe. Moldflow analysis is expected to show the location of weld marks and no defects. Because the difference between the leading edge temperature of the two merged melts is only 1°C and the leading melt temperature is 209°C, they are in a state of smooth fusion, so no welding defects occur as expected. G2 valve gate area does not have obvious welding defects. Analysis shows that it is closer to the G2 needle valve gate. It may be that the G5 valve port area has a complex gradient structure and the leading edge flows slowly. During the G2 valve needle opening time, Failure to flow to the G2 position causes the G2 stream recoil to merge with the G5 forward stream and form defects. For the adjustment of G2 opening time, G2 delayed opening is in line with the process requirements, so the time is set according to a 0.2s gradient, and a total of 4 parameters are set from 1.72 to 1.78, and the test die is punched to observe the

elimination of weld marks, which is more reasonable Needle valve opening period. After the trial mode adjustment, the optimized process parameters of the needle valve opening time are shown in Table 5.

Table 5 Optimization of Needle Valve Opening Time after Mold Test Verification

	G1(s)	G2(s)	G3(s)	G4(s)	G5(s)	G6(s)
Valve opening time (s)	0.93	1.76	0	1.61	0.90	1.76
Injection time(s)	5	4	5.5	4	5	4

## 6. Conclusion

Based on the molding CAE numerical simulation, the SVG mold structure is expected to be verified in terms of the number of gates, pouring points, hot runner selection, reserved dimensions, cooling circuit layout, water inlet selection, and insert materials, etc., and optimized accordingly. The mold scheme enables the organic combination of the mold structure and the molding process to achieve the ideal mold test state. Effectively shorten the mold design and manufacturing cycle, improve product quality, and reduce production costs.

Virtually build an injection molding process based on the molding CAE technology. Under the theoretical framework, from the analysis of plastic material performance, the choice of injection molding machine, the estimation of the molding cycle, the setting of the filling-holding pressure-cooling-warping parameters, and then SVG valve gate opening sequence and time are accurately set, and the scheme is compared and selected, which is a process of continuous modification and optimization of the molding process. In the test mode verification of the injection molding machine, adjusting the parameters of the injection molding machine in combination with the actual production is a further process optimization process. The final verification result reflects the excellent molding effect and good product quality.

Practice has proved that the molding CAE numerical technology and hot runner sequence control technology have good application value in molding such large-size, thin-shell plastic products that require higher appearance.

## References

- [1] Wang Chengjun. Application research and industrialization of compression injection molding technology in flat-screen TV casings [A]. CPC Shenyang Municipal Committee, Shenyang Municipal People's Government, Asia-Pacific Academy of Materials Science. Proceedings of the 15th Shenyang Scientific Academic Conference (Science, Engineering, Agriculture and Medicine) [C]. Shenyang: Shenyang Science and Technology Association, 2018: 5-6.
- [2] Han Ran, Wu Chunming. Application of electric heating high-gloss injection mold technology in flat-panel TV face frame molding [J]. Mechanical and Electrical Engineering Technology, 2009,38 (8): 103-105.
- [3] Zhang Weizhong, Liu Tinghua. Needle valve nozzle and its application in hot runner injection mold [J]. Mold Industry, 2002, 10 (7): 46-49.
- [4] Tan Wensheng, Zhou Jianzhong. Control of welding mark of injection molded parts based on valve casting technology [J]. Application of Engineering Plastics, 2006, 21 (7): 37-39.
- [5] Wang Jialong. Thermoplastic injection molding production technology [M]. Beijing: Chemical Industry Press, 2004: 313-314.
- [6] Xia Wei, Zhang Shenghua, et al. Application of valve casting technology in controlling welding marks of large injection molded parts [J]. China Plastics 2009,23 (10): 61-63.

# 高刚性轻量化轴承滚子无心磨自动 上下料装置的设计

傅洁琼<sup>1</sup>, 刘桥方<sup>1</sup>, 李海林<sup>1</sup>, 杨其升<sup>2</sup>

(1. 广州城建职业学院, 广州 510925; 2. 洛阳喜峰机械有限公司, 河南 洛阳 471000)

**摘要:** 用高强度的碳纤维为材料, 以实现轴承滚子切入式无心磨自动上下料装置高刚性轻量化直线运动模组的结构设计。并通过 CAE 辅助软件, 对理论设计运动模组中重要零部件的负载能力进行分析, 所得到分析结果用于优化设计。最终, 分析的理论成果及结构可从试验上得到验证, 同时试验得出的结果也为 CAE 分析提供了修正的数据和依据。

**关键词:** 滚动轴承; 滚子; 自动上下料装置; 高刚性; 轻量化

中图分类号: TH133. 33<sup>+</sup>2; TG580. 23<sup>+</sup>9 文献标志码: B 文章编号: 1000 - 3762(2018) 12 - 0024 - 04

## Design of Automatic Loading and Unloading Device for Centerless Grinding of Rollers of Lightweight Bearings with High Rigidity

FU Jieqiong<sup>1</sup>, LIU Qiaofang<sup>1</sup>, LI Hailin<sup>1</sup>, YANG Qisheng<sup>2</sup>

(1. Guangzhou City Construction College, Guangzhou 510925, China; 2. Luoyang Xifeng Machinery Co., Ltd. Luoyang 471000, China)

**Abstract:** The carbon fibers with high strength are used as materials to realize structural design for liner motion module of automatic loading and unloading device for plunge - cut centerless grinding of bearing rollers. The load capacity of key parts in theoretically - designed motion module is analyzed by using CAE assistant software, and the analysis results are used for optimal design. Finally, the analyzed theoretical results and structure are verified by experiments. The experimental results provide revised data and basis for CAE analysis.

**Key words:** rolling bearing; roller; automatic loading and unloading device; high rigidity; lightweight

## 1 无心磨上下料装置需求分析

### 1.1 无心磨上下料装置的需求及动作说明

轴承滚子无心外圆磨床在轴承滚子生产中作为主要加工设备, 能提供稳定高效及高精度的外圆加工。利用以直线运动模组为基础的机械手进行自动上下料能显著地提高加工效率和加工稳定性, 同时也是自动化趋势发展的需求。分解其基本动作流程为:

- 1) 双伺服插补将砂轮修成需磨削的滚子形状;
- 2) 将热处理后的滚子依次放入上料槽中;
- 3) 由上料手(气缸 + 空气吸盘) 抓起滚子;

4) 由直线运动模组将滚子准确移动至磨削工位, 气缸下行将滚子放入磨削区, 气缸上行由直线运动模组将上料手退回至上料槽上方(准备抓起下一个待磨削滚子);

5) 导轮进给磨削;

6) 导轮退回, 下料手抓起磨削后的滚子由直线运动模组组合件移动至下料槽上方, 气缸下行放下滚子。

### 1.2 直线运动模组问题分析

现直线运动模组一般由基座、导向系统、传动系统、电动机固定座、传动固定座等单元组成。材料一般使用高强度铝合金或钢材料, 传动系统用滚珠丝杠传动, 其运动精度与刚性虽能满足需求, 但存在体积及质量大的缺点, 如行程为 600 mm 的直线模组, 质量约 25 kg(不含驱动电动机)。这样

收稿日期: 2018 - 08 - 01; 修回日期: 2018 - 08 - 26

不仅占用较大的机台空间,而且对原无心磨床进行大结构的改动,才能装置自动上下料直线运动模组和下料机械手,同时会影响磨床后续的调试与维护。

本设计优化了直线运动模组的结构设计与传动系统,并使用铝合金和碳纤维材料,实现直线运动模组小型化、高刚性和轻量化,并应用于无心磨自动上下料装置中。

## 2 新型直线运动模组设计与分析

### 2.1 直线滚珠导轨的设计分析

直线运动模组的核心部件为直线导向系统和动力传动系统。本设计以广泛应用于直线导向系统的直线滚珠导轨为模组基础,进行类型和型号的选择和有限元分析。

#### 2.1.1 直线滚珠导轨的选型

为达到小型上下料装置模组小型轻量目的,综合考虑承载能力与稳定性,选择台湾 HIWIN 的 MGW15C2R830Z1P 加宽型微型导轨,其基本信息与额定载荷见表 1<sup>[1]</sup>。

表 1 直线滚珠导轨基本信息与额定载荷

Tab. 1 Basic information of linear ball guide and rated load

参数	数值
导轨宽度/mm	42
导轨长度/mm	830
滑块宽度/mm	60
组合高度/mm	16
基本额定动载荷/kN	6.77
基本额定静载荷/kN	9.22
容许 $x$ 向力矩/(N·m)	199.34
容许 $y$ 向力矩/(N·m)	56.66
容许 $z$ 向力矩/(N·m)	56.66

#### 2.1.2 直线滚珠导轨承载能力分析

对 MGW15C2R430Z1P 导轨部件各方向承载能力进行有限元分析,其基本信息见表 2。

表 2 直线滚珠导轨的基本材料性能

Tab. 2 Basic properties of material for linear ball guide

参数	数值
质量/kg	2.4
体积/cm <sup>3</sup>	312.2
密度/(kg·m <sup>-3</sup> )	7 700
屈服强度/MPa	6 204
张力强度/MPa	7 238
弹性模量/GPa	210
泊松比	0.28

承载的有限元分析按实际需要模拟悬臂使用场景,即将导轨的一端固定,另一末端的竖直和水平方向按实际需求经验估计值 98 N 载荷进行分

析模拟,结果见表 3。由表可知,导轨在水平方向刚性约是竖直方向刚性的约 18 倍,而应力也达到了 4.7 倍。

表 3 直线滚珠导轨有限元分析结果

Tab. 3 Finite element analysis results of linear ball guide

参数	承载方式	
	竖直载荷 98 N	水平载荷 98 N
最大应力/(N·m <sup>-2</sup> )	$10.8 \times 10^7$	$2.8 \times 10^7$
最大变形/mm	0.338 0	0.018 4
最大应变	$3.2 \times 10^{-8}$	$1.5 \times 10^{-8}$

### 2.2 直线运动模组结构设计与分析

#### 2.2.1 以直线滚珠导轨为基的结构设计

从上述直线导轨承载能力分析结果来看,其在水平方向承载能力很强,而在竖直方向比较弱。因此,需要通过结构件的优化设计进行竖直方向的加强,并以简单巧妙的方法设计传动系统。

在一般情况下,承载方向与重力方向是一致的,结合表 3 的有限元分析结果,需把导轨承载能力强的水平方向承受载荷,所以将导轨宽面,即水平方向倒置为竖直方向用来承受载荷,但原竖直方向倒置而成的水平方向的承载力则需要加强。在此,为达到上下料装置模组轻量化和高刚性的目的,选择碳纤维复合材料为加强板材料来设计横向板,在传动系统上则使用小巧实用的同步带传动系统,将导轨固定座和电动机座融合成一个零件,同时它也是此直线运动悬臂模组的固定基板,而另一侧则将同步轮的惰轮组件和连接座融合成一个连接板,皮带的张紧设计在电动机座一侧。此设计方案极大地简化了结构,同时实现轻量化与高刚性化,具体结构如图 1 所示。

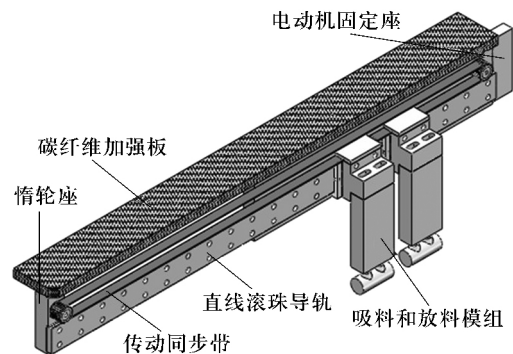


图 1 直线运动模组设计结构图

Fig. 1 Structural design diagram of linear motion module

#### 2.2.2 碳纤维加强板的设计与有限元分析

所使用的碳纤维加强板的长度与导轨的长度均为 830 mm,厚度先设计为 15 mm,宽度为 75 mm,保证其在水平方向的承载能力,以此加强其组合后在导轨水平方向的承载能力。

加强板的碳纤维复合材料选择东丽 T700 ,碳纤维含量为 72% ,树脂含量为 28% ,其材料的基本信息见表 4<sup>[2]</sup>。

表 4 碳纤维复合材料的物理性能信息

Tab.4 Physical properties of carbon fiber composites

参数	数值
质量/kg	1.65
体积/cm <sup>3</sup>	929.4
密度/(kg·m <sup>-3</sup> )	1770
屈服强度/MPa	4500
张力强度/MPa	5550
弹性模量/GPa	185
泊松比	0.307

承载能力的分析计算同样采用一端固定,末端分别承受竖直方向和水平方向的载荷均为 98 N 为例 结果见表 5。

表 5 碳纤维加强板有限元分析结果

Tab.5 Finite element analysis results of plate reinforced by carbon fiber

参数	承载方式	
	竖直载荷 98 N	水平载荷 98 N
最大应力/(N·m <sup>-2</sup> )	20.3 × 10 <sup>6</sup>	7.0 × 10 <sup>6</sup>
最大变形/mm	0.420	0.019
最大应变	8.1 × 10 <sup>-5</sup>	2.4 × 10 <sup>-5</sup>

通过分析,碳纤维加强板质量为 1.65 kg,其刚性要比直线滚珠导轨大 8 倍,其水平方向的刚性承载能力是垂直方向的 21 倍,强度为 3 倍。

将此碳纤维加强板的水平面与直线滚珠导轨的垂直面相结合,使该直线运动模组的承载能力在竖直和水平方向都满足使用要求。

### 2.3 直线运动模组的有限元分析

#### 2.3.1 直线运动模组设计说明

为方便 CAE 软件计算,模拟分析将直线运动模组中的基座、直线滚珠导轨、碳纤维加强板和惰轮座作为一个整体进行有限元分析。其中基座和惰轮座材料均为 6061 铝合金<sup>[3]</sup>,总质量约 9 kg,其刚性模组三维结构如图 2 所示。

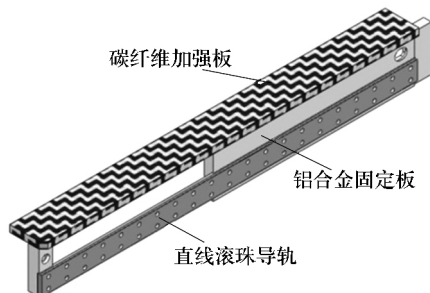


图 2 直线运动模组的整体有限元分析结构图

Fig.2 Overall structure diagram of finite element analysis of linear motion module

#### 2.3.2 直线运动模组有限元分析

与上述的分析方式一样,采用固定块固定,末端面分析以竖直方向和水平方向承受载荷的方式进行分析模拟,结果如图 3 和图 4 所示。

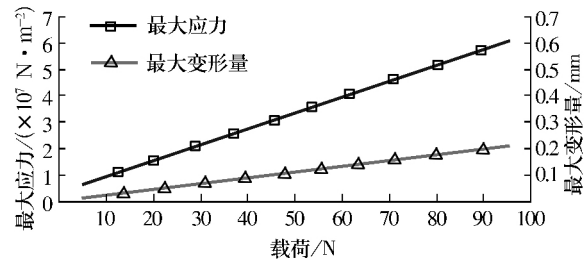


图 3 竖直方向末端载荷-应力/变形量关系

Fig.3 Relationship between stress/deformation-load at end in vertical direction

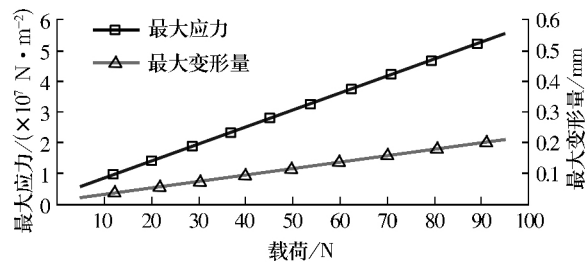


图 4 水平方向末端载荷-应力/变形量关系

Fig.4 Relationship between stress-deformation-load at end in horizontal direction

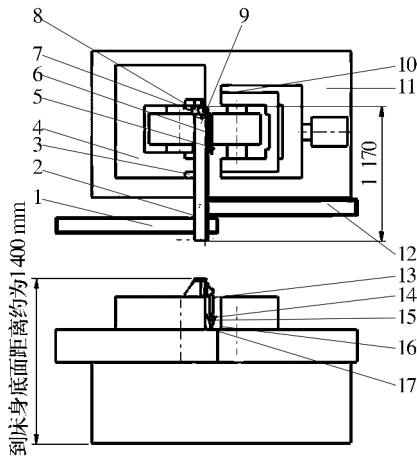
从上述分析的结果来看,该直线运动模组在垂直方向和水平方向完全可以承受 98 N 载荷,承载能力和刚性方面完全可以得到保障。另外模组在垂直方向的载荷或振动可以通过调整碳纤维加强板的尺寸来解决。

## 3 实际应用

对于中小型轴承滚子(特别是  $D_w \leq 20$  mm),由于滚子小而精密,把高刚性轻量化的单导轨悬臂式直线运动模组应用在无心磨上下料装置<sup>[4]</sup>,在设备的实际使用中获得了显著的效果。具体有以下 3 个方面:1) 其单导轨悬臂的运动方式,可以将机械手臂直接固定在砂轮架上,运行稳固可靠,并且不会干涉设备的操作<sup>[5]</sup>;2) 如需更换砂轮时,其调试复位时间也大为缩短;3) 经过高刚性轻量化设计后,模组的质量由 25 kg 减至 10 kg,上下料时的动作快速平稳,提升了加工效率。其具体实际应用如图 5 和图 6 所示。



图5 自动上下料装置应用于轴承精密滚子无心磨床  
Fig.5 Automatic loading and unloading device for centerless grinder for roller of precision bearing



1—上料槽; 2—复合碳纤维加强板; 3—支架; 4—砂轮架; 5—上料手; 6—下料手; 7—驱动电动机; 8—传动同步带; 9—直线运动模组; 10—导轮架; 11—床身; 12—下料槽; 13—气缸; 14—吸盘; 15—工件; 16—导轮; 17—砂轮

图6 应用于轴承生产中无心磨床自动上下料装置布局图  
Fig.6 Layout of automatic loading and unloading device of centerless grinder used in bearing production

### 4 结束语

为实现轴承滚子切入式无心磨上下料装置直线运动模组高刚性轻量化,本设计采用直线滚珠导轨以优化导向系统,同时采用碳纤维板加强模组水平方向的承载力。在结构上将2个主要支撑部件进行强度和刚性的相加,实现了水平和竖直2个方向的同时加强。使其在刚性、强度等力学性能与传统直线运动模组相当的情况下,其总质量仅为传统设计的40%,而使用更为高效与灵活。这种结构直线运动模组可以结合实际需求,借助有限元分析,在实际机构设计中进行灵活的变更与改进。

### 参考文献:

[1] 王华. 数控机床功能部件优化设计选型应用手册: 滚动直线导轨副分册 [M]. 北京: 机械工业出版社, 2017: 89 - 91.  
 [2] 贺福. 碳纤维及其应用技术 [M]. 北京: 化学工业出版社 2015: 45 - 50.  
 [3] 潘复生 张丁非. 铝合金及应用 [M]. 北京: 化学工业出版社 2006: 12 - 13.  
 [4] 张宝珠. 典型精密零件机械加工工艺分析及实例 [M]. 北京: 机械工业出版社 2017: 56 - 57.  
 [5] 日技能士の友編集部. 磨床操作 [M]. 北京: 机械工业出版社 2010: 79 - 80.

(编辑: 侯万果)

### 国家标准委下达 2018 年第三批国家标准制修订计划

2018 年 9 月 27 日,国家标准委以国标委发[2018]60 号文下达了 2018 年第三批国家标准制修订计划。本批计划中滚动轴承领域涉及的计划项目 6 项,如下表所示:

序号	计划编号	项目名称	制/修订	采用国际标准	起草单位	项目周期
1	20181684 - T - 604	滚动轴承 振动测量方法 第 1 部分: 基础	修订	ISO 15242 - 1: 2015	杭州轴承试验研究中心有限公司等	2 年
2	20181685 - T - 604	滚动轴承 外圈上的止动槽和止动环尺寸、产品几何技术规范 (GPS) 和公差值	修订	ISO 464: 2015	洛阳轴承研究所有限公司等	2 年
3	20181686 - T - 604	滚动轴承 振动测量方法 第 2 部分: 具有圆柱孔和圆柱外表面的向心球轴承	修订	ISO 15242 - 2: 2015	杭州轴承试验研究中心有限公司等	2 年
4	20181687 - T - 604	滚动轴承 振动测量方法 第 4 部分: 具有圆柱孔和圆柱外表面的圆柱滚子轴承	修订	ISO 15242 - 4: 2017	洛阳轴承研究所有限公司等	2 年
5	20181688 - T - 604	滚动轴承 振动测量方法 第 3 部分: 具有圆柱孔和圆柱外表面的调心滚子轴承和圆锥滚子轴承	修订	ISO 15242 - 3: 2017	洛阳轴承研究所有限公司等	2 年
6	20181689 - T - 604	滚动轴承 无内圈冲压外圈滚针轴承 外形尺寸、产品几何技术规范 (GPS) 和公差值	修订	ISO 3245 - 2015	洛阳轴承研究所有限公司等	2 年

# 塑料科技®

ISSN1005-3360  
CN 21-1145/TQ

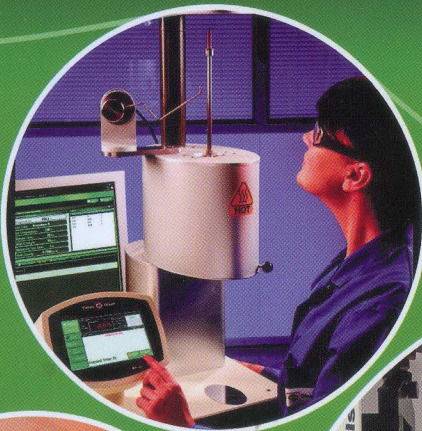
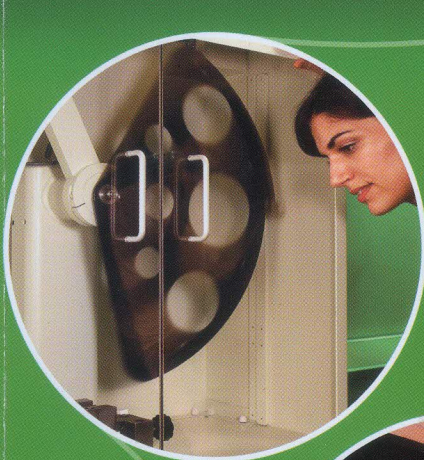
## Plastics Science and Technology

■ 中文核心期刊 ■ 中国科技核心期刊 ■ CA/AJ收录期刊 ■ 荣获首届《CAJ-CD规范》执行优秀奖

### 材料测试解决方案 全面提升橡塑产品竞争力

我们的仪器可进行如下测试：

- 拉伸测试
- MFR
- 悬臂梁测试
- 熔融指数
- 弹性测试
- 维卡测试
- 撕破测试
- 热变形测试
- 硬度测试
- 简支梁指数
- MVR
- 脆性测试



  
**SDL ATLAS®**

SDL Atlas Ltd. 锡莱亚太拉斯有限公司

深圳 电话: 86 (755) 2671 1168  
香港 电话: (852) 3443 4888  
北京 电话: 86 (10) 6581 5766  
上海 电话: 86 (21) 6121 3788  
电邮: info@sdlatlas.com.cn

传真: 86 (755) 2671 1337  
传真: (852) 3443 4999  
传真: 86 (10) 6581 1722  
传真: 86 (21) 6121 3799  
网址: <http://www.sdlatlas.com.cn>

ISSN 1005-3360



9 771005 336074



2018 · 3

第46卷/月刊 (总第311期)

<http://slkj.cbpt.cnki.net>



## 全国塑料制品标准化技术委员会 塑料制品分技术委员会 (SAC/TC48/SC1)秘书处

### 国家轻工业塑料产品质量监督检测大连站 暨辽宁省塑料制品质量监督检验中心

本站是依法批准建立的塑料产品专业检验机构，是经过国家认证认可监督管理委员会和辽宁省质量技术监督局审查认可和授权具有法定权威性和第三方公正性的塑料专业检验机构。



#### 服务内容

- 各种塑料制品、化学建材以及树脂原料的物理机械性能、化学、电性能、卫生性能的分析检测工作。
- 产品质量争议仲裁检验。
- 社会各界与生产企业委托检验。
- 各职能部门或地方政府的委托监督检验。
- 塑料检测及标准化咨询服务。
- 新产品、新材料的鉴定检验及企业标准的制修订服务。
- 塑料检测人员的技术培训。



地址：大连市甘井子区周家街11号 邮编：116033

电话/传真：0411-86600730

E-mail: dlsj@dysy-cn.com, 308838170@QQ.com

#### 行业动态

高强度、抗穿刺BOPE薄膜新产品	31
美国公司发布新型高阻隔金属化聚酯薄膜	35
西班牙能源集团Repsol生产抗冲击性TPOs	39
亨斯迈面向制鞋厂商推出新型快速循环TPU	45
英国塑料联合会与多方专家就海洋垃圾问题开展合作	54
Bertrandt公司和西格里集团推出创新的碳纤维支架技术	61
松原印度工厂着手生产 SONGNOX® 5650抗氧化剂	65
Teknor Apex推出用于汽车车窗密封的低光泽PVC化合物	84
防水卷材火起来！亚洲首条TPO生产线下月青岛投产	84
英国塑料回收商Axion支持垃圾填埋	84
智能车门拉手 帝人创新薄膜科技来助力	90
纽约大学科学家开发深海潜水艇3D打印复合泡沫材料	90
中国石化首款BOPP电容器膜料成功打入市场	96
住友化学向北美市场推出高性能热塑性塑料	96
Belgrade将在2018年加快生产塑料桶内衬	96
快递封装用品新标准发布宜采用生物降解塑料	96
科莱恩亮相2018TCT亚洲展 展示最新3D打印材料及服务	101
茂名石化：成功试产出两种流延聚乙烯膜料	106
西门子和SABIC合作生产热塑性复合材料	110
威猛巴顿菲尔携高科技设备和工艺技术参展Chinaplas	115
俄罗斯首次在道路建设中使用大量PPC塑料	119
欧洲制造商研发出一种高性能PE抗静电膜	124
华曙高科与巴斯夫联合推出新型3D打印PA6材料	128
西班牙Poligal公司在波兰西部建成BOPP工厂	128
孩儿喜牌儿童机能鞋因增塑剂超标被召回	139
Teknor Apex开始在欧洲供应尼龙回料	139
用手看心电图？日本开发出可伸缩薄膜显示屏	139

## 目次

#### 本刊启事

本刊已许可中国学术期刊(光盘版)电子杂志社在中国知网及其系列数据库产品中以数字化方式复制、汇编、发行、信息网络传播本刊全文。作者著作权使用费与本刊稿酬一次性给付。作者向本刊提交文章发表的行为即视为同意我刊上述声明。

《塑料科技》编辑部

# 塑料科技<sup>®</sup>

SULIAO KEJI

中文核心期刊 中国科技核心期刊

■ CA收录期刊 ■ AJ收录期刊

■ 荣获首届《CAJ-CD规范》

执行优秀奖

月刊·公开发行·1973年创刊

邮发代号：8-177

第46卷第3期 (总第311期)  
(2018年3月10日出版)

● 主管：辽宁省经济和信息化委员会

● 主办：大连塑料研究所有限公司  
中国塑料加工工业协会  
深圳市高分子行业协会  
大连市塑料行业协会

● 协办：锡莱亚太拉斯有限公司

● 编委会主任委员：曹俭

● 编委会副主任委员：孙成伦 吴宪  
乔文路

● 编委 (按姓氏笔划排序)：

于文杰 于翔 王成云 王克智  
王海鹰 王敏杰 戈明亮 田福祥  
田岩 冯钠 刘妹 刘俊龙  
何冰强 金晓明 罗居杰 杨雅琦  
戚春晓 甄卫军 雷文

● 编辑及出版：《塑料科技》编辑部  
(116033 大连市周家街11号)

● 电话/传真：(0411) 86601793

● http://slkj.cbpt.cnki.net

● E-mail: slkj@dsy-cn.com

● 名誉主编：于文杰

● 主 编：王海鹰

● 本期编辑：王海鹰

● 英文编辑：王海鹰

● 印刷：大连市东晟印刷有限公司

● 发行：大连市邮政局

● 订阅：全国各地邮政局

ISSN 1005-3360

● 中国标准连续出版物号：CN 21-1145/TQ

● 广告经营许可证：许可证号201019

● 刊名商标注册证：第744147号

● 定价：每本18.00元

● 国外发行：中国国际图书贸易集团有限公司  
(北京市海淀区车公庄西路35号)

● 国外发行代号：M3311

● 广告联络：大连 联系人：肖红

电 话：0411-86598957

传 真：0411-86601793

深圳 联系人：叶远锋

电 话：0755-83461622

传 真：0755-83461657

E-mail: szsj2004@126.com

## ● 理论与研究

- 不同类型聚氨酯微孔膜的制备与性能 ..... 27  
刘美惠, 沈惠玲
- ABS高胶粉对ABS/PET/PETG合金的增韧研究 ..... 32  
王美琳, 刘晓丽, 李志英, 刘凤岐
- PEEK/GF/CNTs复合材料的制备及性能研究 ..... 36  
吴立豪, 曲敏杰, 宁 洋, 乔占凤, 万长宇
- UV本体聚合制备压敏胶的性能研究 ..... 40  
贺贝贝, 解一军
- 溢流槽对微注塑成型iPP制品的增强作用 ..... 46  
刘忠柱, 李乐乐, 郑国强, 秦 琦, 米立伟
- 无机粒子改性PPR复合材料力学性能研究 ..... 51  
李统一, 宋科明, 王 禹, 胡伦根
- GE/AlN/CO-PA导热复合材料的制备与性能研究 ..... 55  
刘 欣, 杨 哲, 魏红林, 房关彪, 何海峰
- PB/红麻复合材料的力学性能研究 ..... 62  
贾 婷, 曲敏杰, 郝俊喆, 成丽清, 陈志娟, 王书唯, 张勇杰

## ● 加工与应用

- 超细活性碳酸钙在PVC电线电缆料中应用的研究 ..... 66  
宋建强, 彭鹤松, 甘昆秀, 冯才敏
- 复合型成核剂在聚丙烯T30S中的应用研究 ..... 70  
王 悦, 黄 捷, 王 波, 汤粤豫, 田小艳

## ● 生物与降解材料

- 竹炭增强膨胀阻燃聚乳酸的制备及其热降解行为研究 ..... 73  
赵 巍, 齐先志, 王晓霖
- 可完全生物降解PLA/PPA/PBS薄膜的制备与性能研究 ..... 78  
张 也, 张会良, 李 义, 佟 毅, 刘志刚
- 阻燃竹纤维增强聚乳酸复合材料降解性能的研究 ..... 85  
庞锦英, 陆春道, 蓝春波, 莫美忠, 刘钰馨, 黄春兰, 谭登峰

## ● 计算机辅助技术

- 基于灰色关联度和BP神经网络的多级注塑成型工艺参数优化 ..... 91  
车应田, 刘泓滨, 火寿平
- 基于Polyflow的塑料流延模具设计与仿真分析 ..... 97  
孙全颖, 曲汐研
- 基于BP-TGA算法的注塑成型工艺参数优化 ..... 102  
曹素兵, 朱 婵
- 挤出机头流道的有限元模拟和优化 ..... 107  
贾 辉, 张礼华, 邱建成

## ● 塑机与模具

- U型装饰卡条热流道注塑模设计 ..... 111  
汤小东
- 聚丙烯装置挤压造粒机切刀使用寿命影响因素及改进方案 ..... 116  
雷佳伟
- 按钮注塑CAE与双斜抽芯机构模具设计 ..... 120  
李有兵

## ● 理化测试

- 婴幼儿塑料奶瓶中二苯甲酮和4-甲基二苯甲酮等光引发剂的  
UHPLC-MS/MS测定 ..... 125  
赵 凯, 周 勇, 丁枫芸, 徐坚琪, 卢 伦, 何晖晖

## ● 助剂

- 六苯氧基环三磷腈对PA6阻燃性能的影响 ..... 129  
周 旺, 龙丽娟, 于 杰

## ● 评述

- 无针熔体静电纺丝的研究进展 ..... 134  
杨 涛, 何雪涛, 丁玉梅, 谭 晶, 杨卫民, 李好义
- 当今世界淀粉塑料行业的发展现状——北美 ..... 140  
郭 斌, 韩梓军, 薛 灿, 银 鹏, 李益欣, 梁 浩
- 单组分膨胀型阻燃剂的研究进展 ..... 144  
刘 巍, 江文雪, 孔 淳, 黄浩祺, 于守武

## ● 专利介绍

- 国外塑料专利 ..... 150
- 中国塑料专利 ..... 151

## ● Theory and Research

- Preparation and Properties of Different Types of Polyurethane Microporous Membranes ..... 27  
*Liu Meihui, Shen Huiling*
- Study on ABS/PET/PETG Alloy Toughened by ABS High Rubber Powder ..... 32  
*Wang Meilin, Liu Xiaoli, Li Zhiying, Liu Fengqi*
- Study on Preparation and Properties of PEEK/GF/CNTs Composites ..... 36  
*Wu Lihao, Qu Minjie, Ning Yang, Qiao Zhanfeng, Wan Changyu*
- Study on the Properties of Pressure-Sensitive Adhesive Prepared by UV Bulk Polymerization ..... 40  
*He Beibei, Xie Yijun*
- Enhancement Effect of Overflow Slot on Micro Injection Molding iPP Products ..... 46  
*Liu Zhongzhu, Li Lele, Zheng Guoqiang, Qin Qi, Mi Liwei*
- Study on Mechanical Properties of PPR Composites Modified by Inorganic Particles ..... 51  
*Li Tongyi, Song Keming, Wang Yu, Hu Lungen*
- Study on Properties of GE/AlN/CO-PA Thermal Conductive Composites and Its Preparation ..... 55  
*Liu Xin, Yang Zhe, Wei Honglin, Fang Guanbiao, He Haifeng*
- Study on Mechanical Properties of PB/Kenaf Composites ..... 62  
*Jia Ting, Qu Minjie, Hao Junzhe, Cheng Liqing, Chen Zhijuan, Wang Shuwei, Zhang Yongjie*

## ● Processing and Application

- Study on Application of Ultrafine Activated Calcium Carbonate in PVC Wire and Cable ..... 66  
*Song Jianqiang, Peng Hesong, Gan Kunxiu, Feng Caimin*
- Study on Application of Compound Nucleating Agent in Polypropylene T30S ..... 70  
*Wang Yue, Huang Jie, Wang Bo, Tang Yueyu, Tian Xiaoyan*

## ● Biological and Degradable Material

- Study on Preparation and Thermal Degradation Behavior of Intumescent Flame Retardant PLA Reinforced with BPC ..... 73  
*Zhao Wei, Qi Xianzhi, Wang Xiaolin*
- Study on Preparation and Properties of Fully-Biodegradable PLA/PPA/PBS Blown Films ..... 78  
*Zhang Ye, Zhang Huiliang, Li Yi, Tong Yi, Liu Zhigang*
- Study on the Degradation of Flame Retardant Bamboo Fiber Reinforced PLA Composites ..... 85  
*Pang Jinying, Lu Chunyi, Lan Chunbo, Mo Xianzhong, Liu Yuxin, Huang Chunlan, Tan Dengfeng*

## ● Computer Aided Technology

- Optimization for Multi-Stage Injection Process Parameters Based on Gray Relational Grade and BP Neural Network ..... 91  
*Che Yingtian, Liu Hongbin, Huo Shouping*
- Design and Simulation Analysis of Plastic Cast Mould Based on Polyflow ..... 97  
*Sun Quanying, Qu Xiyun*
- Optimization on Injection Process Parameters Base on BP-TGA Algorithm ..... 102  
*Cao Subing, Zhu Chan*
- Finite Element Simulation and Optimization for Extrusion Head Runner ..... 107  
*Jia Hui, Zhang Lihua, Qiu Jiancheng*

## ● Plastic Machinery and Mold

- Design of Hot Runner Injection Mold for U-type Decorative Strip ..... 111  
*Tang Xiaodong*
- Influencing Factors and Improvement Scheme of Service Life of Cutting Knife for Extruding Granulator of Polypropylene Plant ..... 116  
*Lei Jiawei*
- Mould Design of Button Injection CAE and Double Inclined Core Pulling Mechanism ..... 120  
*Li Youbing*

## ● Physical and Chemical Tests

- Determination of Benzophenone and 4-Methylbenzophenone in Infant Plastic Bottle by UHPLC-MS/MS ..... 125  
*Zhao Kai, Zhou Yong, Ding Fengyun, Xu Jianqi, Lu Lun, He Huihui*

## ● Additives

- Effect of Hexaphenoxycyclotriphosphazene as Flame Retardant on PA6 ..... 129  
*Zhou Wang, Long Lijuan, Yu Jie*

## ● Review

- Research Progress of Needleless Melt Electrospinning ..... 134  
*Yang Tao, He Xuetao, Ding Yumei, Tan Jing, Yang Weimin, Li Haoyi*
- Present Status of Starch Plastics Industry in North America ..... 140  
*Guo Bin, Han Zijun, Xue Can, Yin Peng, Li Panxin, Liang Hao*
- Research Progress of Single-molecule Intumescent Flame Retardants ..... 144  
*Liu Wei, Jiang Wenxue, Kong Chun, Huang Haozhen, Yu Shouwu*

National Chinese Core Journal  
Source Journal for Chinese Scientific  
and Technical Papers and Citations

- CA and AJ covered
- Outstanding execution prize  
of national CAJ-CD criterion

Vol. 46 / No. 3

Series No. 311

Published on March 10 2018

● Sponsor:

**Dalian Plastics Research  
Institute Co., Ltd.**

**China Plastics Processing Industry  
Association**

**Shenzhen Polymer Association**

**Dalian Plastics Industry Association**

● Publisher and Editor:

**Editorial Office of Plastics  
Science and Technology**

**No.11 Zhou Jia Street, Dalian**

● Post Code: **116033**

● Telephone/Fax:

**(86) (0411) 8660 1793**

● http: //slkj.cbpt.cnki.net

● E-mail: slkj@dsy-cn.com

● Honorary Editor-in-Chief: **Yu Wenjie**

● Editor-in-Chief: **Wang Haiying**

● Duty Editor: **Wang Haiying**

● English Editor: **Wang Haiying**

● Production:

**Dalian Dongsheng Printing Co., Ltd.**

● Distributor Abroad:

**China International**

**Book Trading Corporation**

(35 Chegongzhuang Xilu, Haidian District, Beijing)

● Distributive Code Abroad: **M3311**

● Advertising Sales Manager:

(Dalian) **Xiao Hong**

**Tel:0411-86598957**

**Fax:0411-86601793**

(Shenzhen) **Ye Yuanfeng**

**Tel:0755-83461622**

**Fax:0755-83461657**

**E-mail: szsj2004@126.com**

# 按钮注塑CAE与双斜抽芯机构模具设计

## Mould Design of Button Injection CAE and Double Inclined Core Pulling Mechanism

李有兵 Li Youbing

- 广州城建职业学院, 广东 广州 510925  
- Guangzhou city construction college, Guangzhou 510925, China

**摘要:** 分析了塑料按钮的结构及成型工艺, 针对塑件材料性能、外部形状及内部深腔特征, 设计了对称分布的注塑模具结构, 包括: 将二套双斜导柱的侧向分型抽芯机构用于同一模具, 采用塑件内凹为顶出位和确保开合模行程有效的复位结构及其模具的浇注系统、组合式的型腔、复位及顶出机构等。并就浇注系统进行注射模流分析, 同时得到了: 模具充填时间为0.595 6 s; 塑件顶出时间为82.34 s; 最大注射压力为27.293 5 MPa; 最大锁模力为6.520 7 t, 为注塑按钮制品提供了参考。

**Abstract:** The structure and molding process of the plastic button are analyzed. According to the plastic material properties, external shape and internal deep cavity characteristics, an injection mold structure with symmetrical distribution is designed. It includes the following two parts: the double side inclined guide column's side parting core pulling mechanism is used for the same mold, and the structure of the concave part of the plastic part is used as the top and out position to ensure the effective running of the opening and closing die, and the gating system, the combined cavity, the reset and ejection mechanism of the mould. The injection mold flow analysis of the gating system is carried out. At the same time, the mold filling time is 0.595 6 s, the ejection time of the plastic part is 82.34 s, the maximum injection pressure is 27.293 5 MPa, the maximum clamping force is 6.520 7 T, which provides a reference for injection button products.

**关键词:** 按钮; 注塑CAE; 模具; 双斜侧抽芯

中图分类号: TP391.7

文献标识码: A

**Key words:** Button; Injection CAE; Mould; Double oblique side core pulling

热塑性塑料注塑模具设计时, 模具的成型部件、浇注系统、脱模机构以至于模具的具体加工工艺, 都必须考虑塑料原材料的性能、塑件尺寸、技术要求及制品的使用场合, 以确保满足产品的使用<sup>[1-2]</sup>。下面结合双斜侧抽芯机构在按钮注塑模具中的应用, 就注塑模设计的一般过程进行了探讨。

## 1 结构特点

图1所示为按钮及其实体造型。该产品为一长方体形塑件, 一端为凸圆弧形, 另一端是中间半圆内凹, 在半圆内凹端有一保证壁厚均匀的结构设计, 它是R4.5的半圆扇面, 深24.3 mm的掏空深腔, 长方体二个主表面分布有四个呈扇形排列的凹槽, 一个 $\phi 6$  mm的通孔, 另有一带内六角台阶 $\phi 3.6$  mm的通孔。产品材料为改性丙烯腈-丁二烯-苯乙烯塑

料(ABS), 需对塑件表面进行镀前抛光。

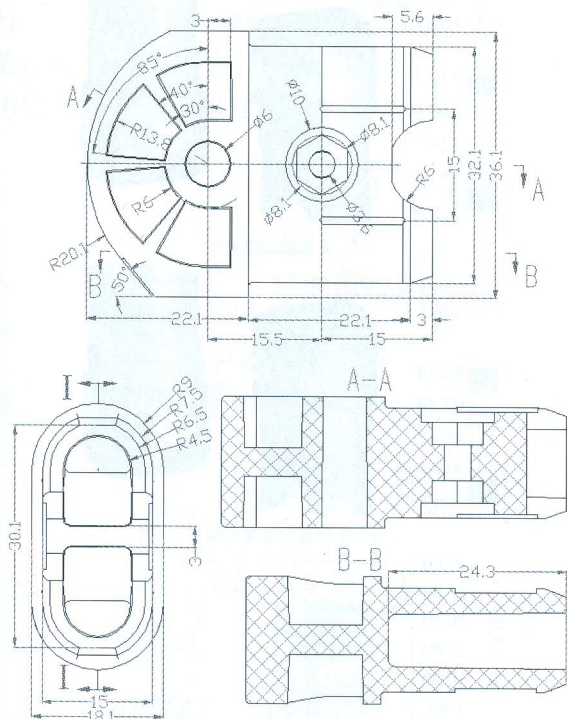
从图1可见, 按钮制品结构复杂, 成型相互垂直的塑件主表面与掏空深腔是注塑模具的设计重点; 按钮结构具有不对称性, 为尽可能使模具受力均匀, 提高注射效率, 降低模具制造成本, 按钮模具采用一模二腔形式。

## 2 成型工艺分析

### 2.1 材料分析

ABS是一种由三种单体聚合而成的非结晶型高聚物, 具有强度高、韧性好、不透明等优点, 综合性能优良、用途广泛, 适合用于生产复杂形状制品, 塑件成型后有较好的光泽。ABS的密度为1.02~1.05 g/cm<sup>3</sup>。因ABS中有丁二烯, 其耐热性不高, 为避免制品与模具黏连, 在注塑时一般设置定模温度为

70~80℃,动模为50~60℃。



(a) 塑件尺寸

(b) 塑件3D

▲ 图1 按钮及造型  
Fig.1 Button and shape

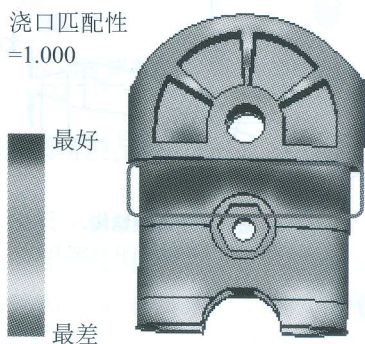
## 2.2 塑件结构与分型

从图1可见,按钮内表面可通过一个型芯成型。考虑到用户使用时与R20.1处圆弧面接触及尽可能达到成型时平衡注射,制品外表面可采用二瓣对开组合凹模和一侧向凹模组合的形式。塑件中 $\phi 6$  mm、 $\phi 3.6$  mm通孔和内六角台阶采用镶嵌型芯成型。

为保证塑件主要表面的成型,使分型面处在最大断面尺寸处,且尽可能与开合模方向平行,按钮的主分型面确定在如图1中I-I所示平面位置。而塑件内掏空深腔的成型可采用一侧向分型与抽芯机构。上述分型面与侧向分型及抽芯机构的构造,也满足了模具注射过程中排气与脱模时的进气需要。

## 2.3 制品工艺质量

按钮整体尺寸不大,具有较大的壁厚,最薄处为2 mm。从图2运用模流分析软件MFI对按钮最佳浇口位置的分析结果中可见,在图2中框选位置即塑件的中间部位可作为浇口开设位置,同时在适当控制原材料干燥度、料流及模具温度的情况下,制品产生缩孔和气泡等缺陷的可能性很小。



▲ 图2 浇口位置分析  
Fig.2 Gate position analysis

## 3 浇注系统

### 3.1 浇注系统设计

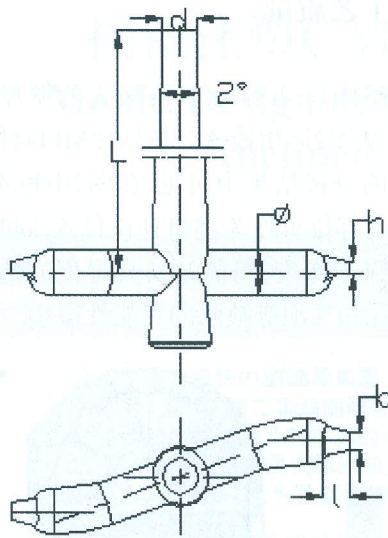
本模具结构为一模二腔,同时塑件外表面不允许有缺陷。考虑生产过程的连续性,为方便取料和实现塑件与浇注系统联接处的自动分离,采用带直流通道与分流道的潜伏式点浇口。为便于拉出主流道凝料,将主流道设计成 $2^\circ$ 圆锥,内表面粗糙度 $R_a$ 为0.8。考虑分流道出料方便,易于制造,热量损失、流动阻力、比表面积等均较小,参考动板与定模的组合形式,分流道采用圆形截面。

按钮塑件体积为 $13.7 \text{ cm}^3$ ,质量为14.4 g。查参考文献<sup>[7]</sup>,选取理论注射量为33 g的注射机,其喷嘴部位直径 $d_0=3.5$  mm,主流道入口(与注射机喷嘴相连处)直径 $d=d_0+(0.5\sim 1)=4$  mm;主流末端直径为:

$$D = d + 2L \tan \frac{\alpha}{2} = 6.3 \text{ mm} \quad (1)$$

式中: $d$ —主流道入口直径, mm; $d_0$ —注射机喷嘴直径, mm; $D$ —流道末端直径, mm; $L$ —主流道全长, mm; $\alpha$ —主流道锥角,  $^\circ$ 。

分流道的设计参考文献<sup>[3-5]</sup>中浇注系统的分流道参数设计部分。浇注系统结构如图3所示。

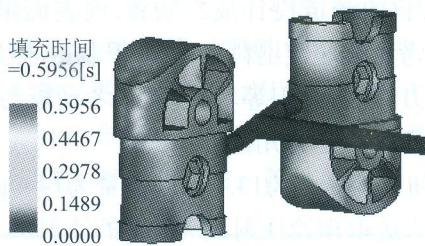


▲ 图3 浇注系统结构

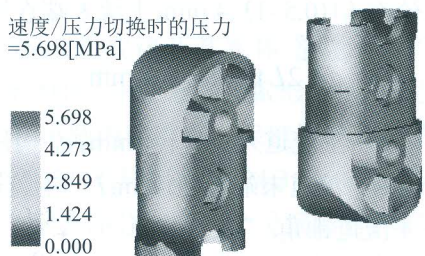
Fig.3 Structure of pouring system

### 3.2 模流分析

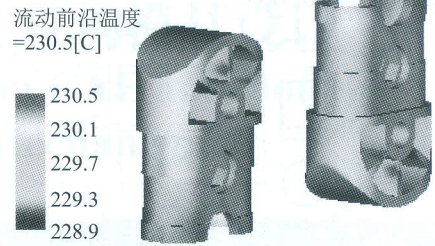
在模具中,浇注系统直接决定了注塑件质量的好坏,借助Moldflow软件对设计的浇注系统进行注塑模流分析,可有效减少试模修模次数。图4为利用MFI对按钮塑件进行模流分析的结果,可见:模具浇注充填需时0.595 6 s(图(a));注射时从速度控制切换为压力控制时的压力5.698 MPa(图(b));熔体流动前沿温度是228.9~230.5℃(图(c));达到塑件顶出时间为82.34 s(图(d));最大注射压力在0.588 7 s时出现,为27.293 5 MPa(图(e));最大锁模力为6.520 7 t,如图4(f)所示。



(a) 充填时间



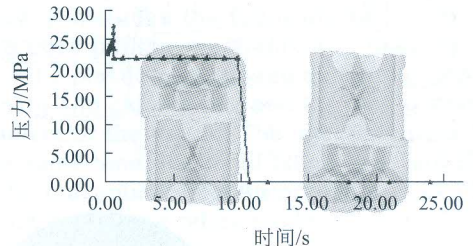
(b) 速度/压力切换时的压力



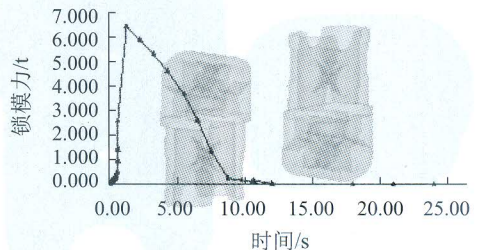
(c) 流动前沿温度



(d) 达到顶出温度时间



(e) 注射压力



(f) 锁模力

▲ 图4 模流分析

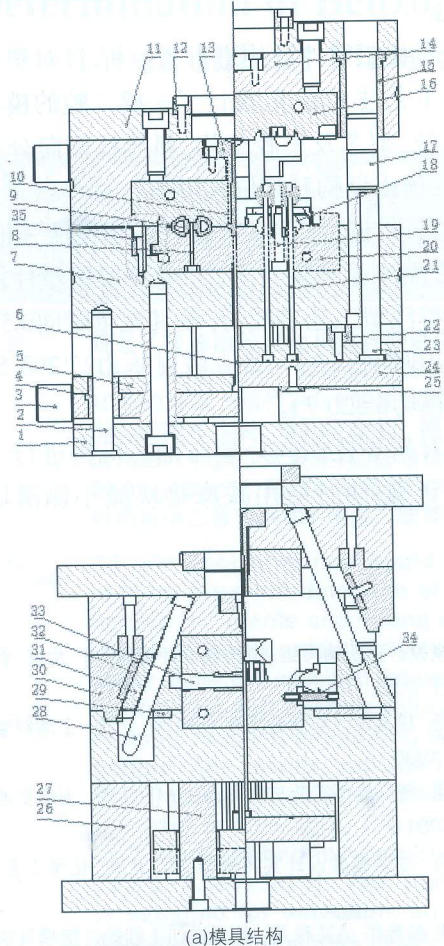
Fig.4 Model flow analysis

由图4(b)可见,料流在型腔中流动末端处压力为0(A、B处有未被填充部分),而塑件中其他部位压力梯度分布均匀,表明注塑期间无滞流、溢料等;从图4(c)熔体流动前沿温度看,注塑时料流前沿温度与料温(熔体注射温度230℃)接近,其温度波动远小于正常的2~5℃,熔体充填理想。上述结果表明,浇注系统设计合理,达到了注塑时的流动平衡,适合按钮塑件注塑成型。

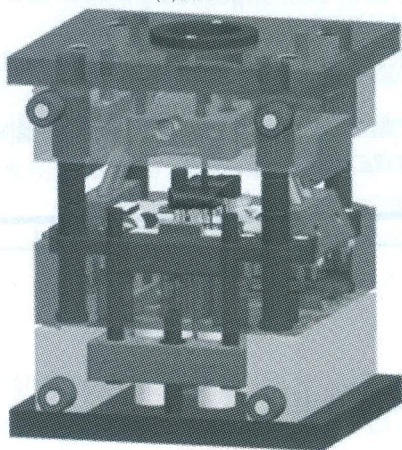
## 4 模具结构

模具的设计主要包括浇注系统、型腔、导向机构、复位机构及顶出机构等。图5为按钮塑件注塑模具结构,图6是模内呈左右对称分布的塑件、浇注

系统与推出系统。模具使用了二套利用开模力进行分型的双斜导柱侧向分型抽芯机构;在顶出机构的设置上,将顶出位置设在工件表面凹槽的脱模阻力较大区域,最大限度地减少产品变形。



(a) 模具结构

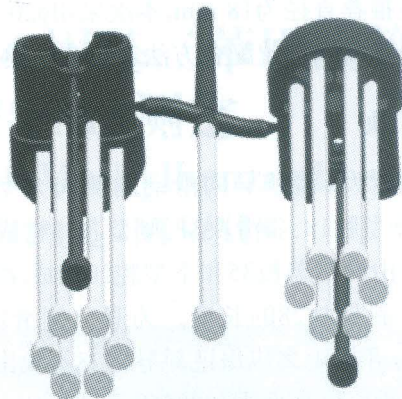


(b) 模具3D

- 1-动模固定板; 2-顶出机构导柱; 3-承重块; 4-顶出机构导套;  
5-顶出固定板; 6-中心顶杆; 7-动模; 8-型芯A; 9-塑件; 10-浇注凝料;  
11-定模固定板; 12-定位圈; 13-浇口套; 14-定模; 15-导套; 16-上型腔;  
17-导柱; 18-侧型腔; 19-型芯B; 20-下型腔; 21-顶出杆; 22-限位块;  
23-回程杆; 24-顶出板; 25-支承钉; 26-垫板; 27-支承柱; 28-斜导柱;  
29-减摩擦垫; 30-斜滑块; 31-斜滑块; 32-减摩擦块; 33-侧型芯; 34-拉钉;  
35-滑槽盖板

▲ 图5 按钮注塑模具结构与造型

Fig.5 The structure and modeling of the injection mould for the button



▲ 图6 模内塑件、浇注与推出系统

Fig.6 Plastic parts, pouring and ejection system in die

## 4.1 型芯及型腔结构

注塑模具采用组合式型腔和型芯。成型按钮外表面的型腔主要由型芯A8、上型腔16、型芯B19、下型腔20和固定于斜滑块31上的侧型腔18组合形成,它们的联结形式见图5模具结构。成型按钮内表面的型腔主要固定于斜滑块31上的侧型芯33。

## 4.2 侧向分型抽芯机构

### 4.2.1 斜导柱

图5中28所示为斜导柱,取其倾角 $\alpha=20^\circ$ 。侧型芯33的理论抽拔距离 $S$ 从图1中可见为24.3 mm。斜导柱的工作长度 $L^{[6]}$ 可由式(2)计算得到:

$$L = \frac{S}{\sin \alpha} = 71 \text{ mm} \quad (2)$$

相应所需开模行程 $H = S \cot \alpha = 24.3 \text{ mm}$ 。为保证模具正常稳定工作,设计时取斜导柱长度为128 mm,开模行程为70 mm。

模具中单一侧型芯的抽芯力为:

$$F_c = Chp(\mu \cos \alpha - \sin \alpha) \quad (3)$$

式中: $F_c$ —侧向抽芯力, N;  $C$ —侧型腔截面平均周长, mm;  $h$ —侧型腔成型部分的深度, mm;  $p$ —塑件包裹侧型芯的包紧力,取 $p=12 \text{ MPa}$ ;  $\mu$ —塑件在热状态时对钢的摩擦系数,取 $\mu=0.2$ ;  $\alpha$ —脱模斜度,取 $\alpha=0.6^\circ$ 。

代入参数计算得出 $F_c=8.5 \text{ kN}$ ,模具采用双斜导柱结构,故每支斜导柱所受抽芯力 $F_c=4.3 \text{ kN}$ 。查参考文献<sup>[7]</sup>中“最大弯曲力与抽芯力和斜导柱倾角的关系”表,当斜导柱倾斜角 $\alpha=20^\circ$ 、抽芯力 $F_c=4.3 \text{ kN}$ 时,最大弯曲力 $F_w=5 \text{ kN}$ 。查“斜导柱倾角、高度、最大弯曲力、斜导柱直径之间的关系”表<sup>[8]</sup>,得到斜导

柱工作段推荐直径为18 mm,本次采用 $\phi 20$  mm的斜导柱。斜导柱以过盈配合方法安装在定模14上。

#### 4.2.2 侧滑块

采用T型导滑槽导向滑动的侧向分型与抽芯机构,由侧型腔18、斜滑块31、侧型芯33构成;T型导滑槽主要由滑槽盖板35和下型腔20构成,滑块行程取决于斜导柱28的长度。为避免侧滑块脱出T型导滑槽,开模距离应保证斜导柱28不脱出斜滑块31。侧向滑块组合形式如图5所示。

模具侧滑块组的锁紧由斜楔块30通过楔紧实现,斜楔块30的楔紧面倾角为 $22^\circ$ 。在锁紧时,斜导柱与侧滑块倾斜孔外侧留有0.4 mm间隙,避免开模时侧滑块与楔紧面间产生干涉。

为减少因滑块长时间使用造成摩擦增大,引起侧向抽芯力的增加,在模具中装有如图5所示的减摩垫29和减摩块32。

#### 4.3 顶出机构

因按钮外部有内凹和二处通孔,为保证顺利脱模,又不影响制品外观,模具中采用了如图6布置的顶出杆。整套顶出机构由穿过下型腔20和动模7的15根 $\phi 3.5$  mm顶出杆、顶出固定板5、顶出板24和顶出机构导柱2、导套4等零件组成。为避免顶出机构超程顶出,模具上采用了限位钉22。

#### 4.4 其他机构

为提高按钮注塑模的工作可靠性,模具中采用了4根回程杆23和固定在回程杆上的回程弹簧组成的先复位机构。它既具有弹簧先复位机构的结构

简单优点,又克服了弹力小,弹簧易疲劳失效的缺陷。

## 5 结语

(1)对按钮塑件结构进行了分析,针对塑件结构和成型工艺技术要求,设计了一模二腔的模具及其浇注系统、型芯及型腔结构、斜导柱侧向分型与抽芯机构、顶出机构和复位机构等。

(2)对设计的浇注系统进行注塑模流分析,结果表明,该浇注系统设计合理,适合按钮塑件注塑成型。所得注塑工艺参数为:模具充填时间0.595 6 s,塑件顶出时间82.34 s,最大注射压力27.293 5 MPa,最大锁模力6.520 7 t。

(3)对斜导柱侧向分型与抽芯机构进行了详细的设计计算,同时使用减摩垫块减小侧滑块的磨损。

#### 参考文献:

- [1] 塑料模设计手册编写组. 塑料模设计手册[M]. 北京: 机械工业出版社, 2002.
- [2] 冯炳尧. 模具设计与制造简明手册[M]. 上海: 上海科学技术出版社, 1990.
- [3] 何冰强. 塑料成型工艺与模具设计[M]. 上海: 上海交通大学出版社, 2011.
- [4] 张维合. 注射模具设计实用教程[M]. 北京: 化学工业出版社, 2007.
- [5] 尚广庆,孙春华,杨莉莉,等. 基于逆向工程的注塑模具快速设计[J]. 机械设计与制造, 2011(10): 226-227.
- [6] 张南. 长距离斜抽芯注射模设计[J]. 模具工业, 2009, 35(6): 57-59.
- [7] 何冰强,高汉华,等. 塑料模具设计指导与资料汇编[M]. 2版. 大连: 大连理工大学出版社, 2009.

### 行业动态

#### 欧洲制造商研发出一种高性能PE抗静电膜

据外媒报道,近日欧洲一家制造商成功应用OCSiAl公司的TUBALL单壁碳纳米管生产了一种高性能PE抗静电膜,与纯膜相比,这些抗静电PE吹塑薄膜的透光率为90%,垂直方向的断裂应力增加约60%,可保持永久导电性。

通过易于处理的TUBALLMATRIX810浓缩物引入0.01 wt.%的TUBALL纳米管,表面电阻率达到 $5 \times 10^9 \sim 1 \times 10^{11} \Omega/\text{sq}$ ,符合ANSI/ESDS541-2003和IEC61340-5-1-2007关于防止包装材料静电效应的标准。与纯膜相比,这些抗静电PE吹塑薄膜的透光率为90%,这是用炭黑无法实现的,此外,垂直方向的断裂应力增加约60%,这提高了该PE膜的耐久性。



# Since 1990



向美国、日本、俄罗斯、中国台湾、泰国、印度等国家和地区，以及国内共5000余家用户表示衷心的感谢！

自从1990年，一项精密恒温槽的科学研究项目立项开始，一家，从无白领蓝领跳槽另立山头的公司；一家，从没有业务员到处奔波兜售的企业，就在孕育着诞生之中！

## 自动黏度测试一揽子解决方案

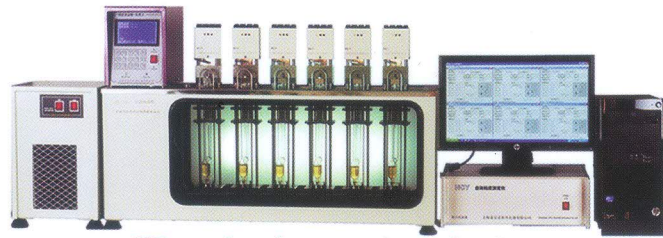
安全 便捷 准确 用于：聚氯乙烯，聚酯，聚酰胺，聚砜，聚碳酸酯，维纶，浆粕，纸浆，硅橡胶，聚乙烯醇，乙酸纤维素，聚丙烯酰胺，聚烯烃。



质量 ZPY自动配液器

容积 RPY自动配液器

WR-2 防渗水 恒温水/油浴振荡器



NCY系列 自动黏度仪



废液收集器

黏度计架

## SWB系列维卡软化点热变形温度仪

专利

ZL201220315849.4



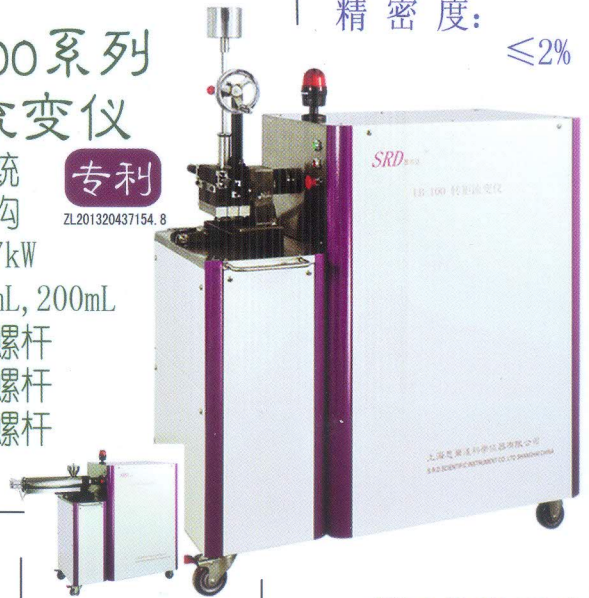
专利设计，测试架自身热变形：0.01mm  
最小施加力：小于47gf，符合ASTM测试要求  
温度分布：优于0.5℃

## LB-100系列转矩流变仪

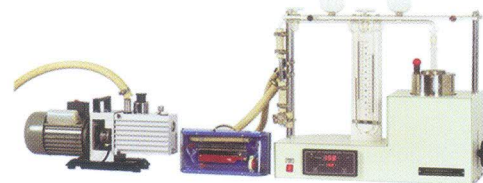
计算机系统  
内藏式结构  
主机：3.7kW  
密炼：60mL, 200mL  
挤出：单螺杆  
锥双螺杆  
平双螺杆

专利

ZL201320437154.8



温度波动： $\leq 0.1^\circ\text{C}$   
8小时温度稳定： $\leq 0.1^\circ\text{C}$   
测试范围：0.02~2000  
精密密度： $\leq 2\%$



SF-1压差法水分仪  
检测聚酯聚酰胺等结构内部水分  
ppm级

## JWC系列精密恒温槽



上世纪经典力作  
专用于  
特性黏度测试  
至今仍独占鳌头

各项温度指标  
优于 $\pm 0.01^\circ\text{C}$

《聚合物常用测试技术及自动化》  
姚汉樑著（思尔达总编）  
化学工业出版社2015出版



# SRD®

中国 上海思尔达®科学仪器有限公司

S.R.D. SCIENTIFIC INSTRUMENT CO., LTD. SHANGHAI CHINA

地址：上海市闵行区梅陇镇 澄建路20号 邮编：201108

邮箱：srdgs@163.com

QQ：1176829322

总机：021-64926506/33504401/33504402/33504403

市场直线：021-64925147

技术支持：13601897101

请浏览我司官网 [www.srdcn.com](http://www.srdcn.com)



(2017)国认监认字(103)号



170010260458



中国认可  
国际互认  
检测  
TESTING  
CNAS L0251

### 科学 公正 准确 服务

## NTSQP 国家塑料制品质量监督检验中心 (北京)

国家塑料制品质量监督检验中心(北京)(NTSQP),经国家质量监督检验检疫总局授权,从事塑料制品的质量监督检验、仲裁检验和各方委托检验,具有法定权威性和第三方公正性。中心分别获得了欧洲 DIN-CERTCO 和美国 BPI 的实验室认可证书。中心是国际标准化组织 ISO/TC138 和 ISO/TC61/SC10, SC11 的技术对口单位,承担着全国塑料制品标准化技术委员会秘书处的工作,与国内外权威的标准化及检验机构有着广泛的交往。



ISSN 1001-9278



地址:北京海淀区阜成路11号

电话:010-68985371, 68983956

网址:www.ntsqp.org.cn或www.plastic.org.cn

邮编:100048

传真:010-68983571

电邮:ntsqp@ntsqp.org.cn

全国性自然科学技术期刊  
国家科委批准  
国家新闻出版署批准  
公开发刊

全国中文核心期刊  
CA 收录核心期刊

中国科学引文索引核心期刊  
中国科技论文统计与分析源期刊



1987 年创刊,月刊  
第 33 卷第 12 期(卷终)  
(总第 309 期)

2019 年 12 月 26 日出版

ISSN 1001-9278

CN 11-1846/TQ

主管单位:中国轻工业联合会  
主办单位:中国塑料加工工业协会  
北京工商大学  
轻工业塑料加工应用研究所

出版:《中国塑料》编辑部

顾问:杨惠娣

主编:张玉霞

执行主编:刘学

责任编辑:赵艳

地址:北京市海淀区阜成路 11 号

邮编:100048

电话:编辑部:010-68985541

广告/发行部:010-68985253

电子信箱:cp@plascina.com.cn

网址: <http://www.plascina.com.cn>

印刷:北京盛旺世纪彩色印刷有限公司

设计制作:北京砚祥志远激光照排技术有限公司

广告经营许可:京海工商广登字 20170105 号

国内发行:北京报刊发行局

邮发代号:82-371

订 阅:全国各地邮局

国内定价:全年 600.00 元

国外发行:中国国际图书贸易总公司

地 址:北京车公庄西路 35 号

邮 编:100044

开 户 名:轻工业塑料加工应用研究所

开户银行:中国工商银行北京市公主坟支行

帐 号:0200004609008803132

法律顾问:北京新元律师事务所

徐康平律师

# 目 次

## 材料与性能

- 快速高吸有机溶剂树脂制备及其性能研究 ..... 耿孝岭,张智嘉,王国军,李万利(1)  
分层可溶性利多卡因聚合物微针的制备与穿刺效果研究 .....  
..... 张嘉荣,庄 俭,吴大鸣,许 红,郜王鑫,孙靖尧(7)  
石墨烯增强聚丙烯/高密度聚乙烯纤维研究 ..... 武卫莉,李 响(11)  
表面改性 CNF 对 PBS/PLA 共混物的湿热老化行为的影响 .....  
..... 朱 艳,张奇锋,贾仕奎,赵中国,陈立贵,曹 乐(16)  
铜离子配合物对聚氯乙烯阻燃抑烟的研究 ..... 邹再旺,崔永岩(23)  
一种新的氨基酸基有机无机杂化水凝胶 .....  
..... 崔林杰,夏传俊,胡亚松,明平灯,陈俊英,黄 霞(28)  
具有半互穿网络结构的 PDMS/PVDF 超滤膜处理水包油型废水研究 .....  
..... 王 勇(33)

## 加工与应用

- 微发泡注塑注气系统气涌现象的可视化研究 .....  
..... 安华亮,信春玲,乔林军,何亚东,闫宝瑞(39)  
热重法测试滴灌带中炭黑含量的方法研究 .....  
..... 雷振凯,王 陞,张 熙,景蔚洁,朱兴成(44)  
PP/PA6 共混比例对其水辅助注塑管件性能及微观形态的影响 .....  
..... 匡唐清,钟罗浩,徐 盼,冯 强,潘俊宇,柳和生(50)  
聚乙烯电熔接头管材熔融区深度与焊接性能关系研究 .....  
..... 郭伟灿,胡裕锐,缪存坚,施建峰(58)

## 助 剂

- 基于呋喃二甲酸的新型生物基增塑剂的制备及其增塑效果研究 .....  
..... 王一鸣,杜永刚,杨明明,王 莉,庄翔杰(63)  
复合型受阻酚抗氧剂的制备及清除 DPPH· 活性研究 .....  
..... 计海峰,宋丹阳,闫玉双,王卫东(69)

## 塑料与环境

- 生物可降解山麻杆韧皮纤维增强 PBS 复合材料的性能研究 .....  
..... 赵 磊,姜为青,刘 华,李桂付,周红涛(73)

## 机械与模具

- 无人机叶片特殊三次脱模机构简化型模具设计 ..... 汤定德,田 科(80)  
塑料机器人一模多异腔注射模设计 ..... 李海林,王锦红,丁立刚,赵永豪(89)

## 综 述

- 塑料保温管材的研究发展 ..... 侯连龙,澹台建礼,贾少伟(94)  
3D 打印用 ABS 研究进展 ..... 叶 旋,涂华锦(101)



# CHINA PLASTICS

China National Natural Science  
& Technology Journal

Worldwide Distribution

National Chinese Core Journal  
CA Covered

China Science Citation Index  
Core Journal

Statistical Source Journal of  
China Scientific Papers  
Monthly

Started Publication in 1987

Vol. 33, No. 12

(Series No. 309)

Code: **ISSN 1001-9278**  
**CN 11-1846/TQ**

**Dec. 26, 2019**

### Administering Authority:

China National Light Industry Council

### Publisher:

China Plastics Processing Industry Association  
Beijing Technology and Business University  
Institute of Plastics Processing &  
Application of Light Industry (IPPA)

Edited by: Editorial Office of China Plastics

Adviser: YANG Huidi

Editor-in-Chief: ZHANG Yuxia

Executive Editor-in-Chief: LIU Xue

Executive Editor: ZHAO Yan

Address: 11 Fucheng Road, Haidian District,  
Beijing 100048, P. R. China

Telephone Number for Each Division:

Editorial: 86-10-68985541

Advertising/Distribution: 86-10-68985253

Web Site: <http://www.plaschina.com.cn>

E-mail: [cp@plaschina.com.cn](mailto:cp@plaschina.com.cn)

### General Distributor:

China International Book Trading Corporation,  
Beijing PO Box 2320, China

## CONTENTS

### Materials and Properties

- Preparation and Properties of Organic Solvent-absorption Resin with Rapid Rate and High Capacity ..... GENG Xiaoling, ZHANG Zhijia, WANG Guojun, LI Wanli(1)
- Preparation and Puncturing Effect of Lidocaine-Containing Polymer Microneedles with Stratified Solubility ..... ZHANG Jiarong, ZHUANG Jian, WU Daming, XU Hong, GAO Wangxin, SUN Jingyao(7)
- Graphene-Reinforced Polypropylene/High-density Polyethylene Composite Fibers ..... WU Weili, LI Xiang(11)
- Effects of Surface-Modified Nanocellulose on Hygrothermal Aging Behavior of PLA/PBS Blends ..... ZHU Yan, ZHANG Qifeng, JIA Shikui, ZHAO Zhongguo, CHEN Ligui, CAO Le(16)
- Study on Flame Retardancy and Smoke Suppression of PVC with Copper Ion Complexes ..... ZOU Zaiwang, CUI Yongyan(23)
- A Novel Amino-Acid-Based Inorganic-Organic Hybrid Hydrogel ..... CUI Linjie, XIA Chuanjun, HU Yasong, MING Pingdeng, CHEN Junying, HUANG Xia(28)
- Disposal of Oil-in-Water Wastewater by PDMS/PVDF Ultrafiltration Membrane with Semi-IPN Structure ..... WANG Yong(33)

### Processing and Application

- Visualization Study of Gas Surge Phenomenon in Microcellular Injection-molding Gas Injection System ... AN Hualiang, XIN Chunling, QIAO Linjun, HE Yadong, YAN Baorui(39)
- Study on Methodology for Measurement Content of Carbon Black in Drip Irrigation Belt by Thermogravimetry ..... LEI Zhenkai, WANG Chui, ZHANG Xi, JING Weijie, ZHU Xingcheng(44)
- Influence of PP/PA6 Blending Ratio on Performance and Morphology of WAIM Pipes ..... KUANG Tangqing, ZHONG Luohao, XU Pan, FENG Qiang, PAN Junyu, LIU Hesheng(50)
- Relationship Between Welding Performance and Depth of Fusion Zone for Electrofusion Joint of Polyethylene Pipes ..... GUO Weican, HU Yurui, MIAO Cunjian, SHI Jianfeng(58)

### Additive

- Preparation and Plasticizing Effect of Novel Bio-base Plasticizers Based on Furanedicarboxylic Acid ..... WANG Yiming, DU Yonggang, YANG Mingming, WANG Li, ZHUANG Xiangjie(63)
- Synthesis of Complex Hindered Phenol Antioxidant and Its Scavenging Activity for DPPH Free-Radicals ..... JI Haifeng, SONG Danyang, YAN Yushuang, WANG Weidong(69)

### Plastic and Environment

- Performance Investigation of PBS Composites Reinforced with Biodegradable Phloem Fiber from *Alchornea Davidii* Franch ..... ZHAO Lei, JIANG Weiqing, LIU Hua, LI Guifu, ZHOU Hongtao(73)

### Machinery and Mould

- Design of Simplified Mold with Special Three-step Demolding Mechanism for Blade of Unmanned Aerial Vehicle ..... TANG Dingde, TIAN Ke(80)
- Design of Multi-cavity Injection Mold for Plastic Robot ..... LI Hailin, WANG Jinhong, DING Ligang, ZHAO Yonghao(89)

### Review

- Research and Development of Thermal Insulation Plastic Pipelines ..... HOU Lianlong, TANTAI Jianli, JIA Shaowei(94)
- Research Progress in ABS Materials for 3D Printing ..... YE Xuan, TU Huajin(101)

## 塑料机器人一模多异腔注射模设计

李海林<sup>1</sup>, 王锦红<sup>1</sup>, 丁立刚<sup>2</sup>, 赵永豪<sup>1</sup>

(1. 广州城建职业学院, 广州 510993; 2. 中山火炬职业技术学院, 广东 中山 528436)

**摘要:**以塑料机器人产品为载体,介绍异型组合产品的结构工艺性,确定该产品采用一模多异腔的成型方案。基于计算机辅助工程(CAE)数值模拟技术优化模具浇注系统的设计,解决流道填充不平衡的问题;同时在流道上增设特殊结构,解决注塑生产后产品的空间存放问题。根据产品的功能要求,在模具结构中设置抽芯机构,以解决产品成型后产生夹线的工艺问题。该模具在实际的生产过程中取得较好效果,为类似模具的设计提供相关的参考与借鉴。

**关键词:**组合型腔;模流分析;注射模

**中图分类号:** TQ320.66+2

**文献标识码:** B

**文章编号:** 1001-9278(2019)12-0089-05

**DOI:** 10.19491/j.issn.1001-9278.2019.12.016

### Design of Multi-cavity Injection Mold for Plastic Robot

LI Hailin<sup>1</sup>, WANG Jinhong<sup>1</sup>, DING Ligang<sup>2</sup>, ZHAO Yonghao<sup>1</sup>

(1. Guangzhou City Construction College, Guangzhou 510993, China;

2. Zhongshan Torch Polytechnic, Zhongshan 528436, China)

**Abstract:** In this paper, the structural manufacturability of special-shaped composite products was introduced by using the plastic robot products as carriers, and the forming scheme of one mold with many different cavities was determined. Based on the CAE numerical simulation technology, the design of the mold gating system was optimized to resolve the unbalanced filling problem occurring in the flow passage. Meanwhile, a special structure was additionally arranged on the runner to solve the problem of space storage for the products after injection molding production. According to the functional requirements of the products, a core pulling mechanism was arranged in the mold to solve the technical problem of thread clamping after the product was formed. The mold achieved good results in the actual production process. This work provided a good reference for the design of similar molds.

**Key words:** combined cavity; simulation analysis; injection mold

## 0 前言

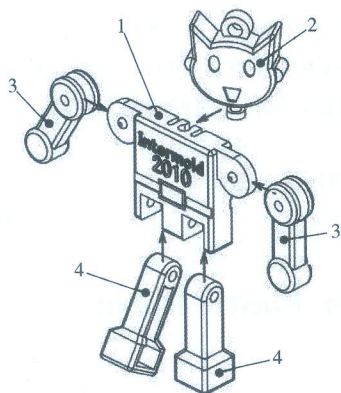
在设计注射模具时,对于由尺寸较大、形状各异的塑料零件组装而成的塑料产品,通常采用一模一腔的结构形式,将不同零件布置在不同模具中注塑生产;而对于尺寸较小、批量不大且材料相同的塑料产品,基于节约产品开发成本的考虑,可以将一套产品上的多个零件同时布置在一套模具中,注塑成型后再将各个塑料零件装配成一个产品。本文涉及到的是一款塑料机

器人,其组成零件尺寸较小,装配后的外形尺寸不大,主要用于充当装饰物悬挂或者小玩偶,所以产品要求外观精致美观,同时还必须保证产品装配后整体着地的平稳性。在模具设计过程中,若以传统的设计思路与方法,则存在模具分型面复杂、填充不平衡、以及机器人立足着地不稳等问题。本例中通过巧妙的选取产品夹线位置、运用 CAE 模拟分析技术、增设模具抽芯机构等方法,有效地解决传统设计方法可能遇到的问题及难点。

## 1 机器人组合件工艺分析

该产品的材料为丙烯腈-丁二烯-苯乙烯共聚物

(ABS),共由4个不同的零部件构成,各部件的名称如图1所示。该产品装配后的最大高度尺寸为40 mm,胳膊平直张开后的最大尺寸为48 mm,产品的平均壁厚为1.2 mm,装配效果如图2所示。由装配效果图可知,主身件1与头部件3存在无法顺利脱模的部位。产品要求能平稳立足着地,故腿件4的底部需具备一定的平面度要求,不允许有夹线及脱模斜度等问题。



1—主身 2—头部 3—胳膊 4—腿

图1 机器人装配爆破图

Fig. 1 Robot assembly blasting map

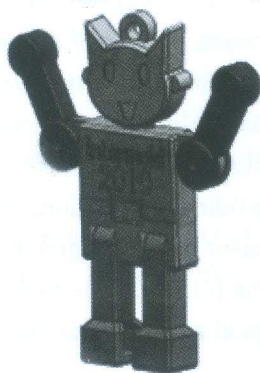


图2 机器人装配立体图

Fig. 2 Robot assembly diagram

## 2 模具结构设计

### 2.1 型腔的数量及布排

模具型腔数量与布局的确定,一般需考虑的因素主要有注塑机的规格参数、产品的精度要求、产品的交货周期、实际生产的经济效率等。本模具中,从产品装配工艺性和生产经济性等因素考虑,确定将装配组件放置同一成型模具内,采用一模六腔的布排形式,如图3所示。采用这种形式布排的好处是每一次注塑生产后可以组装一个产品,能有效避免不必要的浪费,同时还能方便成品数量的统计。

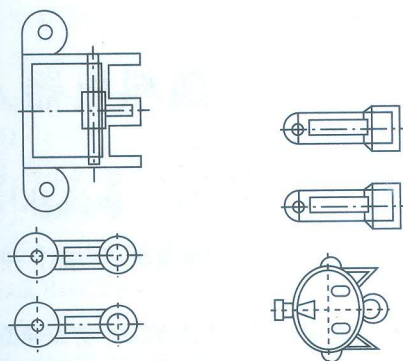


图3 型腔数量与布排

Fig. 3 Number of cavities and cloth rows

### 2.2 分型面的选择

分型面的选择是一个比较复杂的问题,关系到产品的外观质量、影响到模具的具体结构及加工的难易程度,在分型面的选择时需综合考虑多种因素,对于一模多异腔模具而言,主要考虑如何将多异腔的分型面进行台阶的整合单一化,减少凹凸不平的台阶分型面或曲面分型面。

塑料机器人由于各部件形状各异、大小不一,如果按常规思路选取每个部件的最大截面处为分型面,则出现多处凹凸不平的分型面,使得模具零件加工与装配变得复杂。为此,本例中借助常用的三维设计软件,通过调整产品坐标位置,使得所有零件的最大轮廓均处于同一平面位置,如图4所示。从而简化了模具分型面结构,降低模具加工难度。

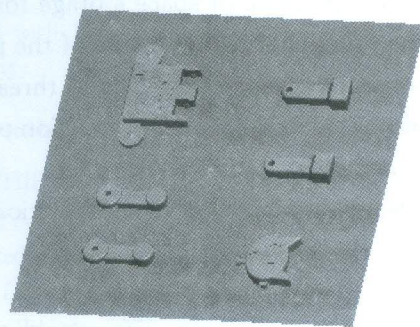
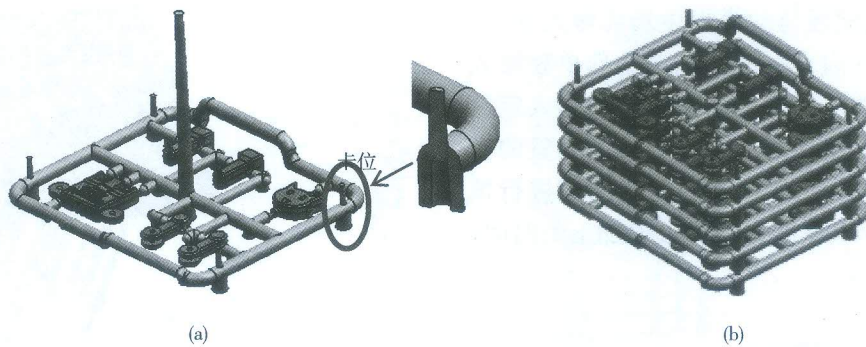


图4 分型面

Fig. 4 Parting surface

### 2.3 浇注系统设计

塑料熔体在注塑压力的作用下,经过浇注系统填充到模具型腔的各个部位,以获得形状完整的、质量优良的塑件。为了便于注塑后产品从模具中取出,模具浇注系统采用框架式辅助流道的形式,如图5所示,将整个产品组件包裹于流道之中,浇注系统结构如图(a)所示;同时在辅助的分流道上增设了4个卡位,方便了产品的后期存放,产品叠放如图(b)所示。



(a) 浇注系统结构 (b) 产品叠放图

图5 浇注系统

Fig. 5 Gating system

由于采用一模多异腔的结构方案,因此各模腔容易出现充填不平衡的工艺问题,从而导致产品容易出现飞边、内应力过大等外在和内在的质量问题。为了避免结构不合理而导致后期模具制作及试生产过程中出现重大工艺问题,在模具设计初期,根据模具的初始结构方案、所选材料的性能以及塑件的大小等因素确定模具的成型工艺参数,如表1所示,利用常用模流分

表1 工艺参数

Tab. 1 Process parameters

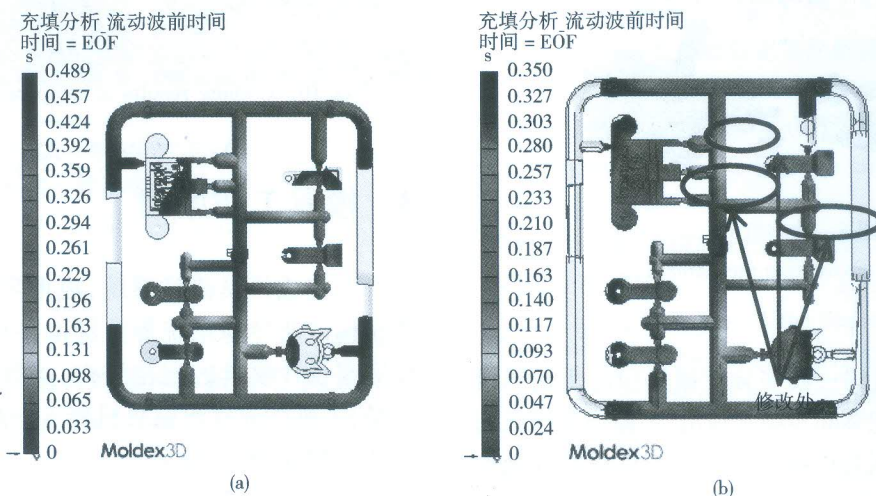
工艺参数	数值
注射压力/MPa	100
注射时间/s	0.5
保压压力/MPa	90
保压时间/s	2
冷却时间/s	13

析软件 Moldex 模拟分析塑料熔体的流动状态,验证浇注系统的合理性。

根据模拟分析结果,确定将部分型腔的分流道尺寸由原始设计的  $\phi 3\text{ mm}$  变更为  $\phi 2.5\text{ mm}$ , 部分型腔的浇口尺寸由原始的  $0.5\text{ mm}$  设计变更为  $0.35\text{ mm}$ , 并在相同成型工艺参数条件下进行模拟过程分析。分析结果图6所示,其中图(a)、(b)分别是设计变更前后的填充过程模拟分析结果状态云图,从状态云图可知,设计变更前各型腔填充不均衡,设计变更后各型腔填充基本均衡,从而保证的产品质量。

### 2.4 成型零件的设计

成型零件的形状与精度决定着产品的质量,其结构设计主要考虑是否节省贵重材料、是否便于加工、排气、后续零件抛光及零件装配等因素,一般来说可以分为整体式与组合式。为了便于零件加工、修配与更换,该模具的成型零件以采用局部镶拼组合式结构为宜,



(a) 优化前充填至 80 % 时的状态云图 (b) 优化后充填至 70 % 时的状态云图

图6 优化对比状态云图

Fig. 6 Optimization contrast of state cloud diagram

即在标准模架中的定模板与动模板中局部镶入动、定模镶件,再将成型组件内表面的小型芯全部单独镶入动模镶件内,成型组件外表面的小型芯单独镶入定模镶件内,如图 7 所示。此种结构不仅节省了大量的贵重金属材料,还能有效利用零件结合处的间隙进行填充时的排气,同时能够大量减少特种放电加工的时间,提高了模具的生产效率。

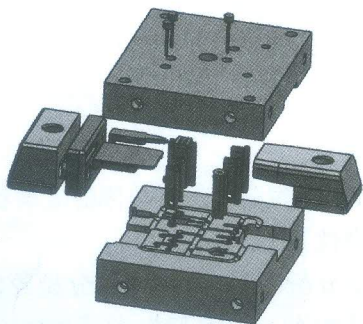


图 7 成型零件  
Fig. 7 Forming parts

### 2.5 抽芯机构的设计

由产品的工艺分析可知,主身件 1 与胳膊件 3 的结构上存在与开模方向不平行的侧孔与侧凹,故在模具结构上需要设计抽芯机构来解决此类问题;同时在腿件 4 底部处上增设了抽芯机构。如果按常规设计的方法处理,则本处无需此机构,但生产出的产品会存在底部不平或者夹线等问题,从而导致使用功能上的缺陷,出现产品无法平稳着地的现象。考虑到制品实际所需的抽芯距与抽芯力都相对较小,故本模具的抽芯机构采用斜导柱与滑块的组合式,其中滑块采用镶拼组合式,以方便加工与节省贵重材料,如图 8 所示。

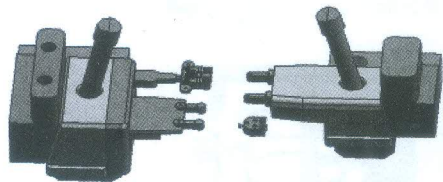


图 8 抽芯机构  
Fig. 8 Extraction mechanism

### 2.6 顶出机构设计

对于框架式流道的一模多异腔模具顶出机构的设计,需保证各腔产品能够同步顺利顶出,不能出现产品与流道分离的情况,否则会影响产品后续的存放或其他的后处理工序。本模具顶出机构设计的重点是考虑推出零件的选择与推出运动过程的导向。结合制品的具体形状,本模具采用推杆与推管联合顶出方式,如图 9 所示。同时在顶出机构中增设导柱与导套进行顶出运动导向,

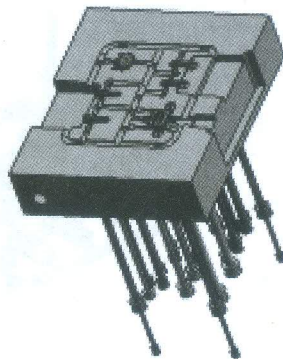


图 9 顶出机构  
Fig. 9 Ejection mechanism

保证顶出过程平稳可靠,从而确保各产品同步脱模。

### 2.7 温度控制系统设计

合理的温控系统不仅能控制产品的精度,还能调节模具注塑生产的周期。设计温度控制系统时必须确保模具的型芯与型腔的温差控制在一定的范围内,以降低产品的翘曲变形程度。本模具注射成型的塑料组件的整体外形尺寸较小,采用 U 形循环冷却回路即可,如图 10 所示。从温控系统状态云图可见,各型腔温差在 10 °C 以内,效果较好。

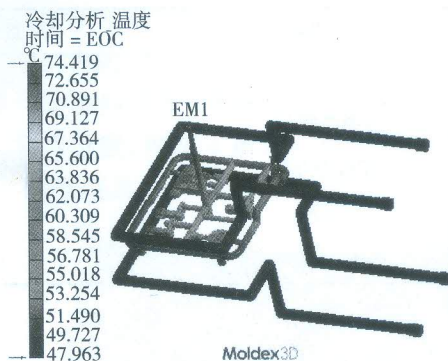


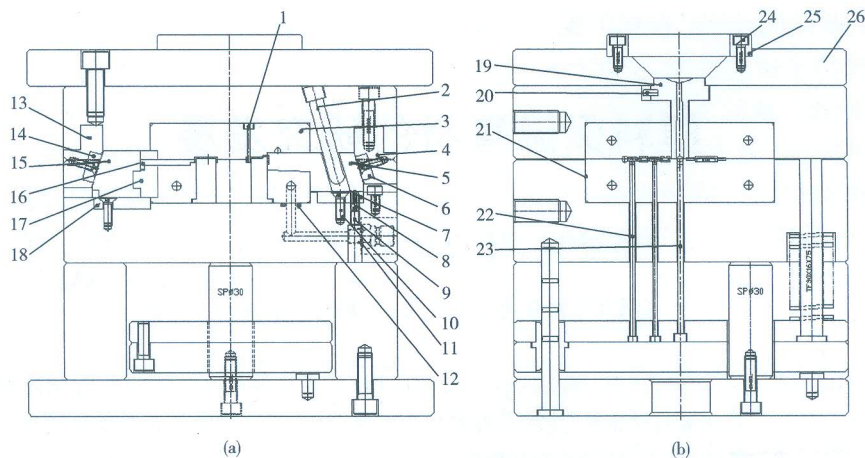
图 10 温度控制系统冷却结果云图  
Fig. 10 Cooling results of temperature control system

## 3 模具工作原理

在完成模具浇注系统、成型零件、推出机构、侧抽芯机构以及冷却系统等关键部件设计的基础上,进一步完善设计模具的定位结构、支撑零件以及其他的相关结构,最终设计出塑料机器人—模多异腔注射模具,主要结构如图 11 所示。

其工作原理如下:模具合模后安装在注塑机上,在一定的温度及压力下,注塑机将熔融塑料通过喷嘴沿模具浇注系统均匀地注入到模具型腔中;在注塑机保压压力和锁模力作用下,塑件在型腔中保压成型,并在冷却系





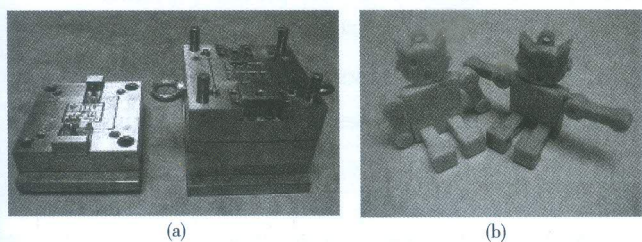
1—定模镶针 2—斜导柱 3—定模镶件 4、13—锁紧块 5—滑块 6、14、18—耐模块 8—定位波子  
9—止付螺丝;10—锥头螺钉 11—接水栓 12—密封圈 15—滑块座 16—滑块镶件 17—滑块压板  
19—浇口套 20—防转销 21—动模镶件 22—推杆 23—拉料杆 24—平头螺钉 25—定位环 26—定模座板  
(a)主视图 (b)侧视图

图 11 模具装配图

Fig. 11 The mould assembly drawing

统作用下冷却、固化;注塑机打开,模具在定模镶件 3 与动模镶件 21 处分型,同时抽芯机构利用开模动作完成侧向分型抽芯;在注塑机顶出力作用下,利用推杆 22、拉料杆 23 等顶出零件将产品与流道浇注系统凝料顶出;在注塑机合模动作作用下模具再次闭合,完成一个注塑周期。

经过后期生产验证,实际模具与注塑产品均能满足使用要求,可为类似产品的模具结构设计提供参考。模具与产品实物如图 12 所示<sup>[2]</sup>。



(a)模具实物 (b)产品实物

图 12 模具与产品实物

Fig. 12 Mould and product

## 4 结论

(1)针对塑料机器人的零件形状与尺寸,设计了一模多异腔的模具结构方案,并解决了多异腔模具分型面不平整的技术问题,节约了产品开发成本;

(2)借助 CAE 模流分析软件工具,对多异腔模具的浇注系统进行平衡填充分析与温度控制系统分析,优化其设计参数,确保产品符合技术要求;

(3)结构中将浇注系统设计成框架式的辅助分流

道结构,并且在辅助流道上设计卡位,方便产品后续存放及表面处理;

(4)根据产品的功能要求,局部增设抽芯机构,保证产品整体的着地平稳性。

## 参考文献:

- [1] 宋玉恒. 塑料注射模具设计实用手册[M]. 北京:航空工业出版社,1998:85-105.
- [2] 赵长荣. 手机充电器底盖注塑模具设计[J]. 工程塑料应用,2014(3):65-68.  
ZHAO C R. Injection Mold Design of Mobile Phone Charger Bottom Cover [J]. Engineering Plastics Application, 2014(3): 65-68.
- [3] 罗文锋. 温控器固定架注塑模设计[J]. 模具技术, 2016(1):9-11.  
LUO W F. Design of the Injection Mould for Temperature Controller Holder [J]. Die and Mould Technology, 2016(1): 9-11.
- [4] 刘庆东. 前模滑块注射模设计[J]. 中国塑料, 2015, 29(9): 100-103.  
LIU Q D. Design of the Slide on Stationary Mould Fixed Half [J]. China Plastics, 2015, 29(9): 100-103.
- [5] 韦煜成. 塑料顶盖注射工艺分析及模具设计[J]. 科技创新与应用, 2017(6): 21-22.
- [6] 杨勇辉. CAE/CAD 技术在塑料模具设计中的应用[J]. 工程塑料应用, 2017(2): 124-126.  
YANG Y H. Application of CAE/CAD Technology in Designing of Plastic Mould [J]. Engineering Plastics Application, 2017(2): 124-126.

DOI: 10.13979/j.1007-7235.2019.02.010

# 一种挤压半空心铝型材的遮盖式一模双孔分流模的结构

李有兵<sup>1</sup>, 邓汝荣<sup>2</sup>

(1. 广州城建职业学院, 广东 广州 510925; 2. 广州科技职业技术学院, 广东 广州 510550)

**摘要:**提出了一种针对半空心铝型材采用遮盖式一模双孔的挤压模结构。通过实际例子,详细介绍了这种模具结构有关参数的选择。主要包括挤压机能力的选择,模孔布置、分流孔设计、下模焊合室结构和工作带的选择。介绍了模具强度的校核方法。将传统的平面模、单孔分流模与这种新的遮盖式双孔模的实际挤压结果进行了对比。这种新的模具结构简单、容易加工。实践表明,采用这种新的一模双孔挤压模结构可显著提高模具的寿命、提高铝型材生产效率和降低成本,所得型材尺寸精度高、表面光亮,是一种值得推广的的模具结构。

**关键词:**半空心铝型材; 一模双孔; 遮盖式; 结构

中图分类号: TG375.4 文献标识码: A 文章编号: 1007-7235(2019)02-0045-05

## A covering type extrusion die with twin cavities for semi-hollow Al-profile

LI You-bing<sup>1</sup>, DENG Ru-rong<sup>2</sup>

(1. Guangzhou City Construction College, Guangzhou 510925, China;

2. Guangzhou Vocational College of Science and Technology, Guangzhou 510550, China)

**Abstract:** A new structure named covering type with twin cavities in a die for the semi-hollow Al-profiles was presented. The determination of structure parameters was introduced in detail through an actual case. The parameters mainly covered the capacity of the extruder, the arrangement of portholes, the structure design of chamber and the selection of bearing. The method of checking the die strength was introduced. The structure of the traditional solid die, the porthole die with single cavity and the covering type structure with twin cavities were compared with the extrusion results. The covering type was simple and easy to process. The practical application shows that the new die structure can enhance the die life, improve the production efficiency and reduce the cost. The profiles obtained are precise in dimension with bright surface. Thus this die structure is worth promoting.

**Key words:** semi-hollow Al-profiles; twin cavities in a die; covering type; structure

随着现代制造技术的进步和发展,人们在铝合金挤压型材生产中追求通过技术创新来大幅提高现有挤压机的生产效率,新的一模多孔挤压技术无疑是最佳的途径之一。而一模双孔挤压技术是实现一

模多孔挤压的基础,是在一套模具上同时同步挤出两根相同的铝型材制品,这对提高挤压机的效能和产品成品率有重要的意义。在铝型材市场需求中半空心型材占相当大的比例。而半空心型材的生产中

收稿日期: 2018-09-10

第一作者简介: 李有兵(1982-): 男,湖南邵阳人,讲师,研究方向: 功能材料的研发与制作。

模具是关键要素。半空心铝型材的模具设计复杂程度较高,解决模具的强度是关键。笔者以一种常见的铝型材实例介绍专门针对半空心铝型材采用的遮盖式一模双孔挤压模具的结构,以及设计中各种参数的选择,供同行参考。

## 1 遮盖式一模双孔挤压模的结构

所谓遮盖式就是改变传统的挤压半空心铝型材采用的平面模结构,而采用一种遮盖式分流模结构。目前半空心铝型材分流模结构中常用的是分割式结构,这种结构易产生拉丝和起筋现象。遮盖式分流模结构是利用分流模上模的中心部位将悬臂遮盖起来,使得悬臂在挤压过程中不直接承受金属的正面压力,将悬臂保护起来;而在分流模的下模,悬臂部分要向上突起,但不与上模接触,突起的顶部与上模之间留有一定的间隙(应力间隙),使得即使上模在挤压过程中向下发生挠曲时,也不会触及悬臂对悬臂施加力的作用。这样就改变了悬臂的受力状态并保护了悬臂,因而大大提高模具的强度。对于一模双孔的模具则充分利用分流桥作为对悬臂的保护,这是考虑到挤压机在挤压筒径向上存在压力梯度,通过合理的布置模孔,避免悬臂特别是悬臂的端部直接承受金属挤压时的正面压力,达到提高模具强度的同时提高铝型材挤压效率。

## 2 模具结构参数的确定

### 2.1 挤压机能力的确定

确定选用挤压机的能力要考虑到挤压产品的变形程度、挤压系数。挤压系数过大,挤压过程中挤压力会过高,容易出现挤压困难,一方面不利于产品成形,另一方面将会降低模具的寿命。挤压系数小则挤压力小,这有利于产品成形,但在一模双孔挤压时,在同样的坯料长度下会使挤出的型材长度减少,导致工艺废料的比增加,降低了成品率。而若增加坯料的长度,挤压筒是有限的,同时会使挤压力急剧上升。这是双孔模具结构设计中必须要考虑的。经验数据表明,在综合考虑的情况下,挤压系数在60~80范围内最为合适,比较有利于产品成形、生产过程控制和模具寿命等。

图1所示为一款民用建筑铝门窗型材,是典型的半空心型材。其断面面积为 $221\text{ mm}^2$ ,舌比经计算为6.5。采用单孔模挤压时一般选择8 MN~11 MN挤压机。采用双孔模挤压则可选择18 MN挤压机,其挤压筒内径尺寸选择 $\Phi 185\text{ mm}$ 。经计算挤压系数

为66.5,挤压机比压为670 MPa。坯料尺寸可选用 $\Phi 180\text{ mm} \times 520\text{ mm}$ 。

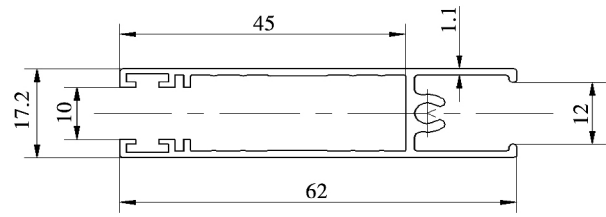


图1 一种铝门窗型材的断面图

Fig. 1 Profile section of a kind of Al door and window

### 2.2 模孔的布置

模孔的布置一方面要有利于挤压成形,可以充分发挥挤压筒的潜能;另一方面必须有利于使模具结构简单、紧凑,有利于模具加工和节省原材料。在18 MN挤压机上挤压图1所示的型材,模孔的布置可以有二种方式,如图2所示。

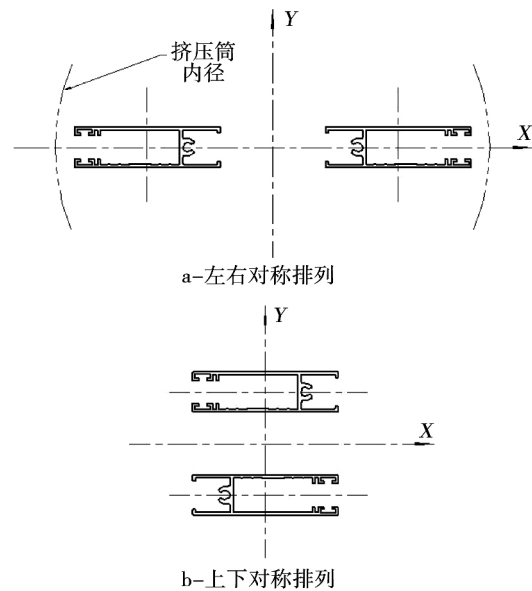


图2 模孔布置方式示意图

Fig. 2 Arrangement of die holes

图2a为左右对称排列,这样的好处在于左右两根型材在挤压时不会发生表面的接触,两根型材都可与滑出工作台接触,挤压容易实现平稳顺利。其不足的是不能充分利用挤压筒的特点,因为一般地说,应使模孔各处尽可能处在中心区域,这样有利于达到挤压成形时各处金属流速容易趋于一致;模孔离挤压筒内壁边缘距离小,一方面要采用宽展的模具结构,这将增加金属流动的复杂程度;另一方面,模具的外形尺寸必须相应增加才能保证模具的

强度。

图 2b 是采用上下对称排列,虽然上下两根型材在挤出时有表面的接触,表面可能会发生轻微的摩擦,但考虑到挤压时的自动牵引装置和型材最终的表面处理方式,这种接触对型材表面质量的影响是可以不考虑的,因此,选用图 2b 方式更为合适。

### 2.3 分流孔的布置

分流孔的布置包括确定分流比、分流孔的大小及分流桥的结构等。这是一模双孔模具的关键之处。根据图 2b 模孔的布置进行设计。第一步根据个人经验,借助 CAD 软件设计出初步的方案,较成熟的有两种分流孔布置的方案,如图 3 所示。第二步是将这两种方案在 UG 软件环境下建立三维模

型,并保存为固定的格式。第三步是将建立的三维模型导入挤压模拟软件 HyerXtrude 中进行模拟运算和观察。最后是对结果进行分析和对比,并结合个人的经验进行必要的修正后再模拟、分析和对比,得出最佳方案。

通过模拟发现,图 3a 的分流孔布置方案金属流速调整较为困难。主要是分流孔  $S_1$ 、 $S_2$ 、 $S_3$  的比例关系较难确定。可以预测,由于制造上的误差致使修模的工作量会增大。另外,虽然分流模的上模中心部位能将悬臂全部遮盖起来,但悬臂的端部因对应分流孔  $S_2$  模拟发现悬臂的变形程度较大,分流孔  $S_2$  面积的变化对悬臂变形有明显的影

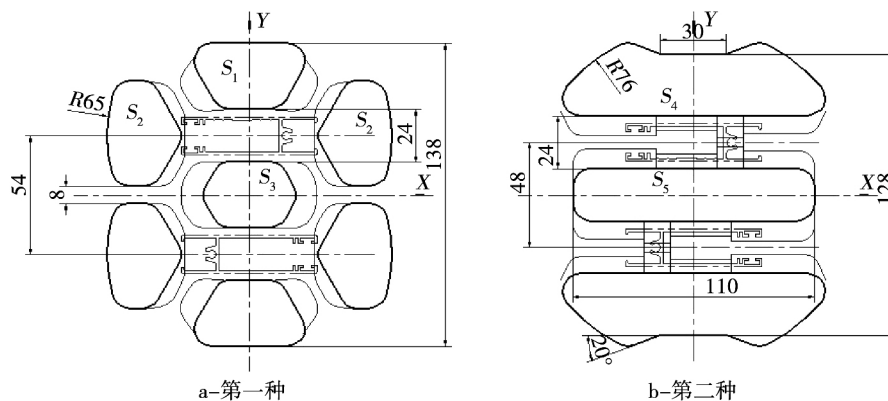


图 3 两种分流孔布置方案示意图

Fig. 3 Two kinds of layout of feeder portholes

图 3b 所示方案,分流孔数量少,仅调整分流孔  $S_4$ 、 $S_5$  二者的面积关系即可,在确定分流孔  $S_5$  的面积的前提下,很容易调整分流孔  $S_4$  的面积就可以使各处的金属流速趋于一致,而且分流孔面积的变化对悬臂不产生影响,这是最关键的。同时,分流孔面积和调整可以对分流桥不进行修正或改变,悬臂也完全置于分流桥的保护下,特别是悬臂的端部不承受直接的金属正面压力,因此,悬臂的强度是最好的。经分析比较,采用图 3b 的方案更合适。其主要参数如下:

- 1) 分流比  $K = 17.3$ 。取挤压比的 25% ~ 30%;
- 2) 分流桥的宽度为 24 mm,厚度为 85 mm;
- 3) 分流孔之间的面积关系为  $S_5 = 0.81S_4$ ; 从模拟发现,当  $S_5 = (0.75 \sim 0.85) S_4$  时,各处金属流速调整较容易趋于一致;
- 4) 分流孔最大外接圆直径为  $\Phi 152$  mm;
- 5) 分流桥结构是结合下模相对应的悬臂突起部

分进行设计,其结构如图 4 所示。

### 2.4 下模焊合室结构与工作带

对于一模双孔挤压模,为了消除模具制造误差对挤压时两根型材同步性的敏感影响,以及消除在两个模孔相邻的中心部位产生金属流动的死区(刚性区)而使型材表面出现粗晶和光亮带现象,必须设计成两个独立的焊合室,使模孔间的成形互不干涉和影响。焊合室之间的隔墙宽度取 6 mm ~ 8 mm,焊合室深度根据挤压的能力取 18 mm,隔墙高度取 10 mm。

由于采用的遮盖式结构,悬臂要向上突起,突起的部分与悬臂模孔间的尺寸关系如图 5 所示。原则是突起部分边缘距离悬臂模孔边缘 2 mm ~ 3 mm。同时,由于悬臂突起部分与上模必须保持一定的应力间隙,为便于加工,间隙取在下模悬臂顶部表面,从模拟中发现,取 0.5 mm ~ 1.2 mm,均对悬臂不产生力的作用,所以取 1.0 mm。



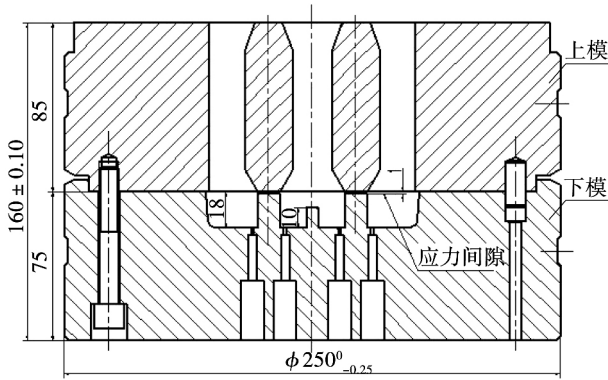


图7 模具结构示意图  
Fig. 7 Die structure

$h$ —分流桥的有效厚度  $\mu\text{m}$ ;

$b$ —分流桥最小宽度  $\mu\text{m}$ ;

$S$ —上模分流桥受压总面积  $\text{mm}^2$ ;

$P$ —挤压机最大比压  $\text{MPa}$ ;

$[\sigma_{\text{弯}}]$ —模具材料在工作强度下的弯曲应力,  $\text{MPa}$ (模具材料为 H13, 取值为  $1150 \text{ MPa}$ )。

根据上述结构进行计算:

$$n = \frac{85 \times 24 \times 2 \times 1150}{24 \times 90 \times 670} = 3.23$$

结果表明, 模具有足够的强度。

但在实践中, 对于一模双孔模具, 特别是半空心

铝型材的一模双孔模具, 必须使用专用的支承模垫, 否则, 模具的寿命会大大降低。图 3b 方案所配合的专用支承模垫内孔结构如图 8 所示。专用支承模垫的厚度不应小于  $70 \text{ mm}$ 。

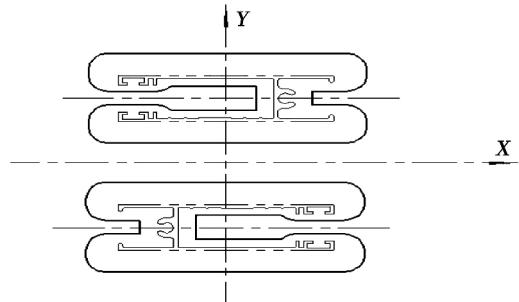


图8 专用支承垫内孔结构示意图  
Fig. 8 Inner hole structure of special die support

#### 4 挤压结果对比

对图 1 所示铝型材采用传统的平面模、单孔切割式分流模结构和遮盖式一模双孔结构的模具进行试模与挤压跟踪, 所得结果对比如表 1 所示。从表 1 数据可以看出, 对于半空心铝型材采用遮盖式一模双孔分流模具有明显的优势, 大大提高了模具的寿命, 降低了型材的挤压模具成本。

表 1 用不同结构模具挤压铝型材的结果对比  
Table 1 Comparison of die structure and extrusion results

模具结构	挤压机能力/MN	型材壁厚偏差/mm	型材表面质量	型材尺寸精度	模具寿命/t Al 材	模具材料/kg
传统平面模	10	超过 0.2	挤压痕深, 表面粗糙	开口易小, 端面壁厚变薄严重	< 1	65
单孔切割式分流模	10	无	挤压痕轻, 表面光亮, 但表面有拉丝、突筋	符合技术要求, 普通级	8.5	52
遮盖式一模双孔分流模	18	无	挤压痕轻, 表面光亮、光滑	符合技术要求, 达高精度	26.7	75

#### 5 结束语

对图 1 所示的半空心铝型材采用遮盖式一模双孔结构挤压模, 试模和实际挤压结果表明: 模具试模一次成功, 模具经过氮化多次使用, 挤压铝型材产量可达  $26.7 \text{ t}$ 。由此得出, 采用这种新的模具结构可以大大提高模具的寿命, 提高铝型材生产效率和降低

成本。同时可以看出, 模孔的布置、分流孔的设计、分流桥的结构以及下模焊合室的结构设计和工作带的选择是半空心铝型材一模双孔结构的关键。在设计过程中, 借助计算机进行模拟更能提高设计的效率和准确率。

(下转第 55 页)

Standard 作为求解器。D 形块和变形体之间设置摩擦系数为 0.1 的接触摩擦属性。模拟完成后,在结果中提取 D 形块的  $y$  向反作用力和位移来绘制  $P-S$  曲线。

模拟与试验的对比结果如图 6b 所示。由图 6 可知,使用依据环向拉伸试验数据拟合得到的指数硬化模型作为仿真模型的材料属性时,得到的结果准确度要高于依据单向拉伸试验数据拟合得到的指数硬化模型。由此可见,本文所使用管材的塑性硬化性能在环向和轴向两个方形上是有一定的差别的,依据本力学模型拟合而得的硬化性能能更加准

确地反映管材的环向性能。

## 5 结 论

1) 铝合金管材经“530℃2 h 固溶处理 + 室温水淬”处理后,环向硬化性能和轴向硬化性能存在一定的差异,不能单纯通过轴向拉伸试验来评价管材的环向塑性硬化性能。

2) 依据本文作者建立的力学模型,通过反向拟合的方法处理环向拉伸试验的数据,得到的指数硬化模型( $\sigma = K\varepsilon_n$ )中的强度系数  $K$  和硬化指数  $n$  能很好地评价管材环形硬化性能。

### 参考文献:

- [1] ARSENE S, BAI J. A new approach to measuring transverse properties of structural tubing by a ring test [J]. Journal of Testing and Evaluation, 1998, 26(1): 26 - 30.
- [2] DICK C P, KORKOLIS Y P. Mechanics and full-field deformation study of the ring hoop tension test [J]. International Journal of Solids and Structures, 2014, 51(18): 3042 - 3057.
- [3] DICK C P, KORKOLIS Y P. Assessment of anisotropy of extruded tubes by ring hoop tension test [J]. Procedia Engineering, 2014, 81: 2261 - 2266.
- [4] DICK C P, KORKOLIS Y P. Strength and ductility evaluation of cold-welded seams in aluminum tubes extruded through porthole dies [J]. Material and Design. 2015, 67: 631 - 636.
- [5] KORKOLIS Y P, DICK C P, KAPLAN A R, et al. Formability assessment of Al-6xxx-T4 tubes for hydroforming applications [R]. SAE World Congress, 2013.
- [6] HE Z B, YUAN S J, LIU G, et al. Formability testing of AZ31B magnesium alloy tube at elevated temperature [J]. Journal of Materials Processing Technology, 2010, 210(6/7): 877 - 884.
- [7] 何祝斌,苑世剑,查微微,等. 管材环状试样拉伸变形的受力和变形分析 [J]. 金属学报, 2008, 44(4): 423 - 427.
- [8] 查微微. 镁合金管材力学性能环向拉伸测试方法 [D]. 哈尔滨: 哈尔滨工业大学, 2007.

(上接第 49 页)

### 参考文献:

- [1] 邓汝荣,黄雪梅. 半空心铝型材挤压模的设计 [J]. 轻合金加工技术, 2015, 43(4): 51 - 54.
- [2] 黄雪梅,郇鹏. 吊挂式铝型材挤压模设计 [J]. 模具工业, 2015, 41(11): 54 - 56.
- [3] 刘静安,邵莲芬. 铝合金空心型材一模两孔挤压模具设计与制造及试挤 [J]. 轻合金加工技术, 2015, 43(9): 49 - 53.
- [4] 刘静安. 铝合金挤压模设计、制造、使用及维修 [M]. 北京: 冶金工业出版社, 1999: 181 - 183.
- [5] 谢建新,刘静安. 金属挤压理论与技术 [M]. 北京: 冶金工业出版社, 2012: 133 - 138.
- [6] 陆玉静,邓汝荣. 型材产生壁厚差的原因及解决方法 [J]. 轻合金加工技术, 2002, 30(8): 29 - 31.
- [7] 陈浩,赵国群,张存生,等. 薄壁空心铝型材挤压过程数值模拟及模具优化 [J]. 机械工程学报, 2010, 46(24): 34 - 39.
- [8] 徐磊,赵国群,张存生,等. 多腔壁板铝型材挤压过程数值模拟及模具优化 [J]. 机械工程学报, 2011, 47(22): 61 - 68.